

**ANALYSIS ON EOR/CO₂ SEQUESTRATION IN SACROC UNIT,
TEXAS USING A COMPOSITIONAL SIMULATOR**

by

Maung Phyoe Wai Aung

THESIS

Presented to the Faculty of Petroleum Engineering Department

New Mexico Institute of Mining and Technology

MASTER OF SCIENCE IN PETROLEUM ENGINEERING

New Mexico Institute of Mining and Technology

August 2009

**ANALYSIS ON EOR/CO₂ SEQUESTRATION IN SACROC UNIT
USING A COMPOSITIONAL SIMULATOR**

By

Maung Phyoe Wai Aung

New Mexico Institute of Mining and Technology, 2009

RESEARCH ADVISOR: Dr. Robert Balch

ABSTRACT

Storing carbon dioxide, CO₂, in oil reservoirs or saline aquifers is one way to reduce greenhouse gases. At the same time, additional oil can be recovered by injection of CO₂. Analyses of CO₂ sequestration and Enhanced Oil Recovery (EOR) in Scurry Area Canyon Reef Operator's Committee (SACROC) unit are presented in this thesis report. The objective of this research study is to understand the potential fate of the injected CO₂ in the oil reservoir while recovering additional oil. First, a simulation study was carried out to match the historical oil production from the pilot test wells, and then the potential for EOR and sequestration using injected CO₂ was analyzed. A good history match for oil, gas and water production volumes and reservoir pressure was obtained.

Second, several cases were studied with different production/injection constraints imposed on the pilot wells. When injection rates were not controlled, the amount of CO₂ injection allowed by the simulator was found to be physically impossible. While controlling the producers using progressively higher GOR limits, the total mass of CO₂ sequestered at realistic rates was highest while recovering the optimal amount of oil. When economics were not taken into consideration and producers were left open during the injection process, the highest cumulative volume of CO₂ was injected, though nearly all was subsequently produced. Re-injection of produced CO₂ must be considered in this case.

Finally, if the pilot area is considered a representative sample of how the entire SACROC unit could be developed and its sequestration/EOR capacity is extrapolated, then a measure of functional sequestration at SACROC can be made. Sequestered tons of CO₂ for each simulation run were compared and contrasted. Estimates of CO₂ annual production rates for coal plants of varying sizes (small, average, and high) are presented. Based on the extrapolation, the case run with highest GOR control on producers is the best EOR scenario and would also store the most CO₂ as measured in years of coal plant output by sequestering annual CO₂ production rates for the longest period of time.

ACKNOWLEDGMENTS

I like to give my special gratitude to Dr. Robert Balch, my research advisor, for his assistance and guidance throughout this research project. Many thanks also to the other members of my advisory committee, Dr. Reid Grigg, Dr. Thomas Engler who is my academic advisor and Dr. Robert Bretz for their advices and support. I also like to appreciate the time and technical guidance provided by Dr. Her-Yuan Chen and John Walter Moreno.

Funding was provided by Southwest Regional Partnership on Carbon Sequestration (SWP) and Department of Energy (DOE). Thanks to the Petroleum Recovery Research Center (PRRC) at New Mexico Tech. I would also like to thank the Texas Bureau of Economics Geology (BEG) and Mr. Merle Steckel of Kinder Morgan CO₂ Inc. for providing the data for this study. My sincere appreciation also goes to Dr. Weon Shik Han. I thank the Computer Modeling Group (CMG) for the technical support on GEM simulator.

I am also grateful to my parents, Tin Aung and Khin Wai Lwin, and my brothers, Toe Aung and Moe Aung, for their contributions to the completion of this work. Special thanks to Dr. Shamsuddin Shenawi, Murad Aliyev, Babajide Ayangade, Ghislain Fai-Yengo, Pinyok Kovisuith and Zaina Soorma for their support.

Table of Contents

Chapter 1: INTRODUCTION	1
Chapter 2: LITERATURE REVIEW	6
2.1. Previous Analyses of CO ₂ Sequestration in Oil and Gas Reservoirs	8
Chapter 3: DESCRIPTION OF GEM-GHG SIMULATOR	11
3.1. Equation of State (EOS)	12
3.2. Viscosity	13
3.1.2 CO ₂ Solubility	15
3.1.2.1 Henry's Law	15
Chapter 4: GEOLOGY AND RESERVOIR DESCRIPTION	17
4.1. Introduction	17
4.1.2 Reservoir Descriptions and History of Production/Injection	19
4.1.2.1 Secondary Recovery (Water Flooding)	20
4.1.2.2 Early Tertiary Recovery (CO ₂ -WAG Project Plan)	20
4.1.2.3 CO ₂ -WAG Project Design	21
Chapter 5: SOUTHWEST REGIONAL PARTNERSHIP ON CARBON SEQUESTRATION AND SACROC PILOT TEST	25
5.1. Introduction	25
5.2. Pilot Area Model Development	28

5.3 Reservoir-Boundary Conditions.....	31
5.4 Properties of the Reservoir	32
5.5 Fluid Data - Initial Conditions.....	34
5.6 Fluids Transport	35
Chapter 6: PILOT TEST WELLS AND HISTORICAL PRODUCTION DATA	37
6.1 Introduction	37
6.2 Reservoir Simulation: History Matching	42
Chapter 7: CO ₂ FLOOD DESIGN FOR ENHANCED OIL RECOVERY AND CO ₂ SEQUESTRATION	59
7.1 Introduction	59
7.2 CO ₂ Flood Design Optimization	60
7.3. Case 1: High Injection Rates	61
Case 2: GOR Constraints at Producers.....	70
Case 3: Shutting-In When Oil Production Rate Falls 5 stb/day	75
Case 4: No Shut-In	78
Chapter 8: CONCLUSIONS AND FUTURE WORK	82
8.1 Conclusions	82
8.2 Future Work and Recommendations	89

List of Tables

Table 3.1 - Parameters of Peng-Robinson Equation of State (PREOS).....	13
Table 5.1 - Summary of the Phast II pilot tests.....	26
Table 5.2- Summary of Reservoir Properties.....	33
Table 5.3 - Oil Composition of the SACROC Unit (Han, 2008).....	34
Table 6.1 - Summary of Historical Production/Injection Data (At the End of 2003)	38
Table 7.1- Description of Input Well Constraints for Simulation Cases	61
Table 7.2- Simulation results of injection and production (Scenario 1, Case 1).....	63
Table 7.3- Simulation results of injection and production (Scenario 2, Case 1).....	66
Table 7.4- Simulation results of injection and production (Case 2).....	73
Table 7.5- Simulation results of injection and production (Case 3).....	76
Table 7.6- Simulation results of injection and production (Case 4).....	79
Table 8.1 - Summary of all Simulation Runs.....	83
Table 8.2 - Summary of Estimated Years that SACROC Stores CO ₂ from Different Power Plants.....	87

List of Figures

Figure 1.1 - Global CO ₂ Emissions from Petroleum Consumption from Different Regions (Source: International Energy Annual, 2009)	2
Figure 1.2 - Global CO ₂ Emissions from Fossil Fuels Consumption from Different Regions (Source: International Energy Annual, 2009)	2
Figure 1.3 - Estimation of Global CO ₂ Emissions from Different Fuel Types (Source: International Energy Annual, 2009)	3
Figure 1.4 - Global Average Temperature Changes in the Past and Future (Source: International Energy Annual, 1999)	3
Figure 4.1 - SACROC Unit Reservoir in the Horseshoe Atoll and contour map of the carbonate reef (Han, 2008).....	18
Figure 4.2 - Cross-Section of the Structural and Stratigraphic of the SACROC Unit (Han, 2008)	19
Figure 4.3 - Different phases and locations of wells in 1973 (Han, 2008)	21
Figure 4.4 - Production and Injection History of SACROC Unit (Han, 2008).....	24
Figure 5.1 - Red area indicates the new pilot area and black dash lines show areas previously flooded with water alternating CO ₂ -gas (McPherson, 2007)	27
Figure 5.2 -Red square box indicates SACROC CO ₂ Injection Pilot Area (Reference: Carbon Sequestration Southwest Partnership Annual Meeting, 2008).....	27

Figure 5.3 - Extracted Reservoir Model with the Top of Structure Map (Scale in Feet).....	29
Figure 5.4 - Pilot-Test 9 × 13 × 22 Reservoir Model with the Top Structure Map (Scale in Feet).....	30
Figure 5.5 - Pilot-Test 25 × 46 × 22 Reservoir Model with the Top Structure Map (Scale in Feet).....	31
Figure 5.6 - Porosity Distribution of the Reservoir Model	32
Figure 5.7 - Permeability Distribution of the Reservoir Model	33
Figure 5.8 - Oil-water Relative Permeability Curve Adopted from Amyx (1960). 35	
Figure 5.9 - Liquid-gas Relative Permeability Curve Adopted from Amyx (1960)36	
Figure 6.1 - SACROC CO ₂ Injection Pilot Area (Reference: Carbon Sequestration Southwest Partnership Annual Meeting, 2008)	37
Figure 6.2 - Oil Production, 58-2	39
Figure 6.3 - Oil Production, 59-2	39
Figure 6.4 - Oil Production, 56-4	40
Figure 6.5 - Oil Production, 56-6	40
Figure 6.6 - Oil Production, 56-17	41
Figure 6.7 - Measured Average BHP of SACROC.....	42
Figure 6.8 - Oil Production History Match, 56-17	44
Figure 6.9 - Oil Production History Match, 56-4	44
Figure 6.10 - Oil Production History Match, 56-6.....	45
Figure 6.11 - Oil Production History Match, 58-2.....	45
Figure 6.12 - Oil Production History Match, 59-2.....	46

Figure 6.13 - Water Production History Match, 56-17	46
Figure 6.14 - Water Production History Match, 56-4	47
Figure 6.15 - Water Production History Match, 56-6	47
Figure 6.16 - Water Production History Match, 59-2	48
Figure 6.17 - Gas Production History Match, 56-17	48
Figure 6.18 - Gas Production History Match, 56-4	49
Figure 6.19 - Gas Production History Match, 56-6	49
Figure 6.20 - Gas Production History Match, 58-2	50
Figure 6.21 - Gas Production History Match, 59-2	50
Figure 6.22 - GOR History Match, 56-17	51
Figure 6.23 - GOR History Match, 56-4	51
Figure 6.24 - GOR History Match, 56-6	52
Figure 6.25 - GOR History Match, 58-2	52
Figure 6.26 - GOR History Match, 59-2	53
Figure 6.27 - Water Cut History Match, 56-17	53
Figure 6.28 - Water Cut History Match, 56-4	54
Figure 6.29 - Water Cut History Match, 56-6	54
Figure 6.30 - Water Cut History Match, 58-2	55
Figure 6.31 - Water Cut History Match, 59-2	55
Figure 6.32 - Water-Oil Ratio History Match, 56-17	56
Figure 6.33 - Water-Oil Ratio History Match, 56-4	56
Figure 6.34 - Water-Oil Ratio History Match, 56-6	57
Figure 6.35 - Water-Oil Ratio History Match, 58-2	57

Figure 6.36 - Water-Oil Ratio History Match, 59-2.....	58
Figure 6.37 - Reservoir Pressure History Match.....	58
Figure 7.1 - Cumulative Oil Production (Scenario 1, Case 1)	64
Figure 7.2- Cumulative CO ₂ Injection (Scenario 1, Case 1).....	64
Figure 7.3- Cumulative CO ₂ Sequestered (Scenario 1, Case 1).....	65
Figure 7.4- Cumulative Oil Production (Scenario 2, Case 1)	66
Figure 7.5- Cumulative CO ₂ Injection (Scenario 2, Case 1).....	67
Figure 7.6- Cumulative CO ₂ Sequestered (Scenario 2, Case 1).....	67
Figure 7.7- Oil Production Rate (Scenario 2, Case 1: 100 MMscf/day).....	68
Figure 7.8- Oil Production Rate (Scenario 2, Case 1: 50 MMscf/day).....	68
Figure 7.9- Oil Production Rate (Scenario 2, Case 1: 25 MMscf/day).....	69
Figure 7.10- Oil Production Rate (Case 2: GOR Constraints 10000 scf/bbl).....	71
Figure 7.11- Oil Production Rate (Case 2: GOR Constraints 50000 scf/bbl).....	72
Figure 7.12- Oil Production Rate (Case 2: GOR Constraints 100,000 scf/bbl).....	72
Figure 7.13- Cumulative Oil Production (Case 2)	74
Figure 7.14- Cumulative CO ₂ Injection (Case 2).....	74
Figure 7.15- Cumulative CO ₂ Sequestered (Case 2).....	75
Figure 7.16- Oil Production Rate (Case 3: Shut-in Below 5 stb/day).....	76
Figure 7.17- Cumulative Oil Production (Case 3: Shut-in Below 5 stb/day)	77
Figure 7.18- Cumulative CO ₂ Injection (Case 3: Shut-in Below 5 stb/day).....	77
Figure 7.19- Cumulative CO ₂ Sequestration (Case 3: Shut-in Below 5 stb/day) ...	78
Figure 7.20- Oil Production Rate (Case 4: no shut-in)	80
Figure 7.21- Cumulative Oil Production (Case 4: no shut-in)	80

Figure 7.22- Cumulative CO ₂ Injection (Case 4: no shut-in).....	81
Figure 7.23- Cumulative CO ₂ Sequestered (Case 4: no shut-in).....	81
Figure 8.1- CO ₂ sequestered rate vs. CO ₂ emission rates from plants (Case 2, 100000 scf/bbl)	88
Figure 8.2- CO ₂ sequestered rate vs. CO ₂ emission rates from plants (Case 2, 10000 scf/bbl).....	88
Figure 8.3- CO ₂ sequestered rate vs. CO ₂ emission rates from plants (Case 3).....	89

List of Abbreviations

HCPV	Hydrocarbon pore volume
MMP	Minimum miscible pressure, psi
Mscf	Thousand standard cubic feet (of gas)
MMscf	Million standard cubic feet (of gas)
MMstb	Million stock tank barrel (of oil)
MMtons	Million tons (of CO ₂)
bbbl	Barrel (of oil)
bscf	Billion standard cubic feet (of gas)

Chapter 1: INTRODUCTION

Global CO₂ emissions have been calculated to exceed 27 billion tons annually and are primarily generated from the combustion of hydrocarbons such as oil, natural gas, and coal (Reichle *et al.*, 1999; Pruess *et al.*, 2003). Once CO₂ is emitted into the atmosphere, it can take approximately 100 years for decomposition (Keeling *et al.*, 2000). With growth in oil and gas demand, the atmospheric concentration of CO₂ has risen up from preindustrial levels of 280 (parts per million) ppm to present-day levels of 365 ppm (Keeling *et al.*, 2000). The Intergovernmental Panel on Climate Change (IPCC) predicts that global temperatures will increase by 1.1 to 6.4° C by 2100 (Metz *et al.*, 2005; Park, 2007) as a result.

Figure 1.1 represents the historical statistics of anthropogenic CO₂ emission globally. Figures 1.2 shows the cumulative volume of CO₂ which were emitted in different regions from consumptions of petroleum and fossil fuels. Figure 1.3 indicates the cumulative volume of CO₂ which are expected to be emitted in the future from various forms of fuels. Figure 1.4 displays the predicted the world average temperature in the past and forecast to 2100.

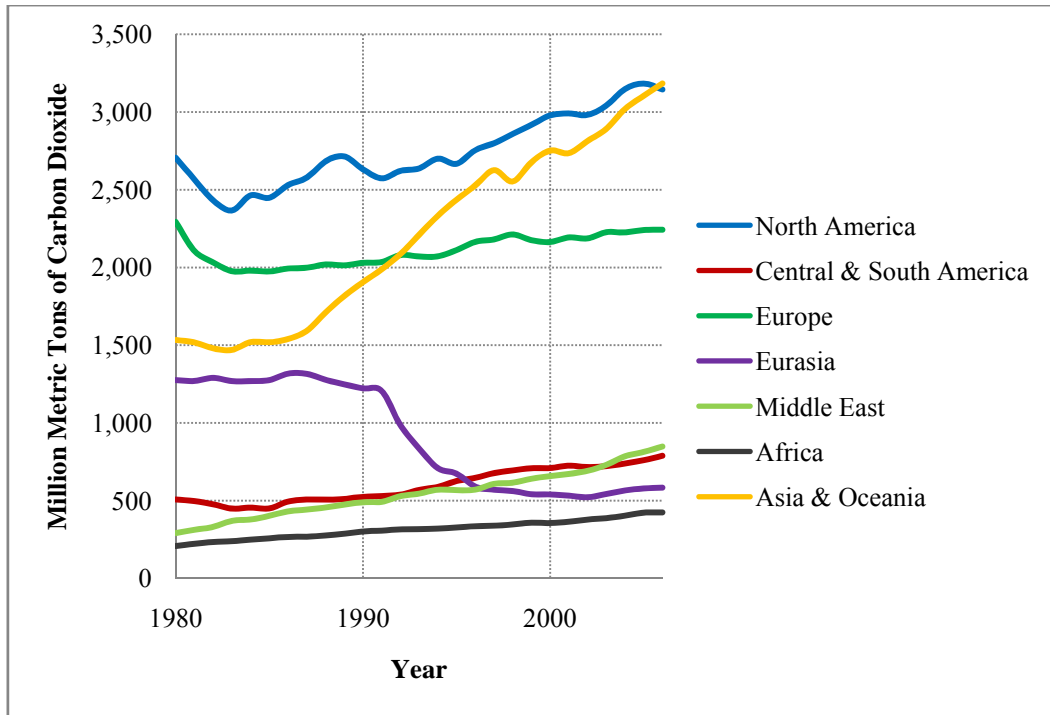


Figure 1.1 - Global CO₂ Emissions from Petroleum Consumption from Different Regions (Source: International Energy Annual, 2009)

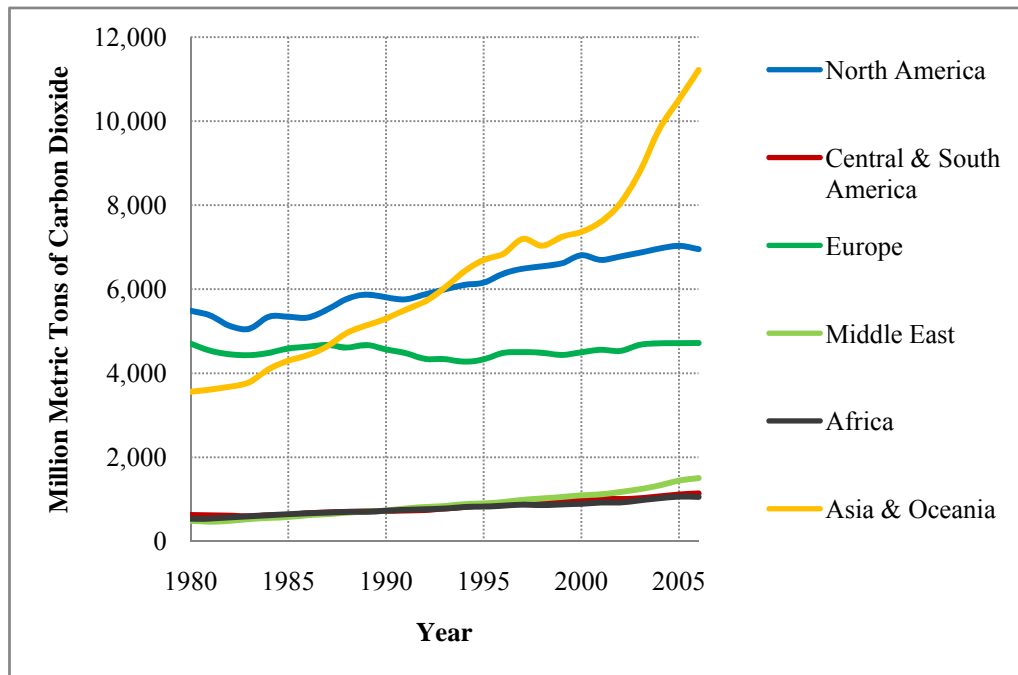


Figure 1.2 - Global CO₂ Emissions from Fossil Fuels Consumption from Different Regions (Source: International Energy Annual, 2009)

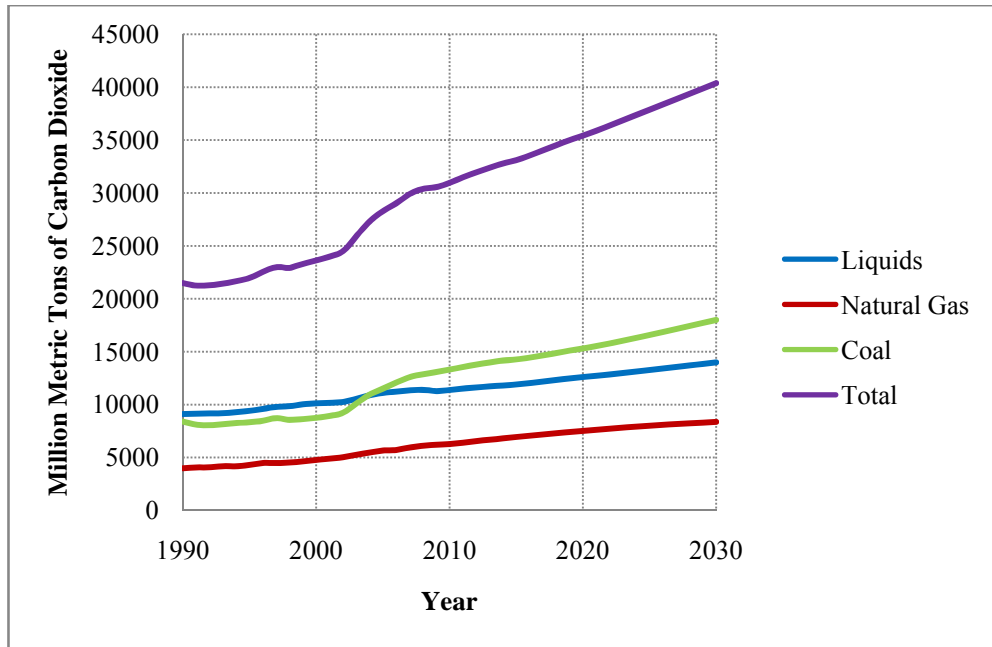


Figure 1.3 - Estimation of Global CO₂ Emissions from Different Fuel Types
 (Source: International Energy Annual, 2009)

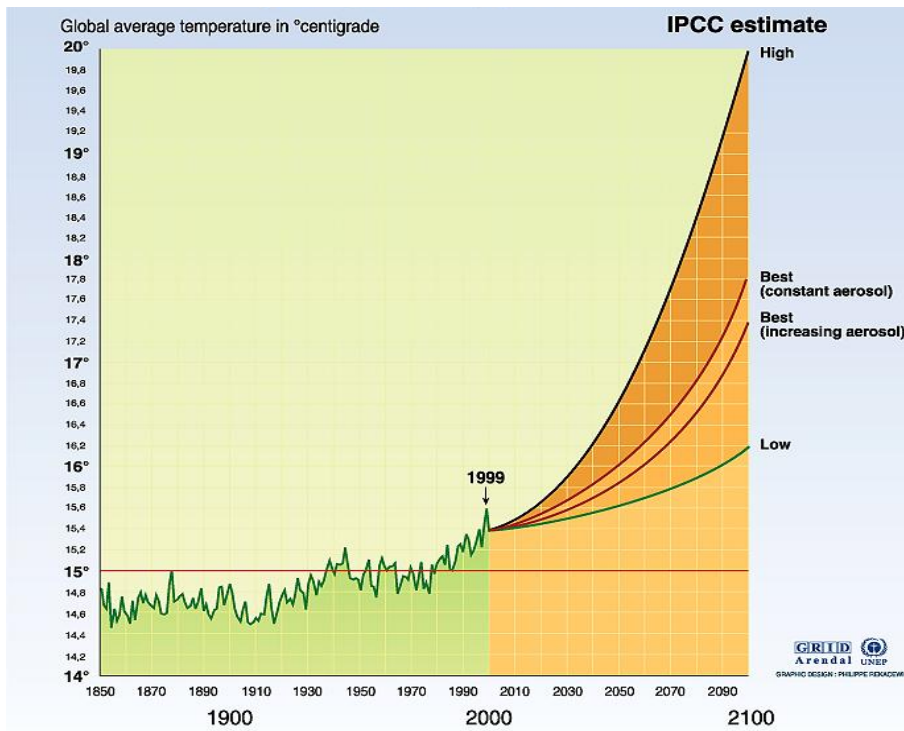


Figure 1.4 - Global Average Temperature Changes in the Past and Future
 (Source: International Energy Annual, 1999)

In order to reduce atmospheric CO₂, the use of fossil fuels as a primary energy source has to be replaced, or methods to capture and store the released CO₂ identified. It is not practical to stop using hydrocarbon fuels as alternative energy sources cannot currently meet the world's energy demand. Therefore, a focus on sequestering CO₂ in deep geological aquifers or depleted oil and gas reservoirs is a key technology if governments choose to reduce CO₂ (Han, 2008).

There are many geological domain options for sequestering CO₂: injecting CO₂ into proven and mature oil and gas reservoirs for the goal of coupled EOR and sequestration; injection into depleted hydrocarbon reservoirs; injection of CO₂ into deep saline aquifers; and methane recovery from the injection of CO₂ into coal seams.

In mature oil fields, there may be remaining oil after primary recovery. Additional oil can be recovered by injecting water or CO₂; therefore, oil fields are considered major targets for performing simultaneous EOR and CO₂ sequestration. Two benefits are provided: additional oil recovery and sequestration. However, injecting CO₂ in EOR projects is somewhat different from those for both coupled EOR and CO₂ sequestration. The former intends to optimize the oil recovery by minimizing the volume of CO₂ while the latter's incentive is to maximize the CO₂ storage while gaining as much incremental production as possible. Carbon dioxide is considered sequestered only if the injected CO₂ remains trapped in the reservoir for geologically significant times.

The focus of this study is to understand the potential fate of the injected CO₂ gas within the reservoir and how much additional oil can still be recovered

while incrementally storing CO₂. The approach was to use compositional simulation on a time scale of ~100 years for most cases.

Chapter 2: LITERATURE REVIEW

Many studies have been made on CO₂ sequestration from different aspects of science and engineering over the last decade. However, research has not been performed in detail for coupled EOR and CO₂ sequestration projects.

Since early 1970's, CO₂ injections for EOR purposes have demanded intensive reservoir engineering efforts which had attempted to reduce the required volume of CO₂ to recover additional oil. One of the goals of coupled EOR and CO₂ sequestration is to increase the amount of CO₂ left behind in the reservoir with the improvement in the oil recovery. CO₂ sequestration is analyzed and evaluated by four major mechanisms by which CO₂ is trapped in the reservoir (Han, 2008).

Supercritical CO₂ can be contained physically in low permeable zones of the reservoir underneath of a cap rock (Bennion *et al.*, 2005). This process mechanism is called *hydrodynamic trapping*. In *residual trapping mechanism*, CO₂ can be trapped in pores as an immobile phase because of capillary forces. With the third method CO₂ dissolves directly by a *solubility trapping mechanism* when it contacts with oil and water (Ghomian, 2008; Han, 2008). The fourth mechanism is called *mineral trapping* in which the CO₂ dissolution can react directly or indirectly with rock minerals and may precipitate as carbonate minerals forming a solid phase (Han, 2008). Among these four mechanisms, the capillary trapping as residual gas saturation is the least studied, however, it is a possible way to store CO₂ (Ghomian, 2008).

CO₂ injections have been performed in oil and gas reservoirs for several EOR purposes. Oil and gas accumulate and are often trapped by structure. This trapping mechanism provides formation integrity and safety for long term sequestration projects. In oil and gas fields, wells and processing facilities are also in place to manage CO₂ injections and monitor the storage process. CO₂ improves oil recovery because of two physical properties: density and viscosity. Liquid phase CO₂ extracts hydrocarbon components from reservoirs more easily than the gaseous-phase CO₂ (Jarrell *et al.*, 2002). Under miscible conditions, the viscosity of CO₂ is much lower than that of water or oil. CO₂ reduces oil viscosity and enables faster flow. CO₂ and oil are not miscible on the first contact but become totally miscible through multiple-contacts in a process in which components of oil and CO₂ are exchanged repeatedly until the oil-enriched CO₂ cannot be separated from the CO₂-enriched oil (Jarrell *et al.*, 2002). This mechanism provides the mechanism by which CO₂ can be injected and stored in oil reservoirs.

Another way to store CO₂ is to inject it into unmineable coal beds at a very deep location while recovering displaced methane gas from the coal. Methane gas is adsorbed onto the surface of the coal at liquid-like densities and is commonly recovered by dewatering and depressuring (Park, 2008). Methane can also be recovered through its characteristics in having higher affinity to adsorb gaseous CO₂ than methane (Park, 2008). Injected CO₂ will flow through fractures in the coal matrix and is adsorbed in pore surfaces while displacing methane gas. Finally, brine water in deep saline formations contains high salinity and is not good for drinking or agriculture. Studies show that saline aquifers have a large capacity for CO₂ storage and can store CO₂ for thousands of years. A million tons

of CO₂ have been captured and stored annually in Sleipner, North Sea (Park, 2008), as an example.

2.1. Previous Analyses of CO₂ Sequestration in Oil and Gas Reservoirs

A simulation study of CO₂ storage in the whole northern platform of SACROC using the Computer Modeling Group's Generalized Equation of States Model (GEM) simulator was conducted by Han (2008). In his work, CO₂ trapping mechanisms and their processes were studied in the area. Two different models, one saturated with brine and another with both brine and water, were developed to analyze CO₂ trapping mechanisms. It was found that mobile, residual and solubility trapping were primary mechanisms during 200 years of simulation in the brine only model (Han, 2008). His model predicted that mineral trapping contained greater amounts of CO₂ over several hundred years. However, in the model with 28% of brine and 72% of oil, it was observed that cumulative CO₂ volume trapped did not vary much over time and both oil trapping and mobile trapping were dominant mechanisms over 200 years. Based on these two analyses, it was concluded that injecting CO₂ into the aquifer below the oil reservoir proved to be more advantageous in storing CO₂ and avoiding potential leakage through the reservoir. His work was meant to provide detailed insight of effective approaches for CO₂ storage.

Ghomian (2008) studied the potential for both EOR and CO₂ storage in mature oil reservoirs in many different conditions. The GEM simulator was also used to investigate the processes. His work investigated various geological and

engineering aspects of oil reservoirs and physical properties of CO₂ to find major factors to help recover the optimal amount of oil and store the maximum amount of CO₂. Analysis was performed on the effect of different oil compositions to determine the appropriate candidate reservoirs for EOR-CO₂ sequestration (Ghomian, 2008). To optimize the oil recovery and the amount of stored CO₂, strategies were implemented employing different injection and production plans, using different well control methods along with mobility control programs such as water alternating gas (WAG) to avoid early CO₂ breakthrough.

A predictive reservoir model was built to model different CO₂ injection scenarios in the Frio brine pilot area (Ghomian, 2008). Simulations were run and results were compared with actual field data. An observation was made that the breakthrough time was close to the measured time in the field while different simulated gas saturation profiles were matched to the results from logs. Injection of CO₂ was also simulated into mature oil reservoirs to increase the amount of oil produced. His study focused on assessing uncertainties in EOR-CO₂ sequestration processes in the sandstone and carbonate reservoirs.

Uncertain variables: water alternating gas (WAG) ratio, CO₂ slug size, hysteresis effects, Dykstra-Parsons coefficient, and correlation lengths were analyzed to see their effects on the cumulative volume of CO₂ stored and cumulative amount of oil recovered. The effect of hysteresis on the amount of stored CO₂ and oil recovered was significant. CO₂ was trapped as residual gas and it increased when hysteresis was included (Ghomian, 2008). For optimizing CO₂ storage, the WAG ratio was the most influential parameter after analyzing the statistical data from the simulation results.

Flood design parameters such as the produced gas-oil ratio constraints, well spacing, production and injection well types, operational constraints for production and injection wells, injection scheme (WAG or continuous CO₂ injection), shut-in and open status, recycling, Kv/Kh and average reservoir permeability were studied in his work. The most sensitive design parameters were found to be the produced GOR constraints, well spacing and injection method (WAG or continuous CO₂ injection) (Ghomian, 2008).

The reservoir simulation study of Han (2008) did not perform a history matching in the area of the northern platform SACROC on 55 years of production and injection. The model focused on various sequestration mechanisms. Hence, the first objective of this thesis is to extract a pilot test area from the application of 9 million geo-cellular original reservoir model of the northern platform of SACROC unit. The geo-cellular model includes geological structures and stratigraphic data. Second goal is to achieve an acceptable history matching that accounts for fluid and pressure distributions in 55 years. Final goal is to perform reservoir simulation to optimize the amount of oil recovery and the maximum amount of CO₂ using different flood design parameters.

Chapter 3: DESCRIPTION OF GEM-GHG SIMULATOR

A simulation study of CO₂ injection into the reservoir was performed using a three-dimensional and multi-compositional simulator, GEM (Generalized Equation of State Model), developed by CMG (Computer Modeling Group). The GEM simulator can carry out three phase flow with multi-component fluids and can simulate reservoir management processes such as: miscible/immiscible gas injections, gas cycling and re-cycling (Computer Modeling Group, 2007). The gridding method used in this simulation is block centered. Well data such as wells location, perforations, and production data are specified or imported while rock and PVT properties are added to the reservoir model.

The GEM simulator uses both the Peng-Robinson (1976) and Soave-Redlich-Kwong (1972) equations of states (EOS) to calculate phase behavior and thermodynamic properties of reservoir fluids (*User's Guide*, Computer Modeling Group, 2007). In GEM, the solubility of gases in the aqueous phase is modeled using Henry's law.

The GEM simulator was further developed into a fully coupled geochemical compositional equation-of-state simulator, GEM-GHG (Generalized Equation of State Model and Green House Gas), which allows users to simulate the CO₂ storage in the reservoirs and be able to determine the storage in the forms of dissolution, gas, liquid, supercritical fluid and trapped fluid (*User's Guide*, Computer Modeling Group, 2007). It can also be used to simulate chemical equilibrium reactions between aqueous species, and kinetic reactions of minerals.

In Section 3.1, the equations-of-state and fundamental parameters used to model this simulation study are discussed.

3.1. Equation of State (EOS)

Both GEM and GEM-GHG can be used to predict the density of pure and mixture components by using Peng-Robinson or Soave-Redlich-Kwong Equations of State (*User's Guide*, Computer Modeling Group, 2007). The Peng-Robinson Equation of State (commonly referred to as PR EOS) was used to calculate the phase equilibrium compositions, densities and thermodynamic properties of reservoir fluid properties of different phases. The GEM also supports various correlations to compute properties such as viscosities (*User's Guide*, Computer Modeling Group, 2007). Peng-Robinson equation of state is described as:

$$p = \frac{RT}{V - b} - \frac{a \alpha}{V(V + b) + b(V - b)} \quad \dots\dots\dots 3.1$$

Where,

$$a = \Omega_a \frac{R^2 T_c^2}{p_c}$$

$$b = \Omega_a \frac{RT_c}{p_c}$$

$$\alpha = [1 + m(1 - \sqrt{T_r})]^2$$

$$m = 0.3795 + 1.54226\omega - 0.1644\omega^2 + 0.016667\omega^3$$

Table 3.1 - Parameters of Peng-Robinson Equation of State (PREOS)

p	Pressure	ω	Acentric values
p_c	Critical pressure	b	Coefficient in PR EOS for mixture effects
R	Ideal gas constant	Ω_a	0.45724
T	Temperature	Ω_b	0.07780
T_c	Critical temperature		
T_r	Reduced temperature		
V	Molar volume		
a	Coefficient in PR EOS for mixture effects		

3.2. Viscosity

In order to calculate the viscosity of the reservoir fluids, Pedersen's correlations were used (Pedersen *et al.*, 1987).

$$\frac{\mu_{mix}(P, T)}{\mu_o(P_o, T_o)} = \left(\frac{T_{c,mix}}{T_{c,o}}\right)^{-1/6} \left(\frac{P_{c,mix}}{P_{c,o}}\right)^{-2/3} \left(\frac{MW_{mix}}{MW_o}\right)^{-1/2} \left(\frac{\alpha_{mix}}{\alpha_o}\right) \dots\dots\dots 3.2$$

Where,

μ = Viscosity

T_c = Critical temperature

P_c = Critical pressure

MW = Molecular weight

α = Rotational coupling coefficient

The subscript "mix" represents the mixture property, and the subscript "o" refers to the reference substance property. The reference substance for the Pedersen's correlation is methane. The critical temperature and pressure of mixtures are calculated with mixing rules which are the function of the component critical temperatures and pressures, and mole fractions. The molecular weight of the mixture is calculated with the following equation.

$$MW_{mix} = coef_1(MW_w^{coef_2} - MW_n^{coef_2}) + MW_n \dots\dots\dots 3.3$$

Where,

MW_{mix} = Weight fraction averaged molecular weight

MW_n = Mole fraction averaged molecular weight

The rotational coupling coefficient can be calculated as follows:

$$\alpha = 1 + coef_3(\rho_r^{coef_4} MW^{coef_5}) \dots\dots\dots 3.4$$

Where,

α = Rotational coupling coefficient

ρ_r = Reduced density of the reference substance

The coefficients ($coef_1$ to $coef_5$) are default values introduced by Pedersen *et al.* (1984) (Chang, 2008).

The calculated phase (gas, oil and water) densities are calculated and identified by comparing with the pre-defined reference density in the GEM simulator.

3.1.2 CO₂ Solubility

Either Henry's Law or flash calculation methods can be used to model the solubility of fluid components into others in GEM.

3.1.2.1 Henry's Law

CO₂ solubility can be modeled with Henry's law in the following form.

$$p\phi_i = H_i x_i \dots\dots\dots 3.5$$

Where,

p = Pressure

p_{ref} = Reference pressure

ϕ_i = Fugacity coefficient of component

H_i = Henry's law constant for component

Henry's law constant (H) is calculated from,

$$\ln(H_i) = \ln(H_i^{ref}) + \frac{v_i^\infty(P - P_{ref})}{RT} \dots\dots\dots 3.6$$

where,

H_i = Henry's law constant for component

H_i^{ref} = Henry's constant of component i at reference pressure

T = Temperature

R = Universal gas constant

v_i^∞ = Molar volume at infinite dilution of component

Henry's constant is a function of temperature only and is practically independent of pressure under 74 psi (5 atm).

Chapter 4: GEOLOGY AND RESERVOIR DESCRIPTION

4.1. Introduction

The SACROC unit is the world's second oldest site where CO₂ flooding operations have been performed, located in Scurry County, west Texas within the Midland Basin (Han, 2008). It is situated on the South East flank of the Horseshoe Atoll which is 175 miles long and 3000 foot in thickness covering 3.9 million acres and a northward-opening arc of upper Pennsylvanian carbonate deposits in the basin (Figure 4.1) (Saller *et al.*, 2006). The Horseshoe Atoll, a subsurface accumulation of limestone, is a coral reef mound which is composed of organic debris bonded by crystalline calcite and lithified carbonate mud (Saller *et al.*, 2006).

The SACROC unit is 25 miles long and with a width of 2~9 miles, covers an area of 90,000 acres (Han, 2008). It is located in a Pennsylvanian age limestone reef (the Strawn, Canyon, and Cisco formations) with the Wolfcamp Series of the Lower Permian acting as the caprock (Figure 4.2) (Han, 2008). The oil production is from reef limestones of Strawn, Canyon, Cisco, and Wolfcamp age in the called Canyon, and Strawn Formations (Vest, 1970). The reservoirs are overlain by an impervious shale formation (Vest, 1970).

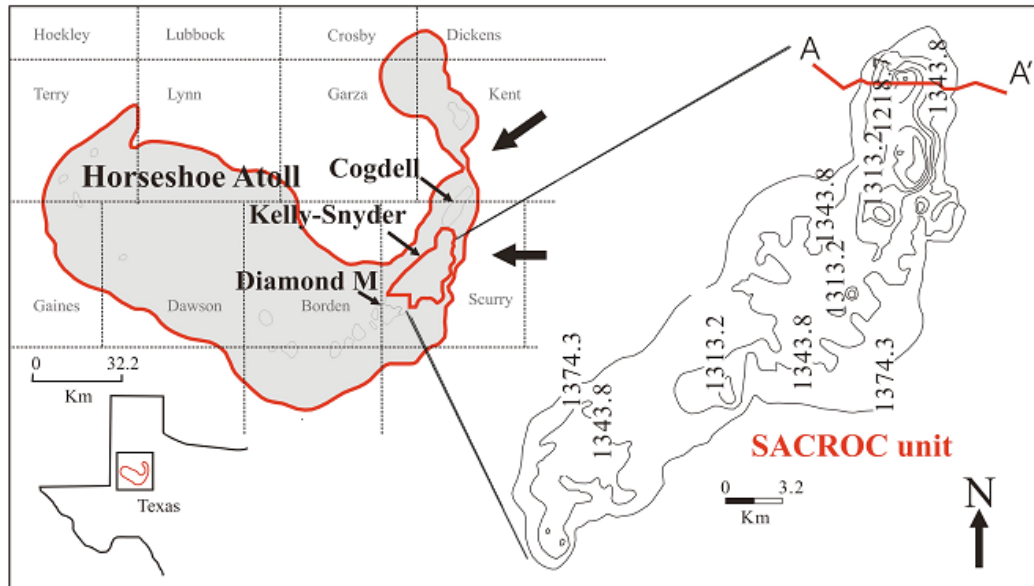


Figure 4.1 - SACROC Unit Reservoir in the Horseshoe Atoll and contour map of the carbonate reef (Han, 2008)

Figure 4.2 represents a cross-section of the geological and stratigraphical structure of the SACROC unit area. The constituents of the Canyon and Cisco Formations are limestone and also include trace amounts of anhydrite, clay, sand, chert, and locally-present shale (Han, 2008). In most of the Midland Basin, the rocks which are from the Pennsylvanian system are composed of nonfossiliferous shale and siltstone (Saller *et al.*, 2006). Rocks which are associated with the Wolfcamp series of the lower Permian system consist of shale, sandstone and fossiliferous limestone shale, sandstone, and siltstone (Han, 2008).

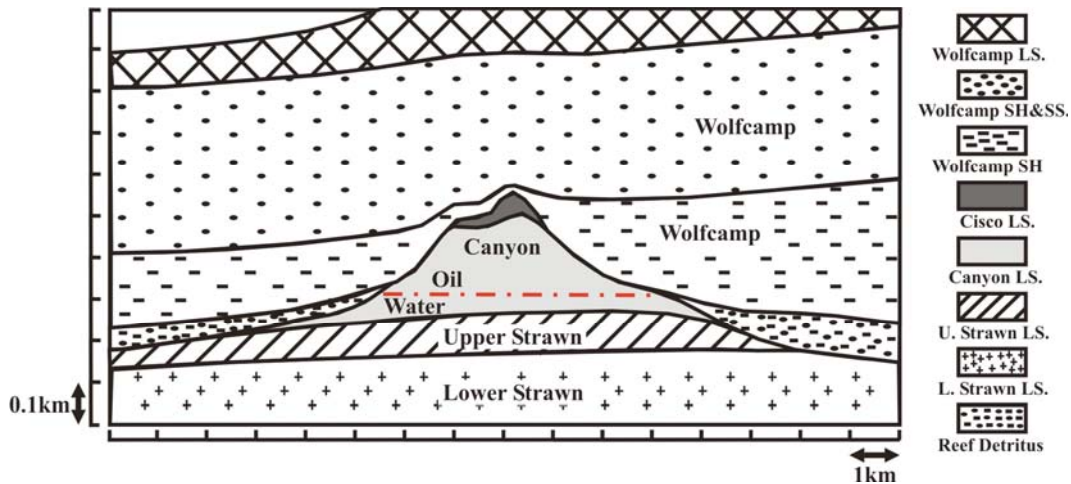


Figure 4.2 - Cross-Section of the Structural and Stratigraphic of the SACROC Unit (Han, 2008)

There have been studies conducted to understand the long-term sealing capacity of the formation above the Canyon reservoirs. This has led to the investigation of the integrity of the seal for the purposes of the geological sequestration of CO₂. The Wolfcamp shale of the lower Permian provides an impervious seal above the overlain formations- Cisco and Canyon (Han, 2008). The horizontal permeability to the shale is 9 mD and the vertical permeability is less than 0.05 mD (Han, 2008).

4.1.2 Reservoir Descriptions and History of Production/Injection

In November 1948, the Standard Oil Company of Texas (later became Chevron) formed the SACROC unit, which comprises about 98% of the Kelly-Snyder Field. 2.73 billion STB of oil-in-place was estimated for the Canyon reef limestone formation by Standard Oil (Dicharry *et al.*, 1973).

4.1.2.1 Secondary Recovery (Water Flooding)

Initially the field produced oil with solution gas drive, however, the reservoir pressure dropped below the bubble point pressure after producing only 5% of OOIP (Han, 2008). It was then necessary to raise and maintain reservoir pressure to continue production.

In 1953, the Texas Railroad Commission approved the foundation of SACROC (Scurry Area Canyon Reef Operators Committee) Unit. A pressure maintenance project was approved in the area by the Commission and injection was designed for a center to edge scheme as opposed to a pattern flood (Burkett, 1970; Han, 2008). The project started with 53 perimeter water injection wells at the rate of 132,000 barrels of water per day (BWPD) (Han, 2008). The reservoir pressure of many areas of the Unit rose above bubble point pressure, 1805 psi, in less than two years and water injection subsequently swept 72% of the total reservoir volume with oil saturation decreasing to 26% (Han, 2008). A material-balance calculation shows that about 1.2 billion STBO still remained at the end of the water injection program (Dicharry *et al.*, 1973). Since a large volume of oil was still left after the water flooding project, additional enhanced oil recovery (EOR) methods were necessary to produce additional oil.

4.1.2.2 Early Tertiary Recovery (CO₂-WAG Project Plan)

The SACROC engineering committee considered three EOR methods: (1) re-injecting dry residue gas, (2) an enriched gas-miscible process, and (3) CO₂-

miscible enhanced oil recovery (Dicharry *et al.*, 1973). The engineers decided against dry residue gas injection because the reservoir pressure was too low to maintain the minimum miscibility pressure (MMP) between re-injected gas and oil (Han, 2008). Therefore the committee chose the CO₂-miscible enhanced oil recovery method after laboratory testing. Han (2008) summarized the several characteristics reported by the laboratory tests in his dissertation.

4.1.2.3 CO₂-WAG Project Design

The SACROC engineering committee had to stagger the injection of CO₂ and divided the unit into three areas and phases, since the required amount of CO₂ was not available to meet all targeted injection rates simultaneously (Figure 4.3) (Han, 2008).

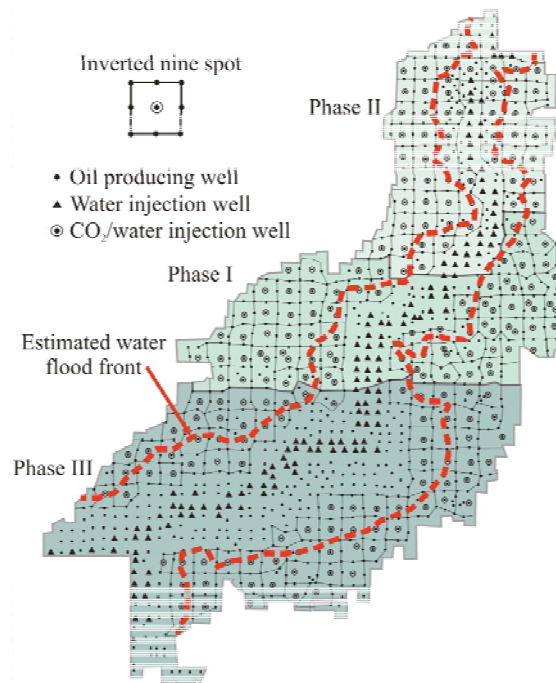


Figure 4.3 - Different phases and locations of wells in 1973 (Han, 2008)

The initial plan included 174 inverted nine-spot patterns (Han, 2008). Later, the plan was modified to add an additional 28 patterns. A Water-Alternating-Gas (WAG) injection method was selected instead of the continuous slug method. Dicharry (1973) reported that the initial plan was to inject 2.8% HCPV (WAG ratio of 0.47:1) after the continuous CO₂ slug volume of 6.0% HCPV had been injected. However, the committee chose to inject 3.6% water for a WAG ratio of 0.6:1. While the original plan was to inject CO₂ as the first injecting fluid, a 6% HCPV slug of water was injected ahead of the first CO₂ slug (Han, 2008). While the reservoir pressure was high in the areas near the center-line water injectors, many areas of the field were not pressured to the minimum miscibility pressure of 1600 psi, and required repressurizing ahead of CO₂ injection.

Prior to Phase I CO₂ injection, 21.5 million barrels of water were injected into 56 out of 66 of Phase I's nine-spot patterns in October 1971 (Han, 2008). The average reservoir pressure increased to 2400 psi in two years time (Langston *et al.*, 1988; Han, 2008). The water injection prior to CO₂ injection was repeated before Phase II and Phase III injections (June 1972 to December 1973). The Phase II area saw an increase in pressure to 2209 psi while the pressure rose from 1816 psi to 2696 psi in the Phase III area (Han, 2008). Due to the pre-CO₂ water injection, the oil rate increased from 30,000 bbl/d to 100,000 bbl/d in Phase I (Han, 2008). Phase II saw an increase in oil production from 40,000 bbl/d to 80,000 bbl/d (Langston *et al.*, 1988; Han, 2008). Phase III had an oil rate increase of 40,000 bbl/d after the pre-CO₂ water injection began in April, 1973.

Although laboratory studies indicated that the CO₂ breakthrough would occur after three years of injection, breakthrough happened after just six months

(Han, 2008). CO₂ production reached its peak in November 1972. The main causes of the premature CO₂ breakthrough were determined to be preferential flow paths for CO₂ gas and low pressure zones which created an immiscible gas drive (Han, 2008). Between 1972 and 1985, the water injection rates were increased to maintain the MMP so that CO₂ could be more miscible in the oil. The amount of available CO₂ remained relatively small and the CO₂ injection wells were sparsely scattered (Han, 2008).

In the late 1990's, SACROC had new operators and the oil production had not responded dramatically despite unsuccessful efforts to maintain pressure above the MMP. In August 2000, Kinder Morgan CO₂ purchased the SACROC field and implemented an injection program they termed 'a modern CO₂ operation' (Han, 2008). The 'modern CO₂ operation' was defined as: (1) targeting residual oil after water flooding, (2) controlling the reservoir pressure by injecting water before CO₂ and the operation of water curtain wells surround the area, (3) implementing smaller well spacing, 40 acres, (4) no CO₂ injection in areas where there was already a high CO₂ relative permeability, and (5) only injecting CO₂ into places where water floods were previously successful (Han, 2008).

Kinder Morgan used a series of water injectors termed as a 'water curtain' to close down the boundaries between injection patterns so that fluids would not migrate past the production wells. The water curtain also maintains the reservoir pressure at the desired level (Han, 2008). Kinder Morgan observed the CO₂ flood to be more successful along the water flood center-lines. Figure 4.4 displays the production and injection history of SACROC Unit.

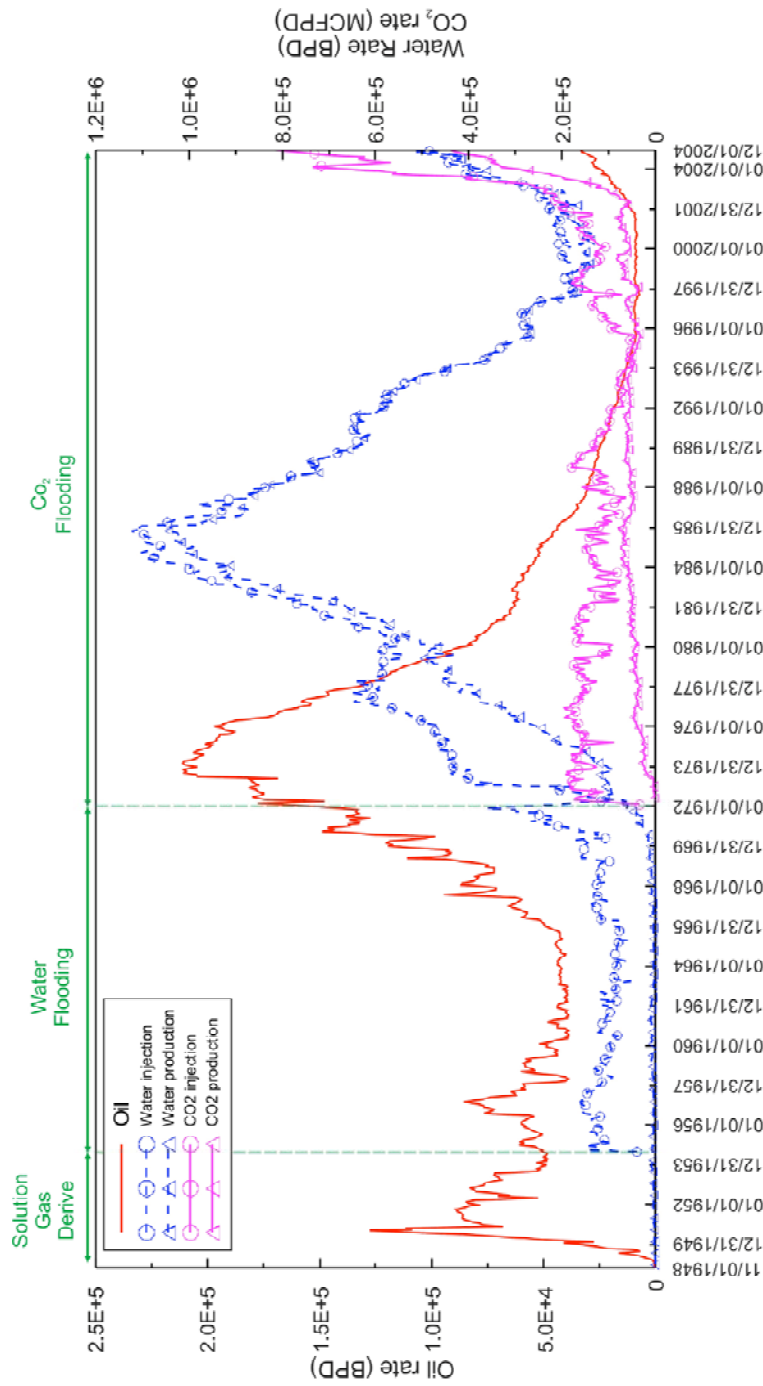


Figure 4.4 - Production and Injection History of SACROC Unit (Han, 2008)

Chapter 5: SOUTHWEST REGIONAL PARTNERSHIP ON CARBON SEQUESTRATION AND SACROC PILOT TEST

5.1. Introduction

The Southwest Regional Partnership on Carbon Sequestration (SWP) was selected by the United States Department of Energy (DOE) and the National Energy Technology Laboratory (NETL) along with seven other regional partnerships to study technologies to capture and store atmospheric carbon in various geological domains in the southwestern United States.

The SWP is made up of diverse technical experts representing science, engineering, economics and public outreach. It operates in Arizona, Colorado, Oklahoma, New Mexico, Utah, Kansas, Nevada, Texas, and Wyoming. Academic institutions, state and federal government agencies, oil companies, and the Navajo Nations are representative organizations.

The SWP has three phases. Phase I was started in 2003 and is involved with characterization. The goal was to evaluate and demonstrate the means to achieve an 18% reduction in carbon intensity by 2012 (McPherson, 2006). Accomplishments in Phase I included (1) analysis, characterization and transportation of CO₂ storage options in the region, (2) analysis and summary of CO₂ sources, (3) analysis and evaluation of CO₂ sequestration and capturing methods used in the region, (4) comparison of different CO₂ sequestration methods and ranking the most appropriate methods for Southwest regions, (5)

acquiring the in-place regulatory requirements of the area, and (6) acquiring public knowledge and acceptance of sequestration approaches (McPherson, 2006). Phase I was completed in December 2005.

The Phase II project was initiated to evaluate and validate the sequestration technologies with different pilot tests in Southwest region. McPherson (2007) summarized the pilot tests of Phase II in the Table 5.1.

Table 5.1 - Summary of the Phast II pilot tests

Location	Pilot Types	Date	Amount and Duration of Injection
Aneth Field, Utah	EOR-CO ₂ Sequestration	Started in August, 2007	~300,000 tons per year for 3 years
San Juan Basin, New Mexico	- ECBM-CO ₂ Sequestration - Small scale terrestrial sequestration	Started in December, 2007	~75,000 tons per year for 1 year
SACROC Unit, Texas	EOR-CO ₂ Sequestration	Started in March, 2008	~150,000 tons per year for 2 years
Southwest Region	Regional Terrestrial Analysis	Started in 2007	N/A

At SACROC, a new injection test site was originally located on the southern edge of Northern platform but was re-located to the South Platform (Figure 5.1) to address oil field operations logistical problems (McPherson, 2007).

The new demonstration site is a 5-spot pattern centered on the producer well, 56-17, surrounded by four injectors: 58-2, 59-2, 56-6 and 56-4 (Figure 5.2).

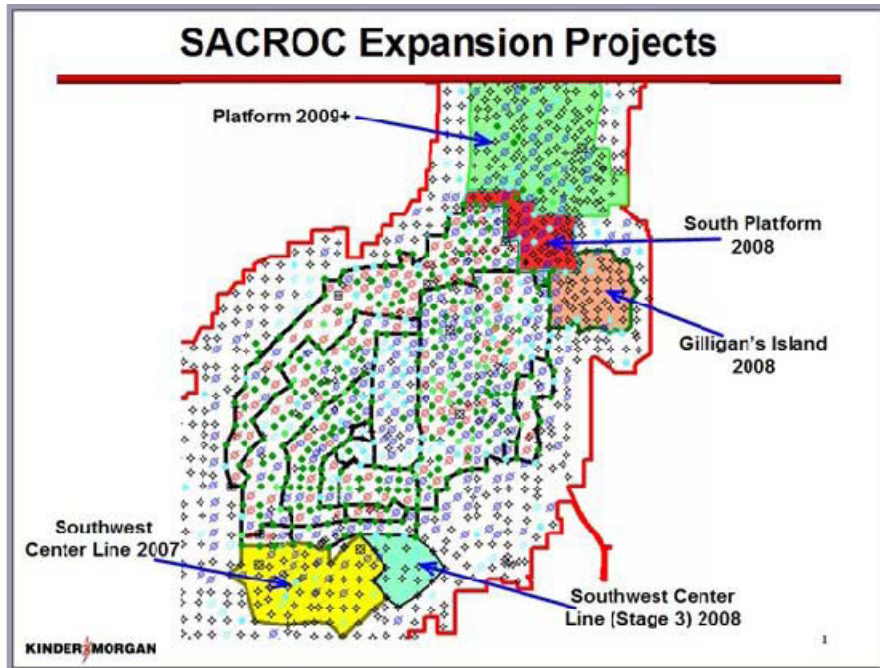


Figure 5.1 - Red area indicates the new pilot area and black dash lines show areas previously flooded with water alternating CO₂-gas (McPherson, 2007)

Figure 5.2 - Red square box indicates SACROC CO₂ Injection Pilot Area (Reference: Carbon Sequestration Southwest Partnership Annual Meeting, 2008)

5.2. Pilot Area Model Development

A 9 million grid element model of the entire northern platform of SACROC was created by the Texas Bureau of Economic Geology (BEG) and its reservoir properties were determined and modeled with core data, well logs, stratigraphic interpretation, and three-dimensional seismic data (Han, 2008). The heterogeneity of reservoir properties was detailed in this high-resolution geocellular model. This simulation study focused on modeling of the pilot test area to perform coupled EOR and CO₂ sequestration operations.

To perform this simulation study, an initial grid model of the CO₂ pilot test site with grid block dimensions of $36 \times 73 \times 22$ was extracted from the original nine million grid cells ($149 \times 87 \times 221$). This model of the pilot test site is approximately 7211 feet in width and 7291 feet long and has a thickness of 840 feet. A 3-D view of the inverted five-spot injection pattern at the site is shown in Figure 5.3.

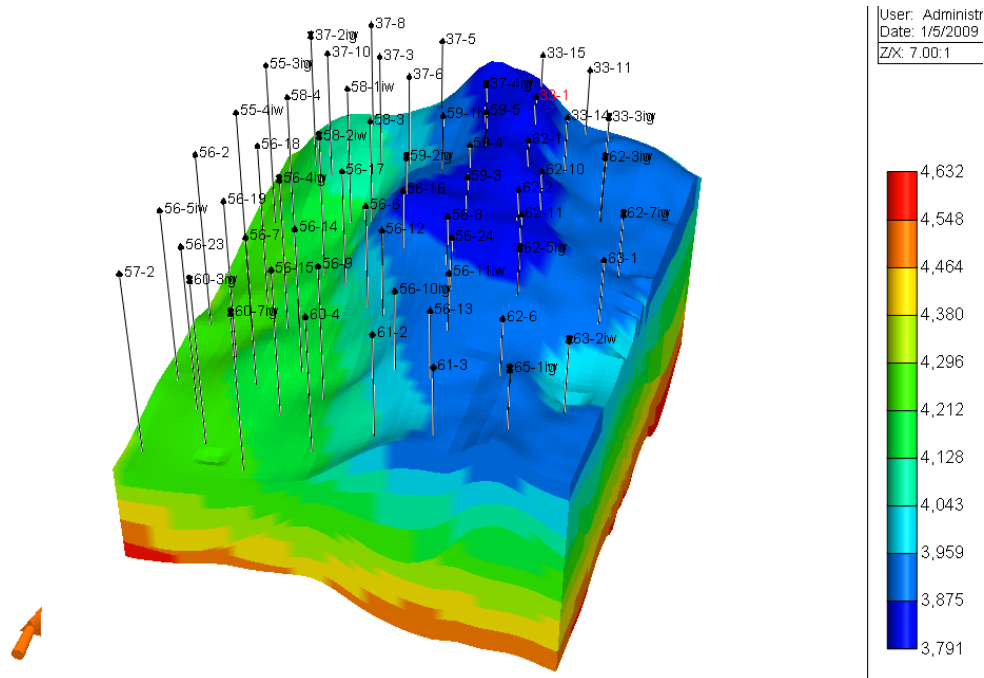


Figure 5.3 - Extracted Reservoir Model with the Top of Structure Map (Scale in Feet)

However, even this reduced area model with 57,816 grid blocks still took significant computer resources (1 week per run on a computer with 16 GB RAM and four 2.66 GHz processors) to simulate the production and injection activities for the 55 years of production. Since multiple runs and scenarios were anticipated a further reduction in field area was attempted using a smaller model ($9 \times 13 \times 22 = 2574$ grid blocks) which included only the pilot wells. (Figure 5.4). This yielded unrealistically high bottomhole pressure behavior that appeared to be a result of pressure build-up at the injection wells. An attempt to reduce the pressure by using a multiplier of 25% for injection rates on wells at the edge of the model failed to completely address this overpressure problem in the simulator. It was ultimately determined that there was no justification for using this method because of the permeability contrast in this area. Increasing the test area to include

additional full patterns around the test wells fixed this problem and allowed the simulator to honor boundary conditions.

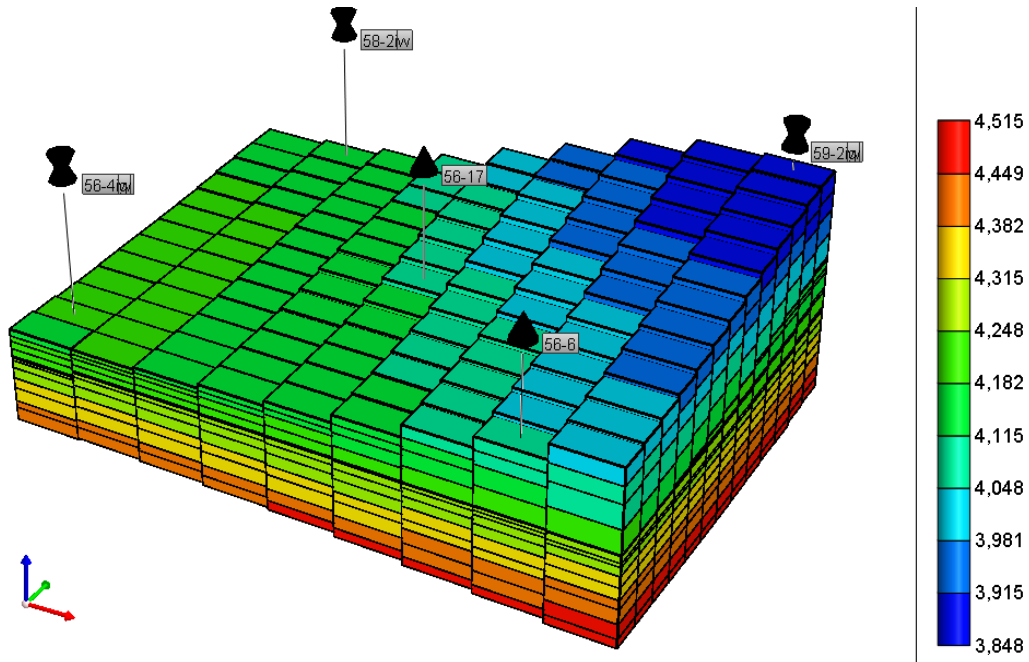


Figure 5.4 - Pilot-Test $9 \times 13 \times 22$ Reservoir Model with the Top Structure Map (Scale in Feet)

A model with grid cells ($25 \times 46 \times 22 = 25,300$) was later created for further simulation studies (Figure 5.5) once initial models were refined.

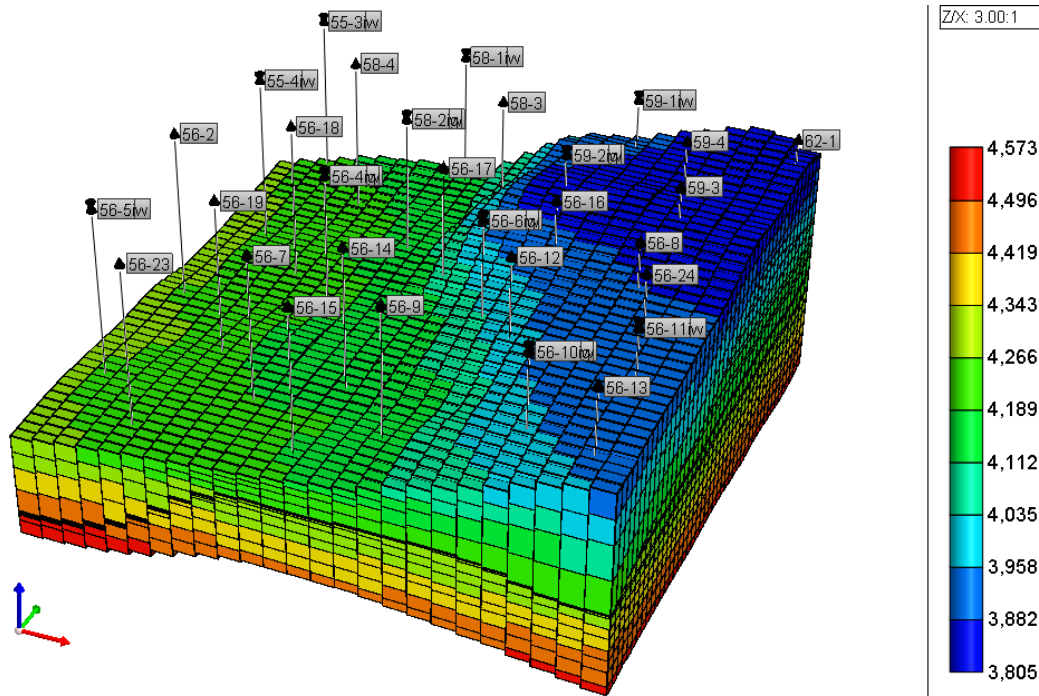


Figure 5.5 - Pilot-Test $25 \times 46 \times 22$ Reservoir Model with the Top Structure Map (Scale in Feet)

5.3 Reservoir-Boundary Conditions

The upper boundary of this model was designed to be a no flow boundary since the Wolfcamp shale formation acts as a seal, as confirmed from the analyses of water chemistry in each formation (Han, 2008). The lower boundary is also considered no flow, since the underlying Strawn formation has very low permeability (Han, 2008). All four sides of the model are treated as closed flow boundaries with no fluid influx from outside of the model; this simulates the effect of the water curtains.

5.4 Properties of the Reservoir

Reservoir properties were extracted from the 9 million geocellular model constructed by the BEG. Permeability was predicted from seismic surveys and well logs. The reservoir is characterized by permeability of 1.0×10^{-5} to 600 mD (Figure 5.7). The anisotropy (kv/kh) is measured at 0.4 from directional measurements on cores of SACROC (Han, *Electronic Written Communication*, 2008). The vertical permeability is then calculated from the anisotropy. Porosity is also measured with a combination of wire line logs and seismic data (Han, 2008) (Figure 5.6). The porosity ranges from 0.001 to 23 % and average water saturation is 28 %.

The initial reservoir pressure was reported to be 3122 psi while the average reservoir temperature was set at 130° F throughout the reservoir (Langston *et al.*, 1988). Reservoir properties are summarized in the Table 5.2.

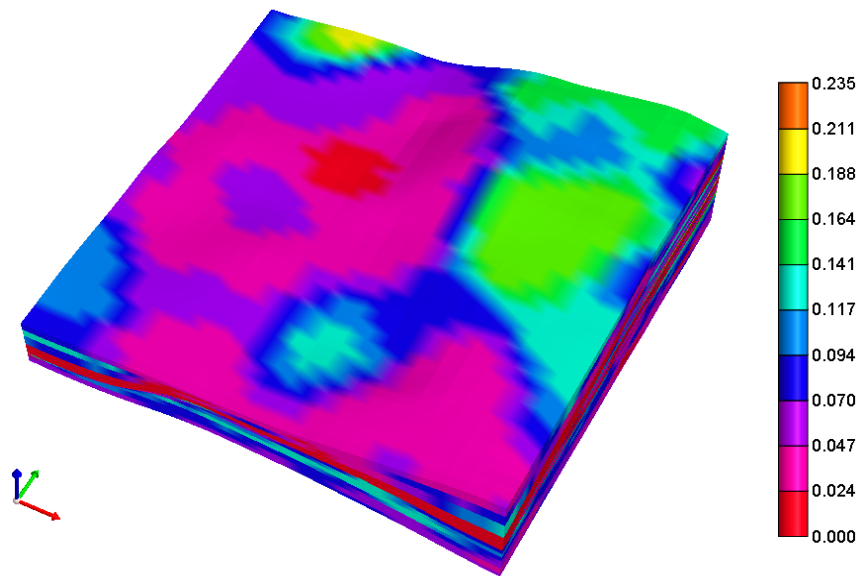


Figure 5.6 - Porosity Distribution of the Reservoir Model

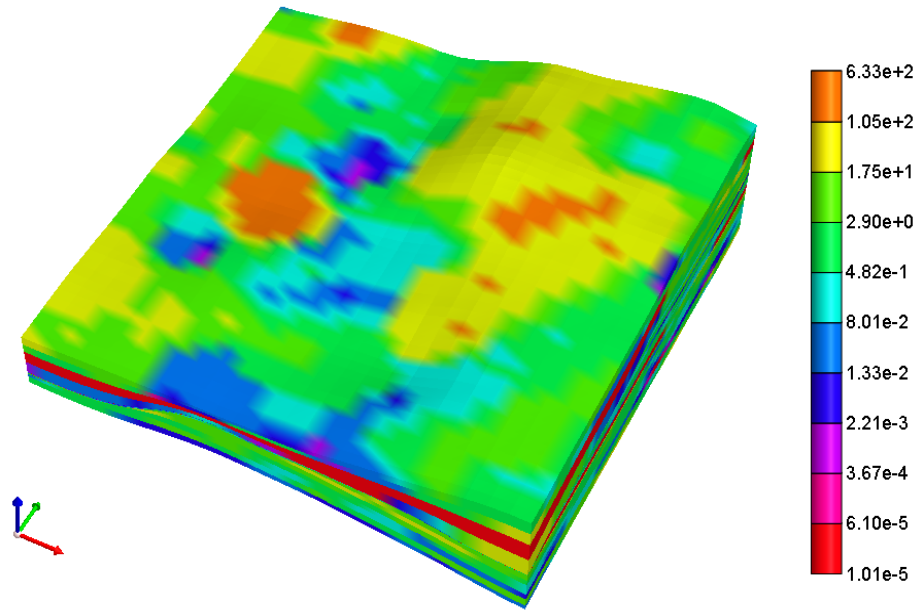


Figure 5.7 - Permeability Distribution of the Reservoir Model

Table 5.2- Summary of Reservoir Properties

Length (feet)	5008
Width (feet)	4595
Thickness (feet)	840
Reservoir Temperature (°F)	150
Initial Reservoir Pressure (psia)	3122
Constant Boundary Pressure (psia)	3122
Rock Compressibility (1/psi)	4.1×10^{-6}
Dip Angle of Reservoir (°)	0
Salinity (ppm)	100,000

5.5 Fluid Data - Initial Conditions

The initial reservoir oil gravity of 42° API was initially used and the composition of the oil is described in Table 5.3. The reservoir was modeled with the historical saturation data of water and oil of 28 % and 78 %, respectively (Vest 1970). The built-in Peng-Robinson Equation of State (PREOS 1976) was used to calculate the fluids' properties: density and fugacity. It was found that fluid densities did not match the original recorded data. Therefore using another PVT simulation program called PVTsim simulator, the fluid densities were tuned with Peng-Robinson-Peneloux Equation of State and then imported to GEM. The viscosity is calculated by the correlations of Jossi, Stiel, Thodos and/or Pedersen. The modeling of aqueous phase solubility was done with Henry's law (Li and Nghiem, 1986).

Table 5.3 - Oil Composition of the SACROC Unit (Han, 2008)

Composition	Mole Percent	Molecular Weight
C1	0.2865	16.04
C2	0.1129	30.07
C3	0.1239	44.10
I-C4	0.0136	58.12
N-C4	0.0646	58.12
I-C5	0.0198	72.15
N-C5	0.0251	72.15
FC6	0.0406	86.00
C7+	0.3015	275.00
CO ₂	0.0032	44.01
N ₂	0.0083	28.01

5.6 Fluids Transport

As discussed above, the heterogeneous property values of permeability and porosity were obtained from the original 9 million grid cells of SACROC model. The measured relative permeability data set of a West Texas limestone published by Amyx (1960) was used (Figure 5.8). The effects of capillary pressures are quite negligible in the field-scale simulations (Aziz and Settari, 1979). Therefore, capillary pressures for this simulation were ignored.

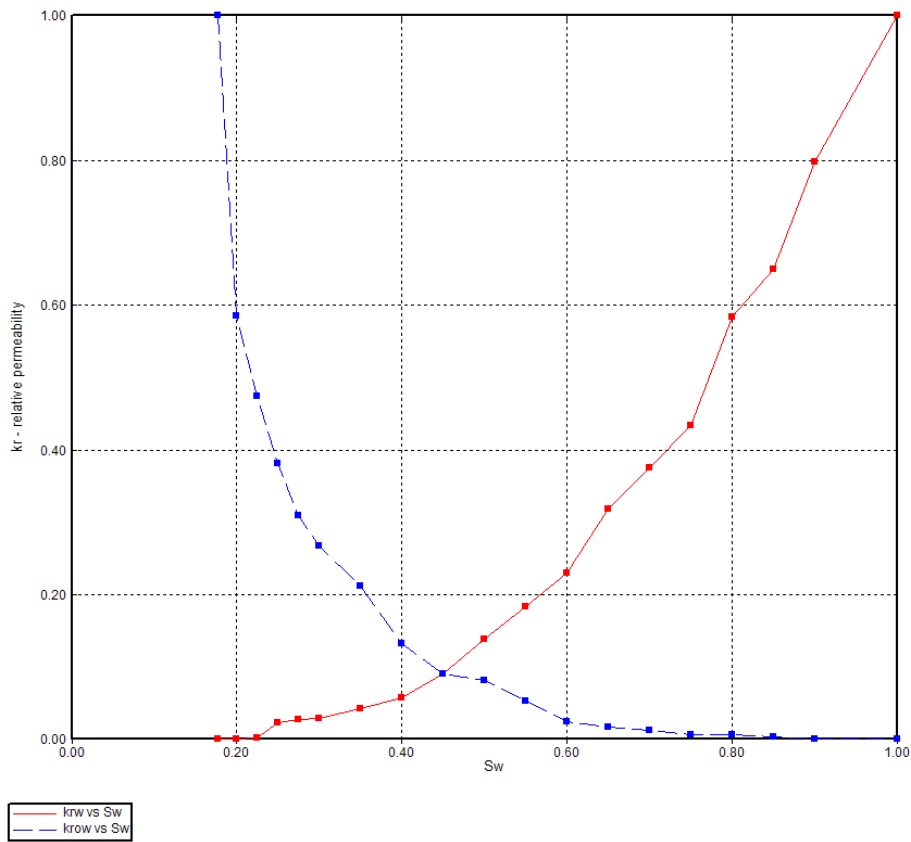


Figure 5.8 - Oil-water Relative Permeability Curve Adopted from Amyx (1960)

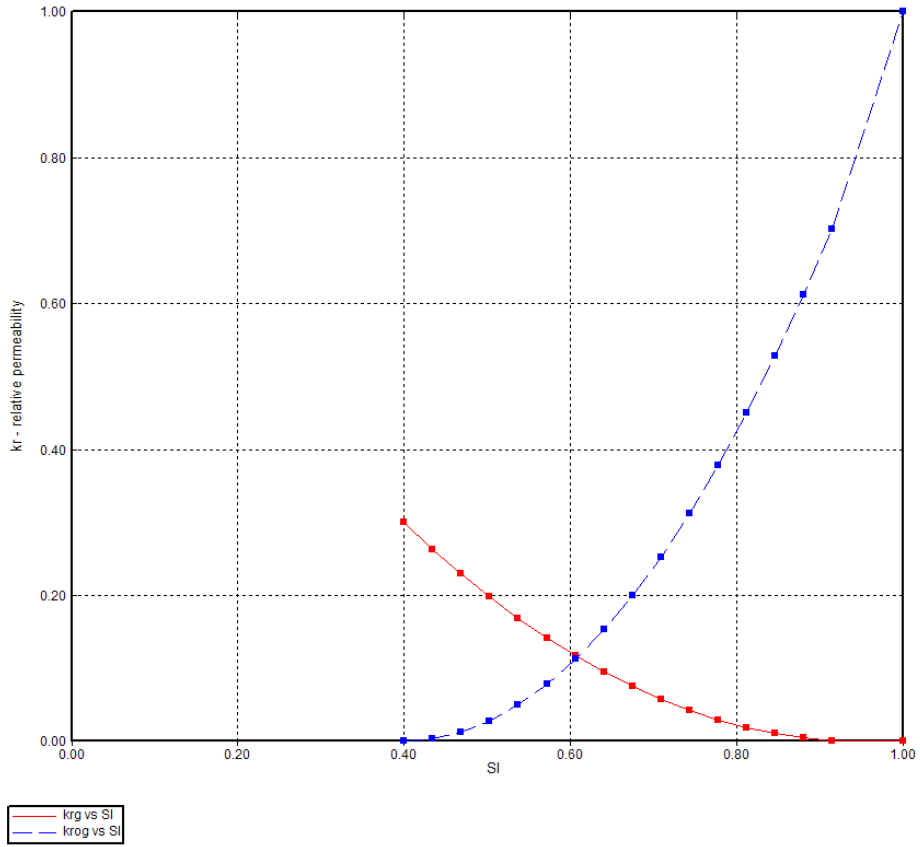


Figure 5.9 - Liquid-gas Relative Permeability Curve Adopted from Amyx (1960)

Chapter 6: PILOT TEST WELLS AND HISTORICAL PRODUCTION DATA

6.1 Introduction

The SACROC unit EOR/CO₂ Sequestration pilot test project is located in SACROC, west Texas. The pilot area for this study includes 5 inverted wells- a producer in the center surrounding by 4 injectors (Figure 6.1).

Figure 6.1 - SACROC CO₂ Injection Pilot Area (Reference: Carbon Sequestration Southwest Partnership Annual Meeting, 2008)

The first production in this pilot test area started from 56-4 and 58-2 in September 1949 followed by 56-6 and 59-2 in November, 1949. Some of the wells were converted into water injectors in the early 1950's. Table 6.1 summarizes the production start dates, cumulative oil/water and CO₂ production, and peak oil rate. The production and injection data were obtained from Kinder Morgan Inc.

Table 6.1 - Summary of Historical Production/Injection Data (At the End of 2003)

Well	First Date of Production	Max. Oil Rate (stb/day)	Cum. Oil Production (Mstb)	Cum. Water Production (Mstb)	Cum. Water Injection (Mstb)	Cum. CO ₂ Production (MMscf)	Cum. CO ₂ Injection (MMscf)
56-17	Jan-84	43	83.7	3512.7	0	0.3	0
56-4	Sep-49	150	391.9	386.8	16503.9	0	2.27
58-2	Sep-49	142	125.9	0	38483.2	0	0
56-6	Nov-49	347	1681.3	16253.9	0	0.73	0
59-2	Nov-49	181	454.8	2	24130	0	2.53

Monthly oil rates for the pilot test wells are provided in Figures 6.2 - 6.6.

Well 56-17 was used as an oil producer while other four wells were injectors.

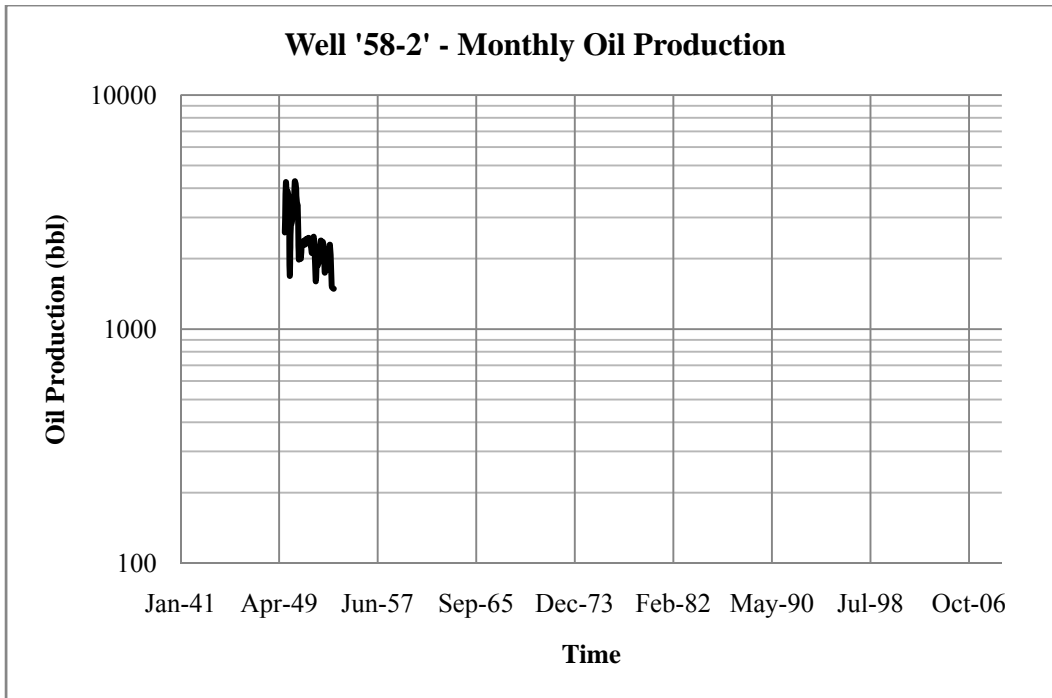


Figure 6.2 - Oil Production, 58-2

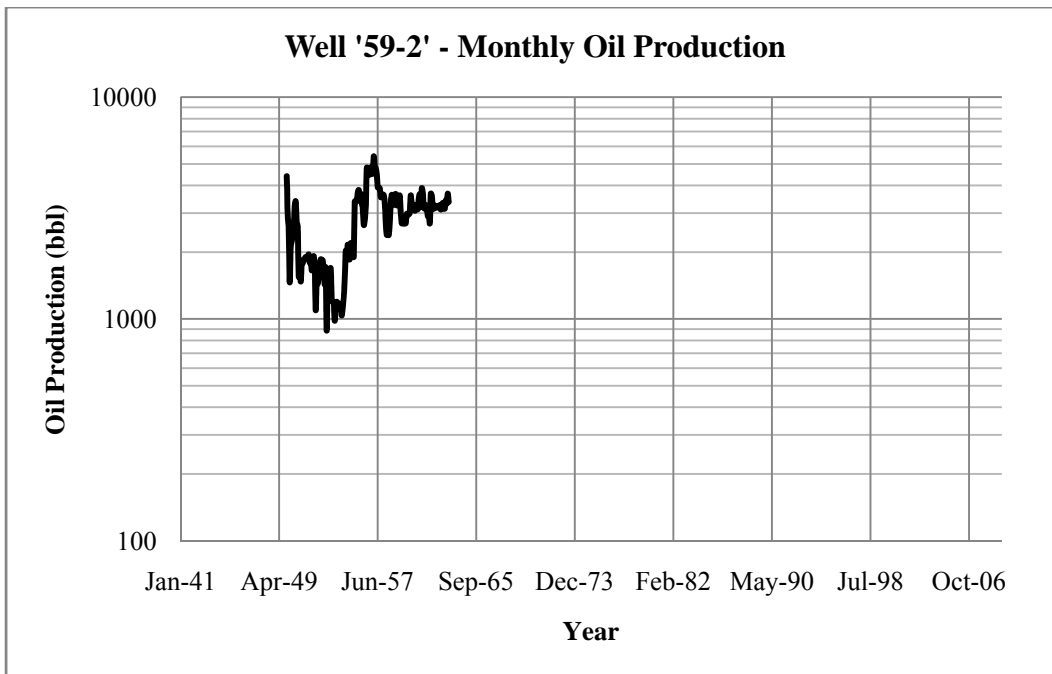


Figure 6.3 - Oil Production, 59-2

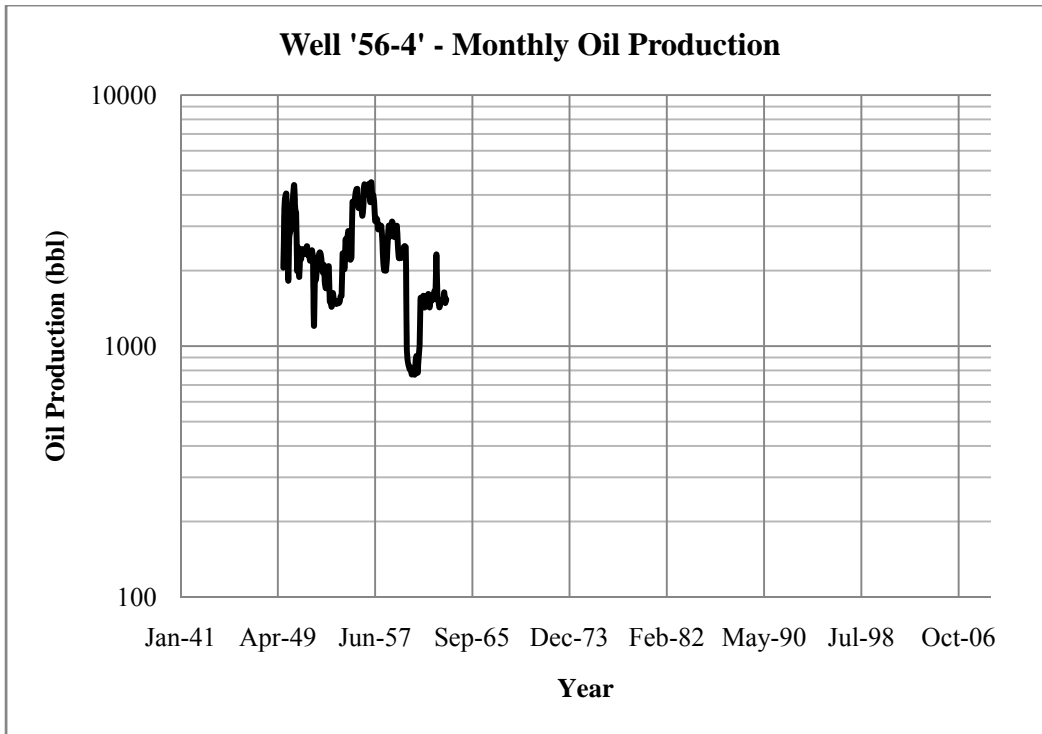


Figure 6.4 - Oil Production, 56-4

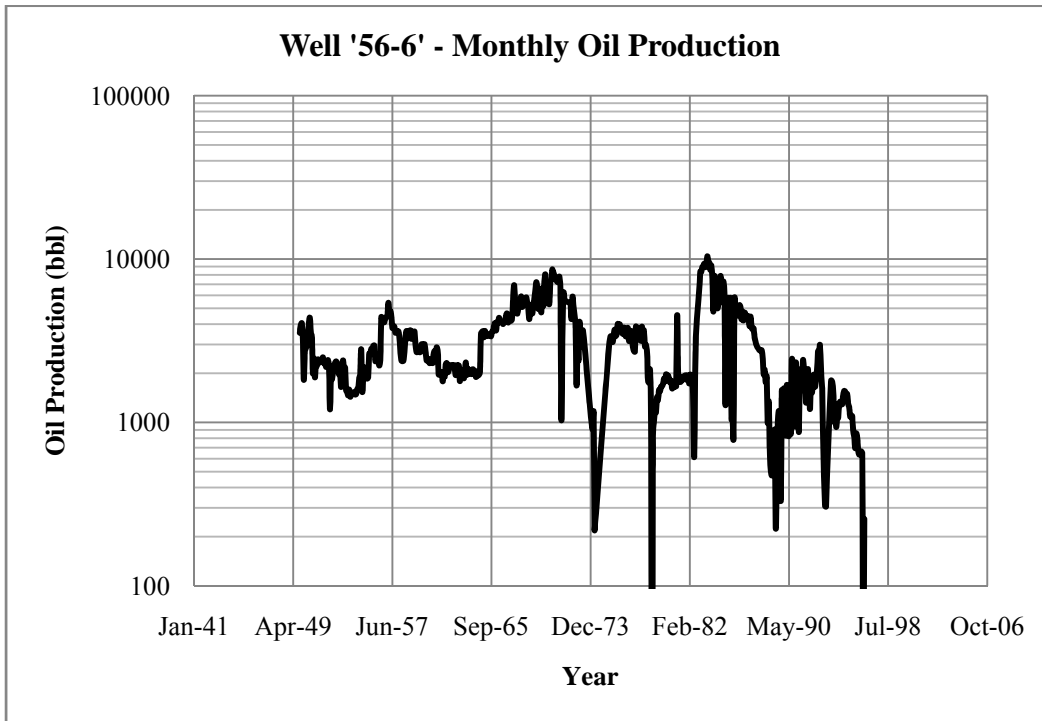


Figure 6.5 - Oil Production, 56-6

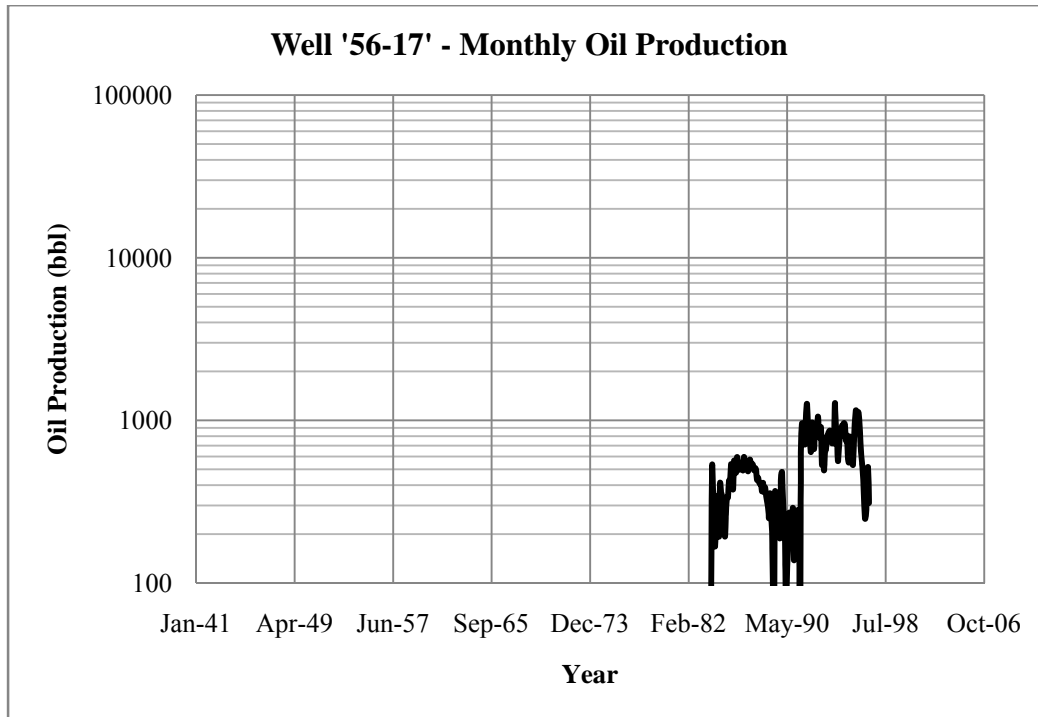


Figure 6.6 - Oil Production, 56-17

Bottomhole pressure (BHP) is provided as an average for the entire SACROC unit and BHP data of individual wells were not available for this study (Figure 6.7). The bubble point pressure was reported to be 1805 psi (Han, 2008). Therefore the average BHP of the entire SACROC was matched by the simulator's output bottomhole pressures during history matching.

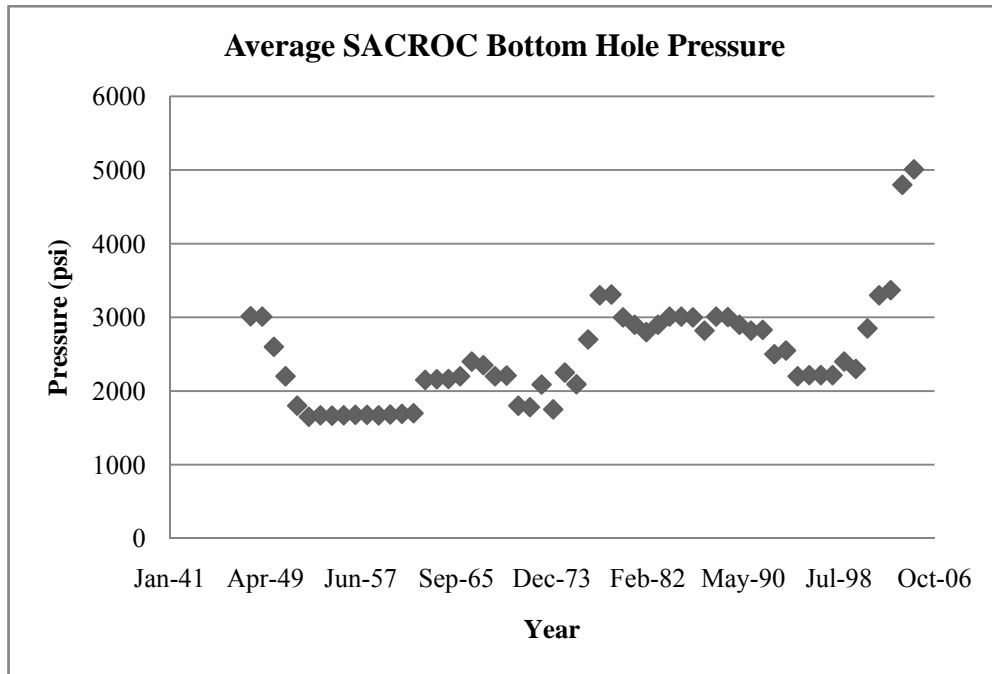


Figure 6.7 - Measured Average BHP of SACROC

6.2 Reservoir Simulation: History Matching

Simulations were constrained using oil rates of producing wells and water/CO₂ injection rates of injectors while history-matching water, hydrocarbon gas production rates, and average SACROC field bottomhole pressures. For faster simulations, oil production rates were averaged quarterly. In the original model, areas with low permeability were reported as zero values in the grid data which impacted the simulation and caused convergence issues. Therefore, it was suggested that the smallest non-zero value (1.0×10^{-5} md) of the permeability be ignored while the thickness is less than 0.0328 foot (Bob Brugman, *Electronic Written Communication*, 2008) since such small grids may dominate the run time of the model unnecessarily. The keyword *PVCUTOFF 50* was applied to null any

grid block with a pore volume less than 50 cubic feet. The time step calculation in the simulator was set to use smaller steps in order to avoid the convergence failures. Each simulation run of 55 years took around a day if nothing unusual occurred. If there were many convergence problems, the simulator would need to be restarted after efforts to fix the problem and this could add significantly to run time.

Figures 6.8 to 6.36 show the history match of oil, gas and water production rates of each well in the pilot area. Gas-oil ratio (GOR), water-cut and water-oil ratio matches of pilot wells are also presented. In general, the history matching results were quite good except the water production rate matches. The reservoir model produced more water than was reported. The simulated water production rates were not able to match the actual data except for well 56-4 and 59-2 while water-cut history matches reflect the rates. The gas-oil ratios are slightly underestimated as compared with the actual measured data in the wells because only a single set of PVT data was available. The simulated average reservoir pressure stays close to the measured average pressure of the whole SACROC Unit (Figure 6.37).

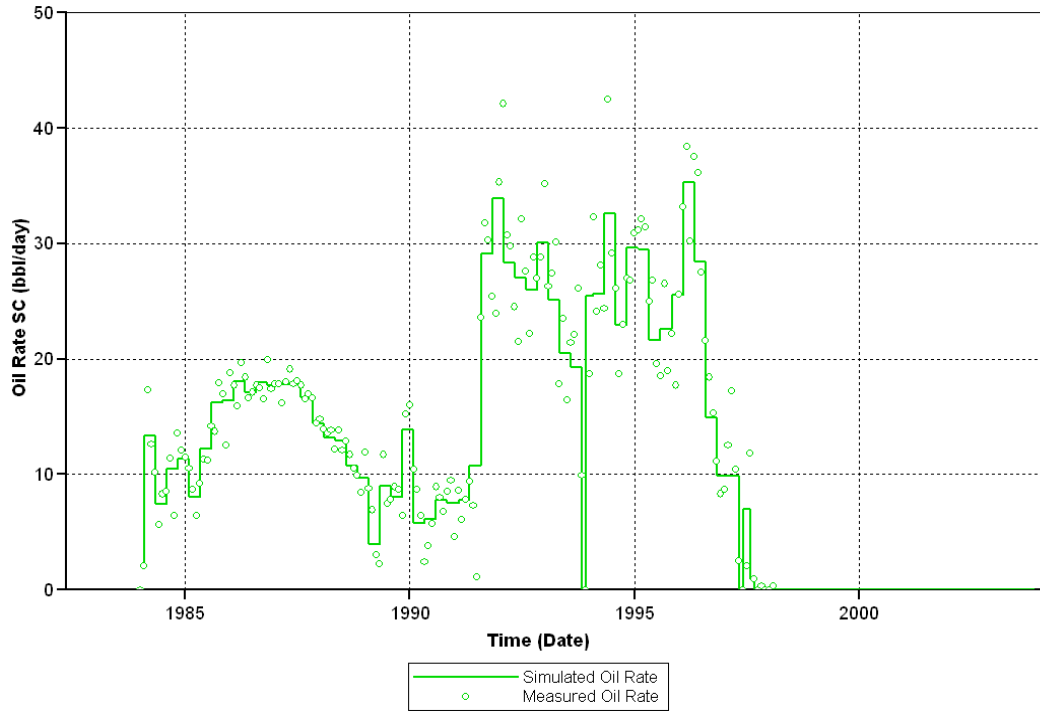


Figure 6.8 - Oil Production History Match, 56-17

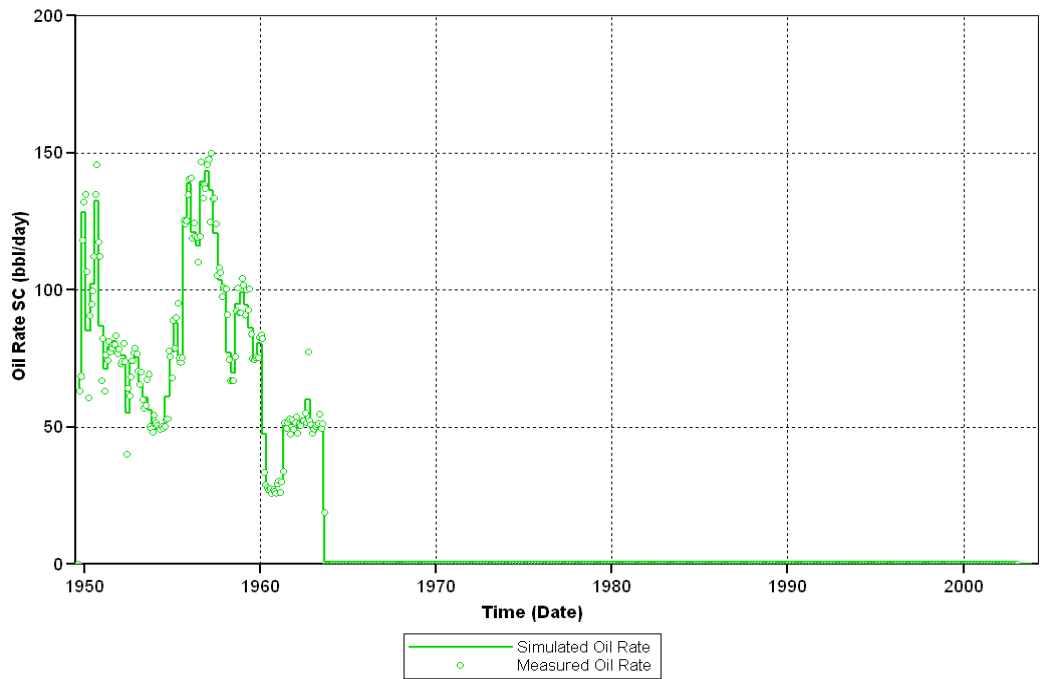


Figure 6.9 - Oil Production History Match, 56-4

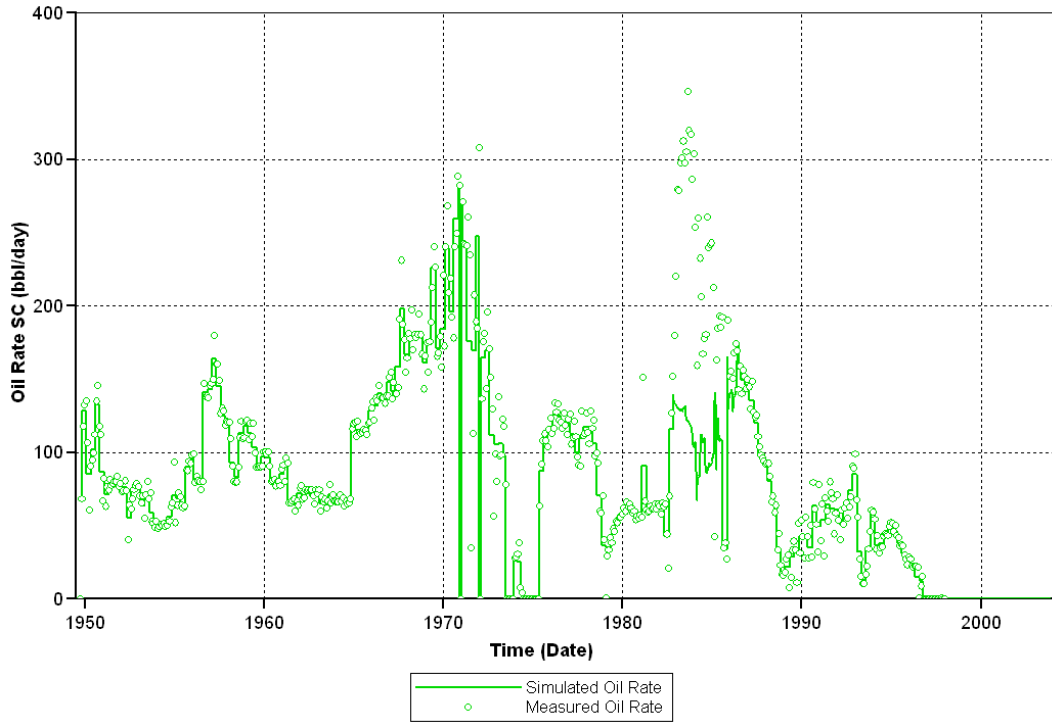


Figure 6.10 - Oil Production History Match, 56-6

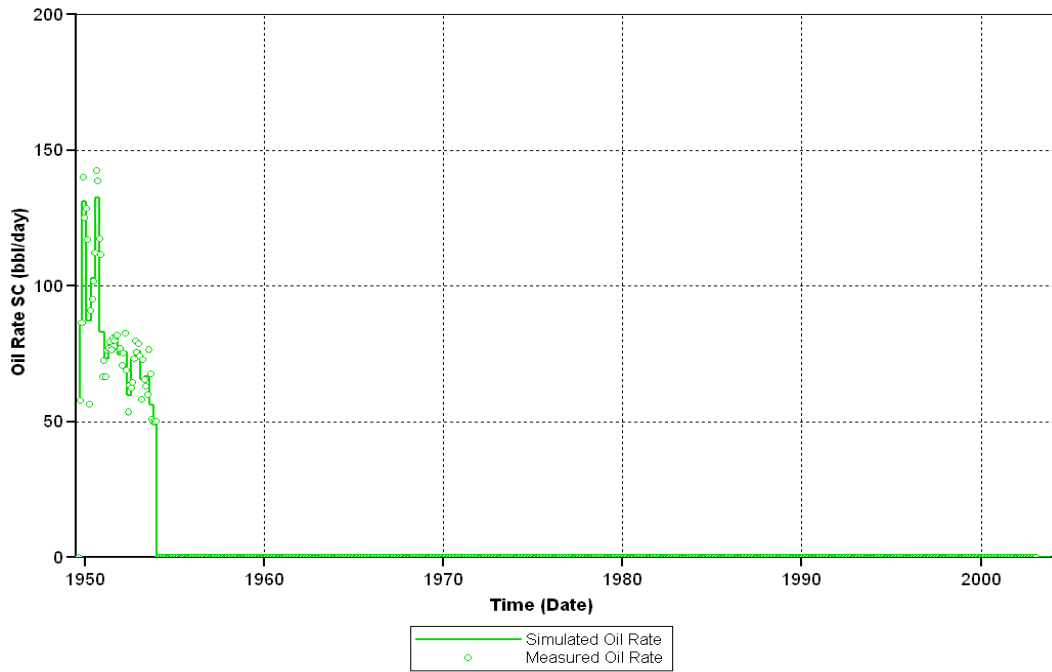


Figure 6.11 - Oil Production History Match, 58-2

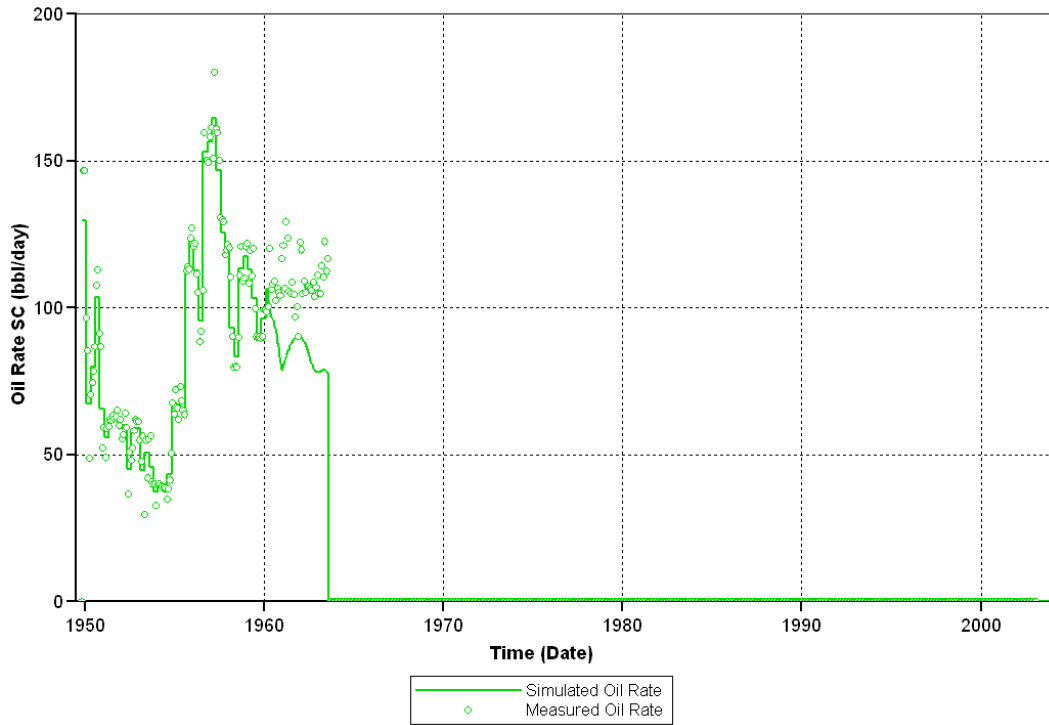


Figure 6.12 - Oil Production History Match, 59-2

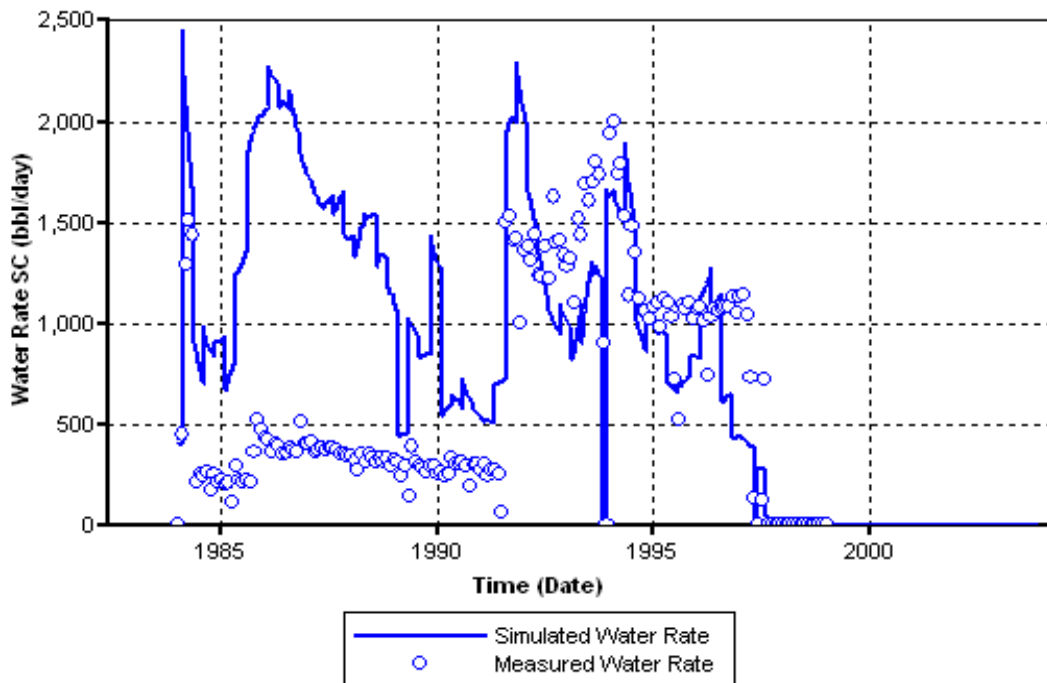


Figure 6.13 - Water Production History Match, 56-17

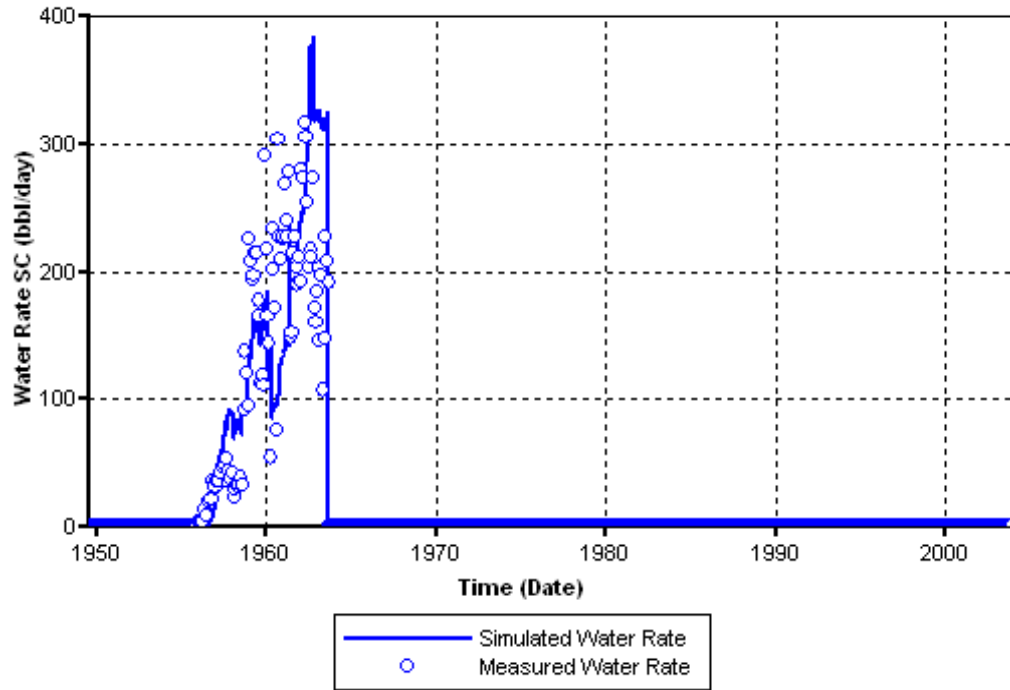


Figure 6.14 - Water Production History Match, 56-4

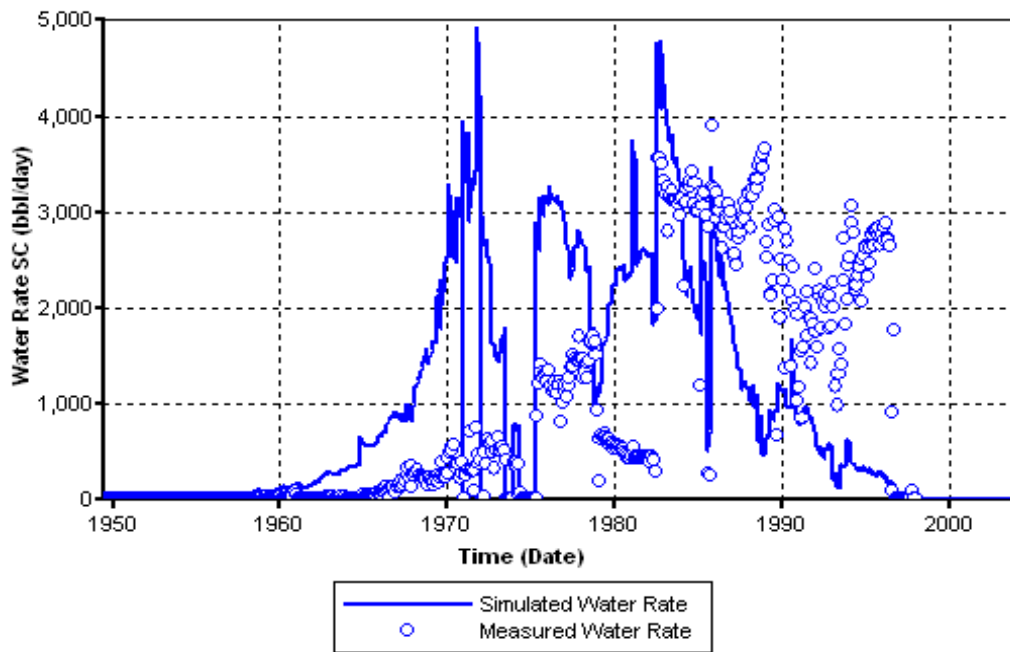


Figure 6.15 - Water Production History Match, 56-6

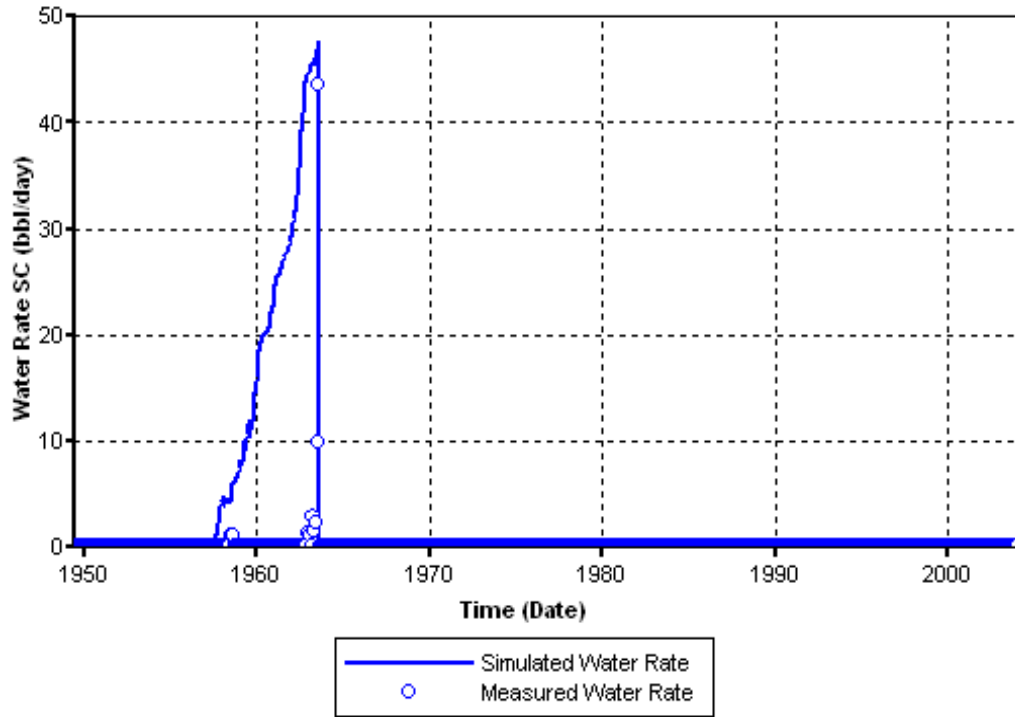


Figure 6.16 - Water Production History Match, 59-2

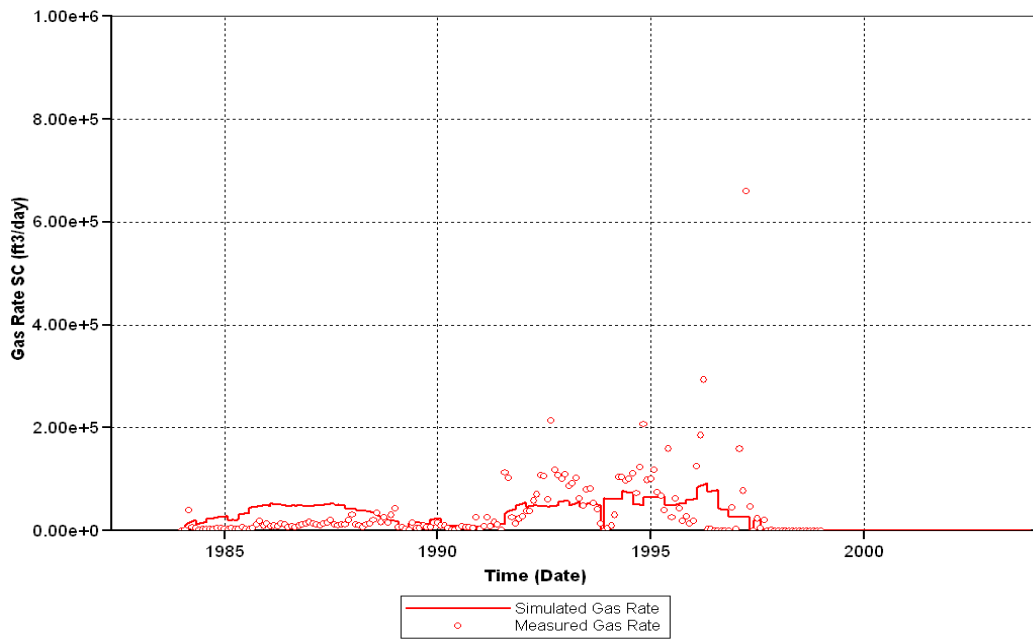


Figure 6.17 - Gas Production History Match, 56-17

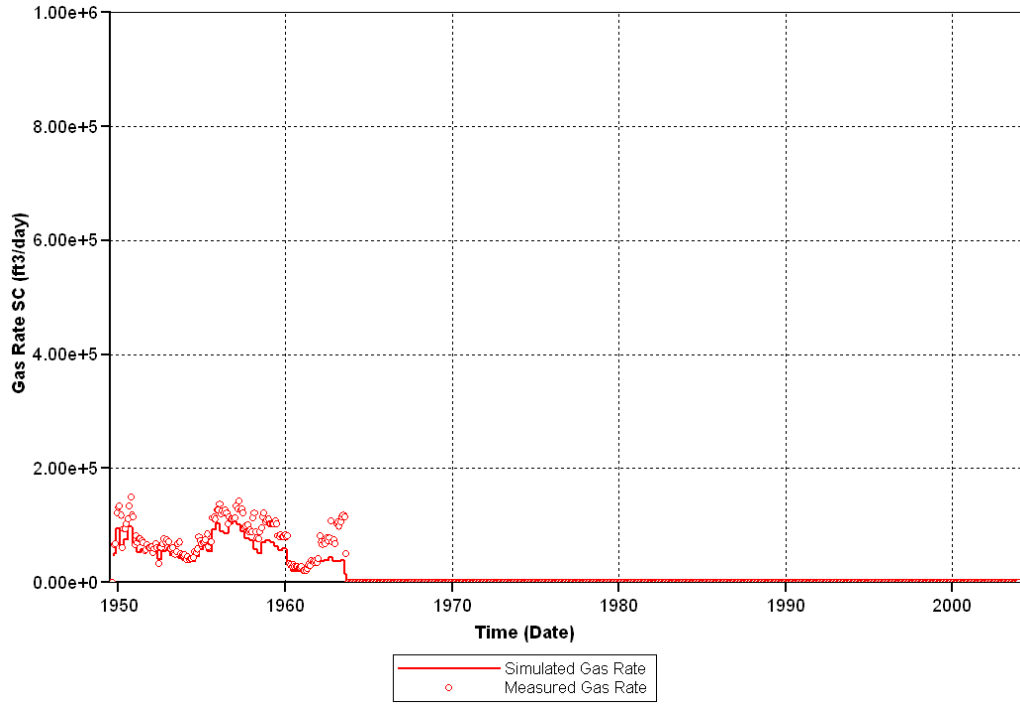


Figure 6.18 - Gas Production History Match, 56-4

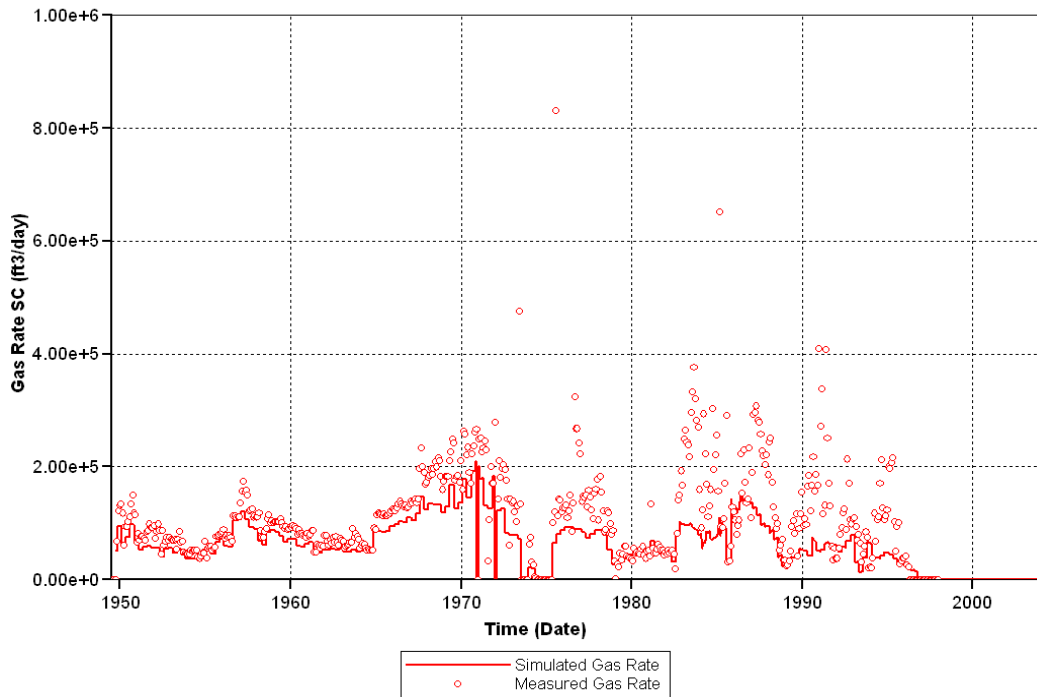


Figure 6.19 - Gas Production History Match, 56-6

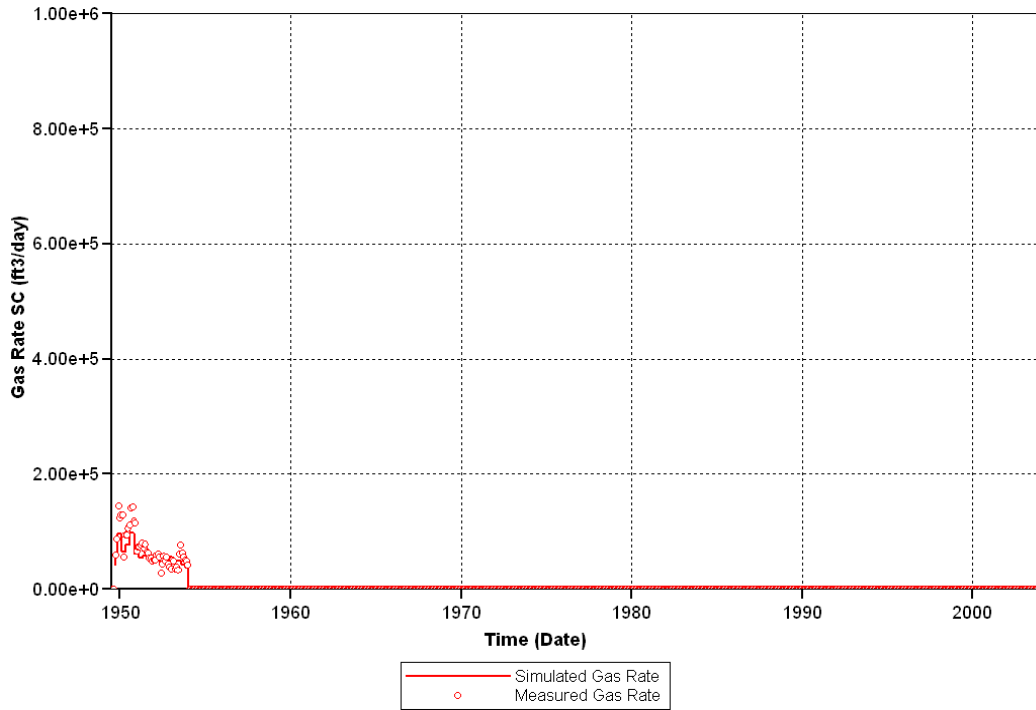


Figure 6.20 - Gas Production History Match, 58-2

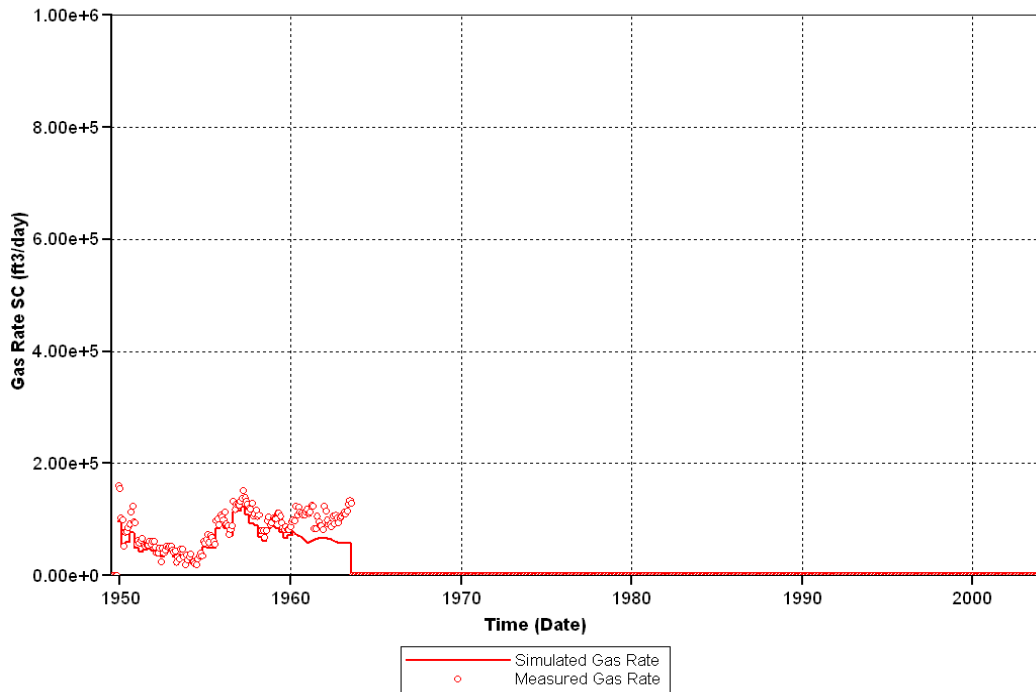


Figure 6.21 - Gas Production History Match, 59-2

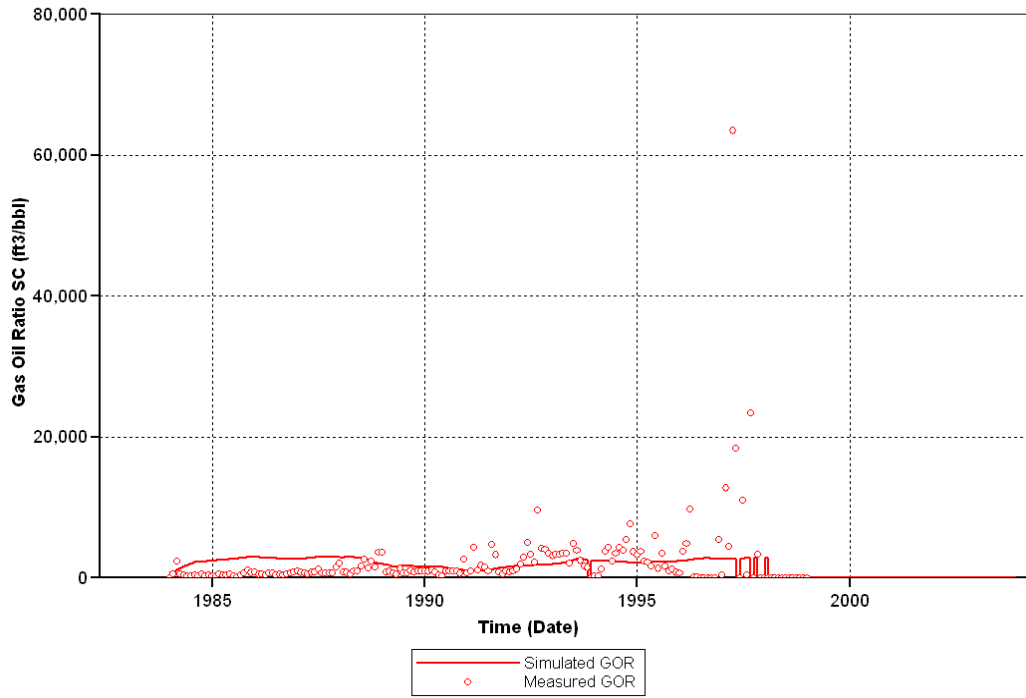


Figure 6.22 - GOR History Match, 56-17

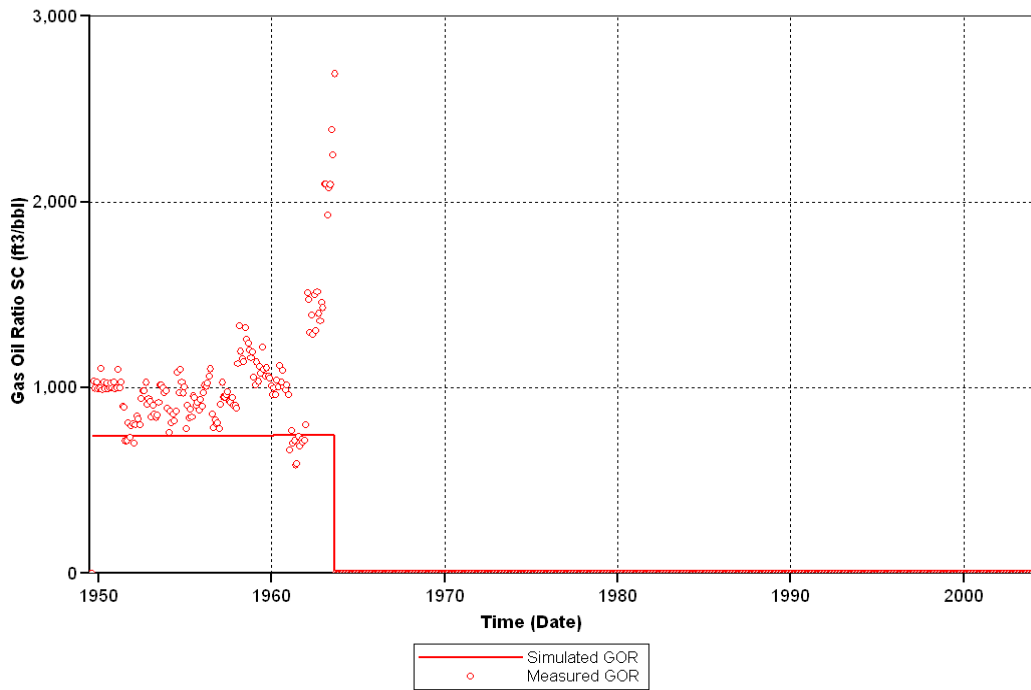


Figure 6.23 - GOR History Match, 56-4

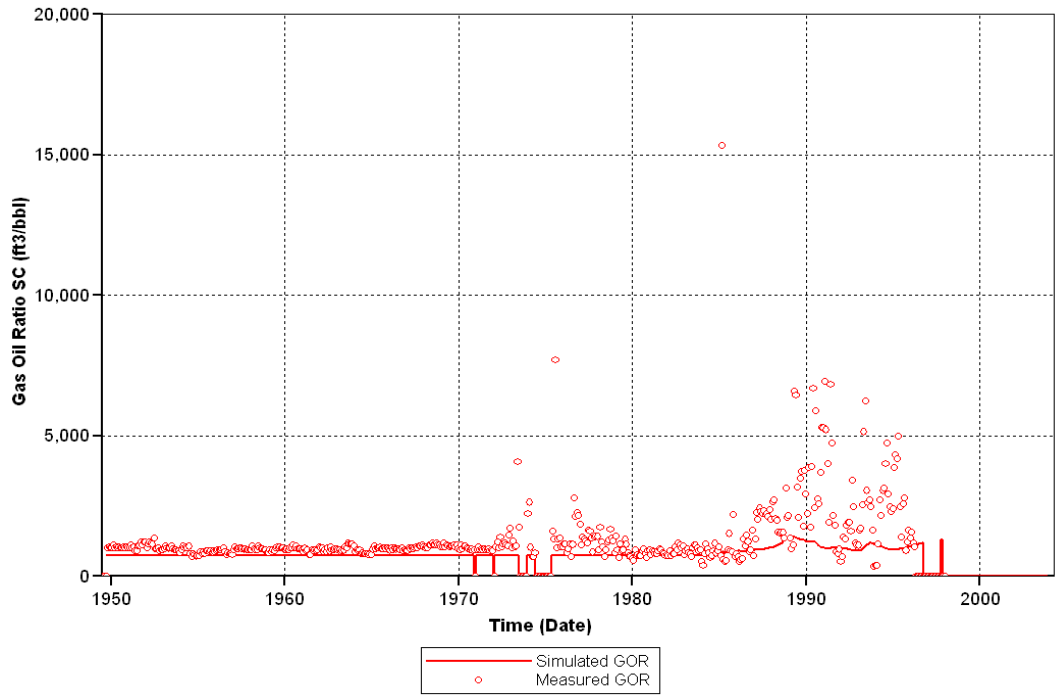


Figure 6.24 - GOR History Match, 56-6

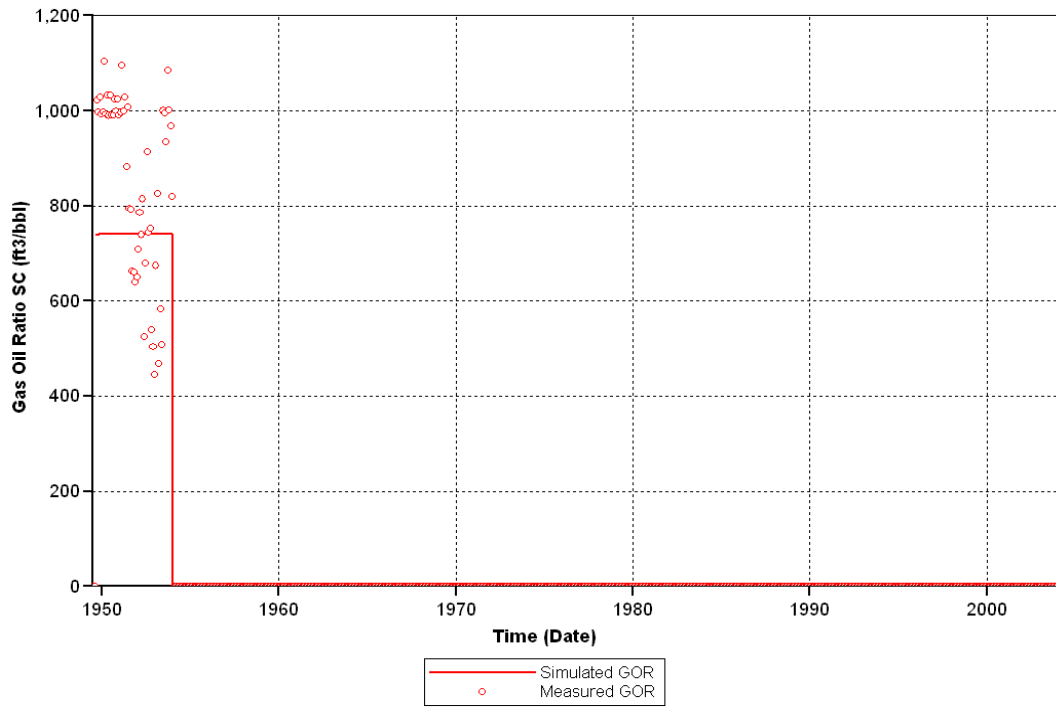


Figure 6.25 - GOR History Match, 58-2

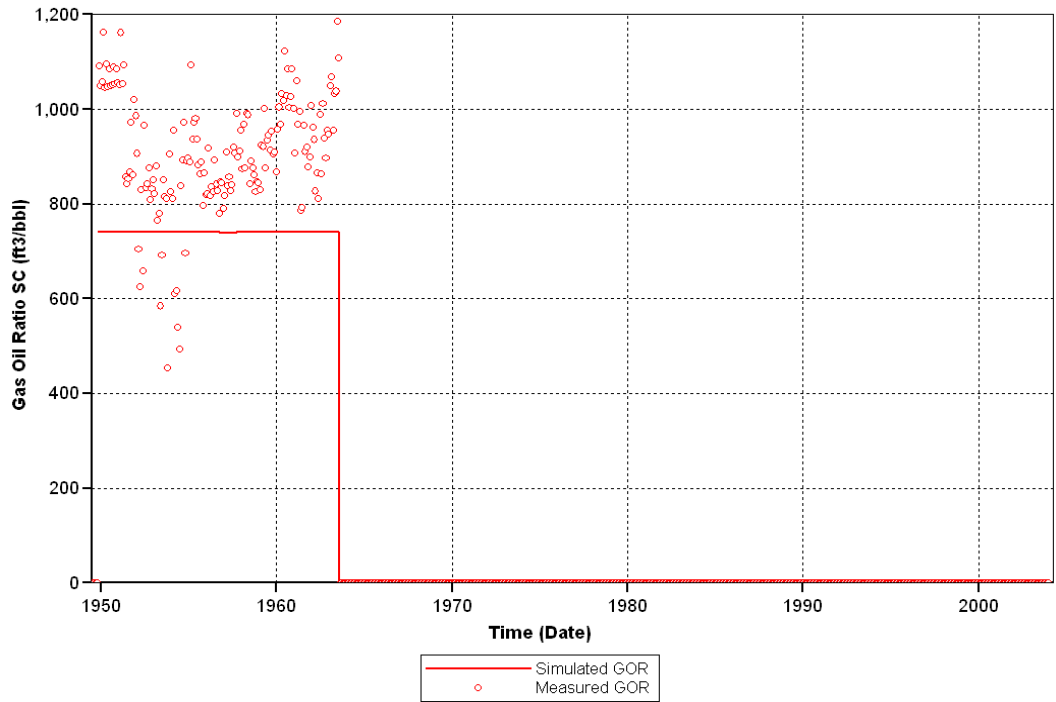


Figure 6.26 - GOR History Match, 59-2

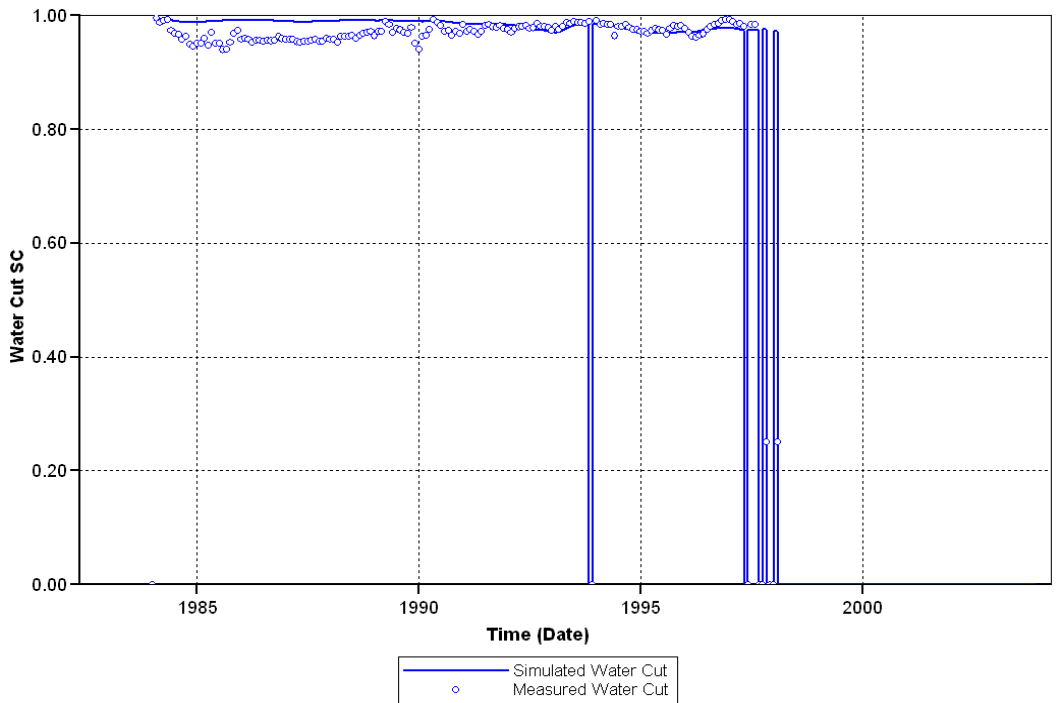


Figure 6.27 - Water Cut History Match, 56-17

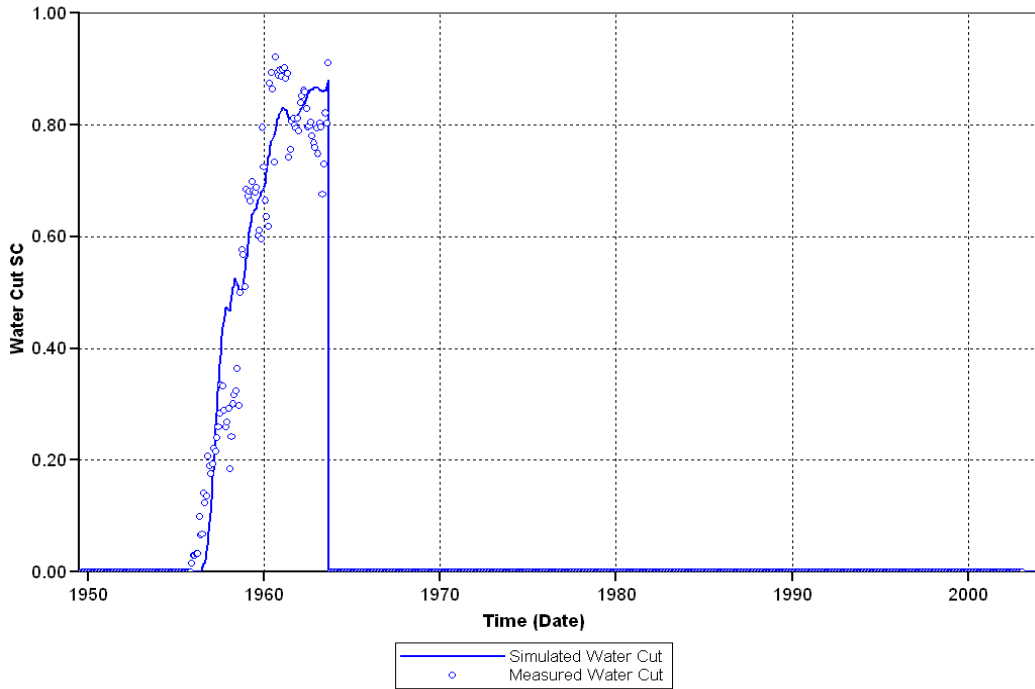


Figure 6.28 - Water Cut History Match, 56-4

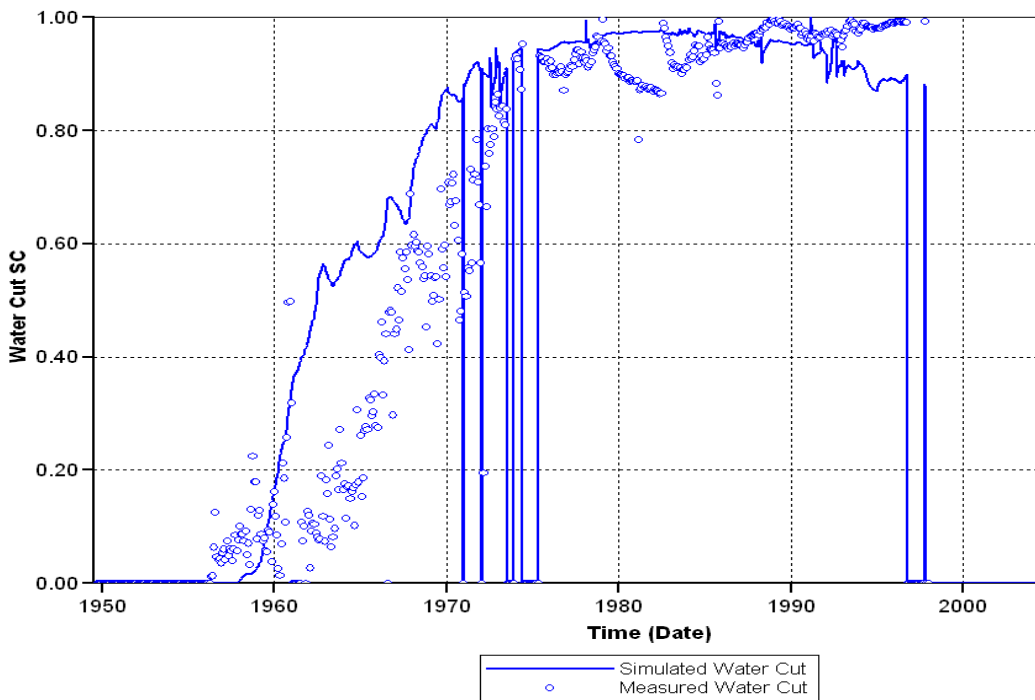


Figure 6.29 - Water Cut History Match, 56-6

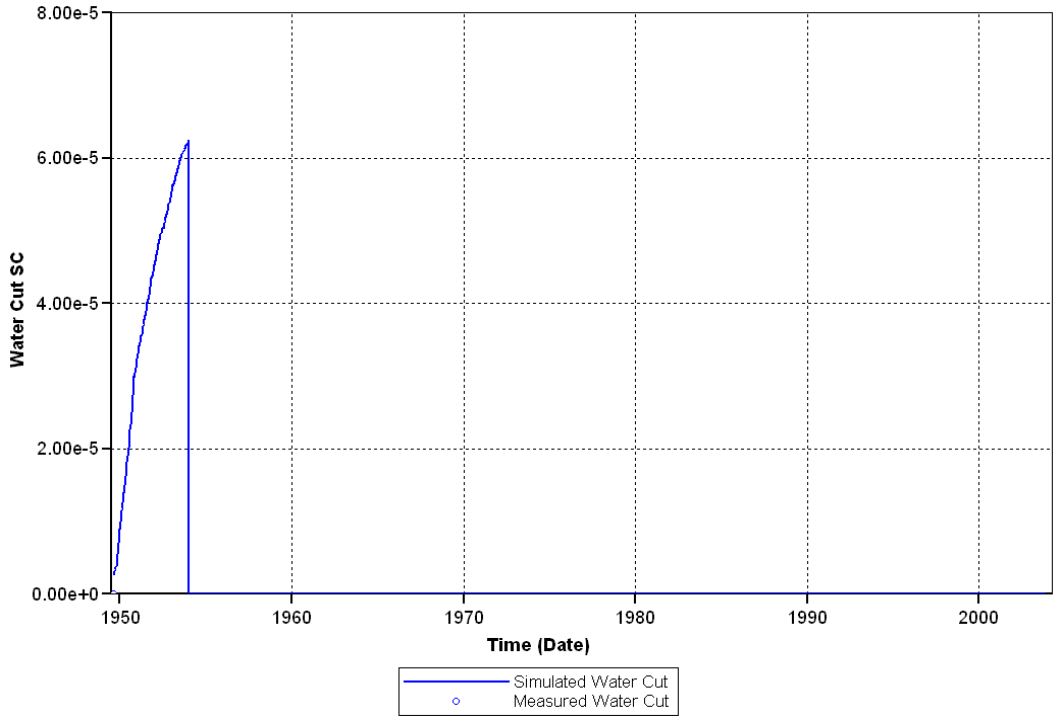


Figure 6.30 - Water Cut History Match, 58-2

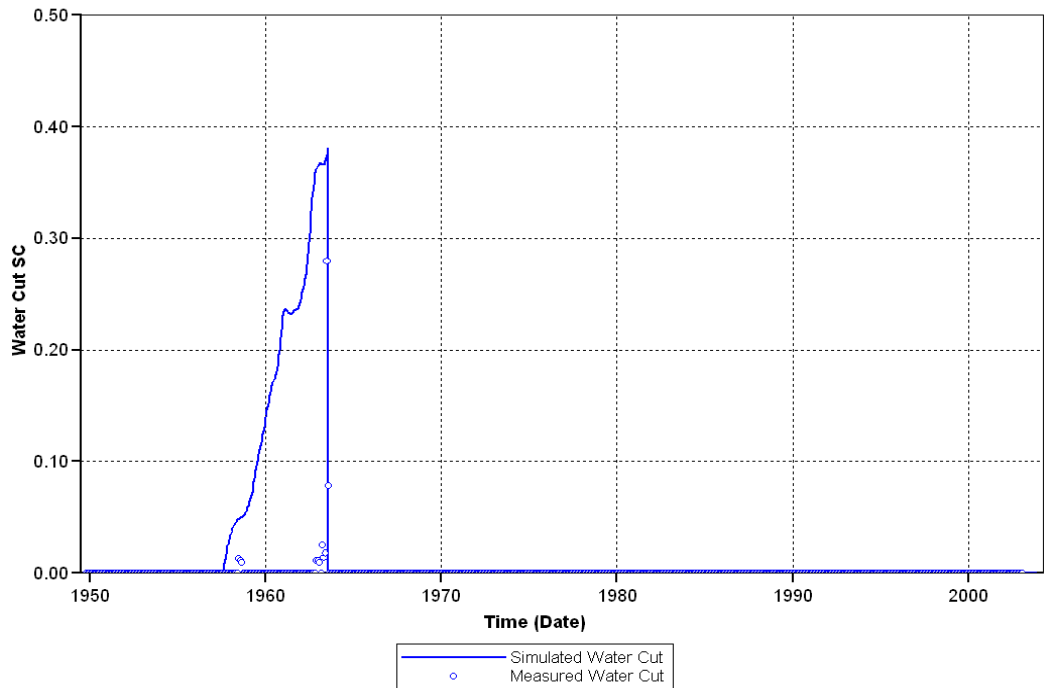


Figure 6.31 - Water Cut History Match, 59-2

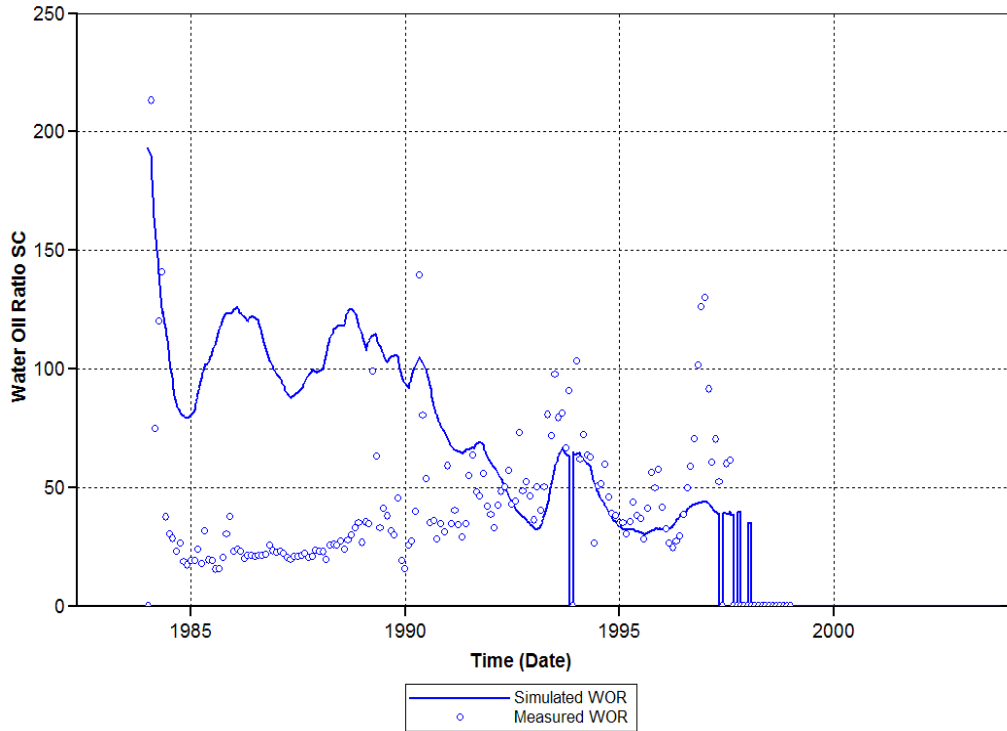


Figure 6.32 - Water-Oil Ratio History Match, 56-17

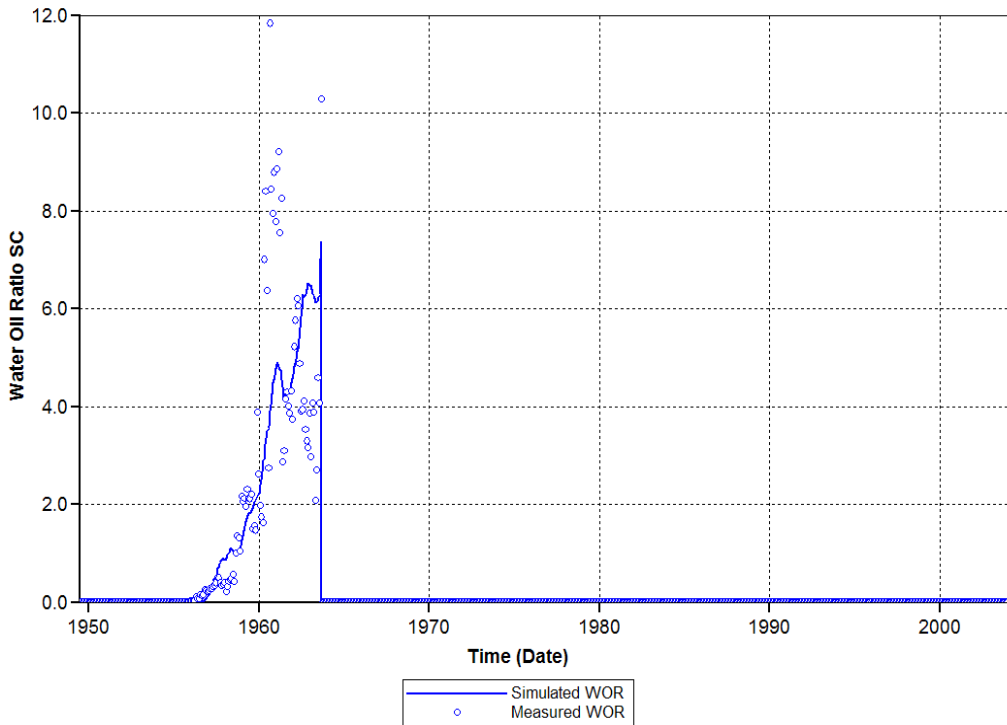


Figure 6.33 - Water-Oil Ratio History Match, 56-4

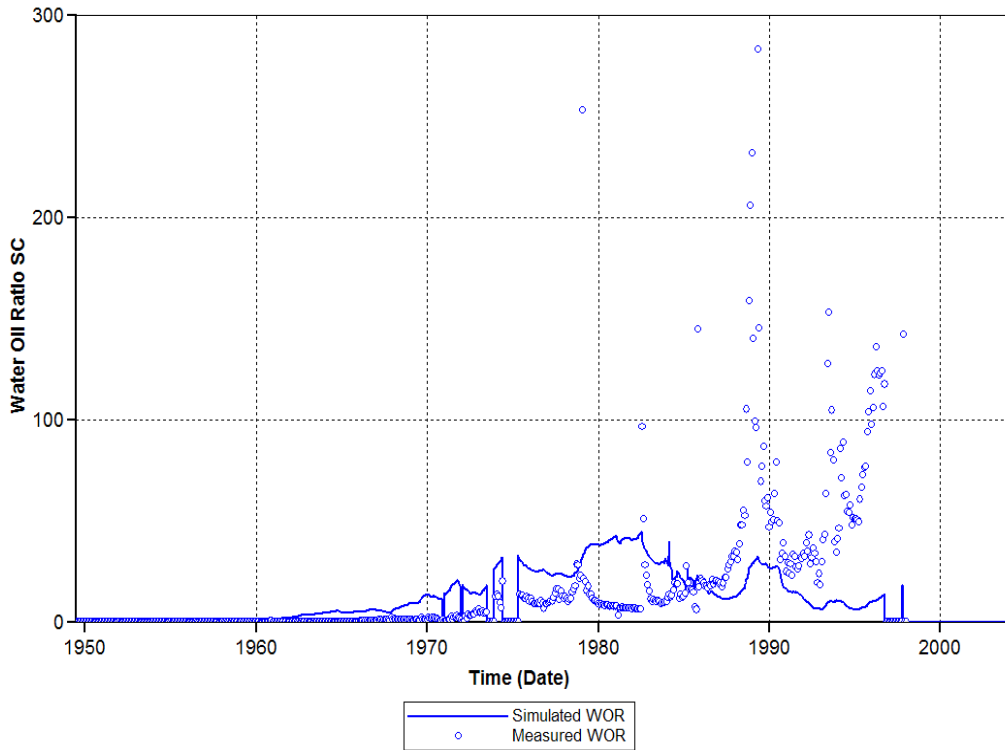


Figure 6.34 - Water-Oil Ratio History Match, 56-6

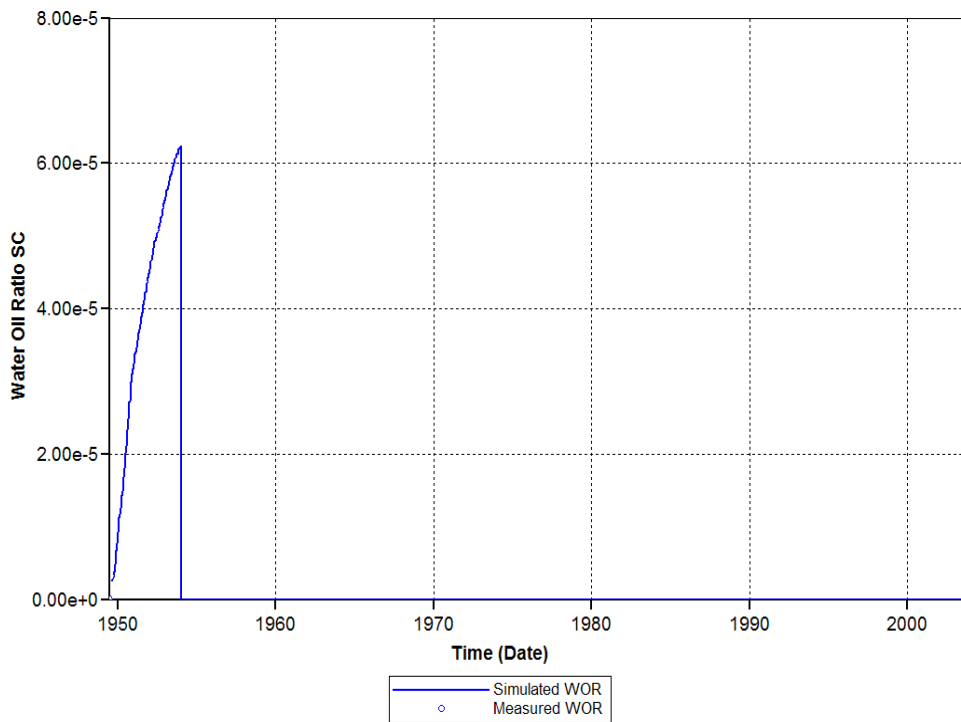


Figure 6.35 - Water-Oil Ratio History Match, 58-2

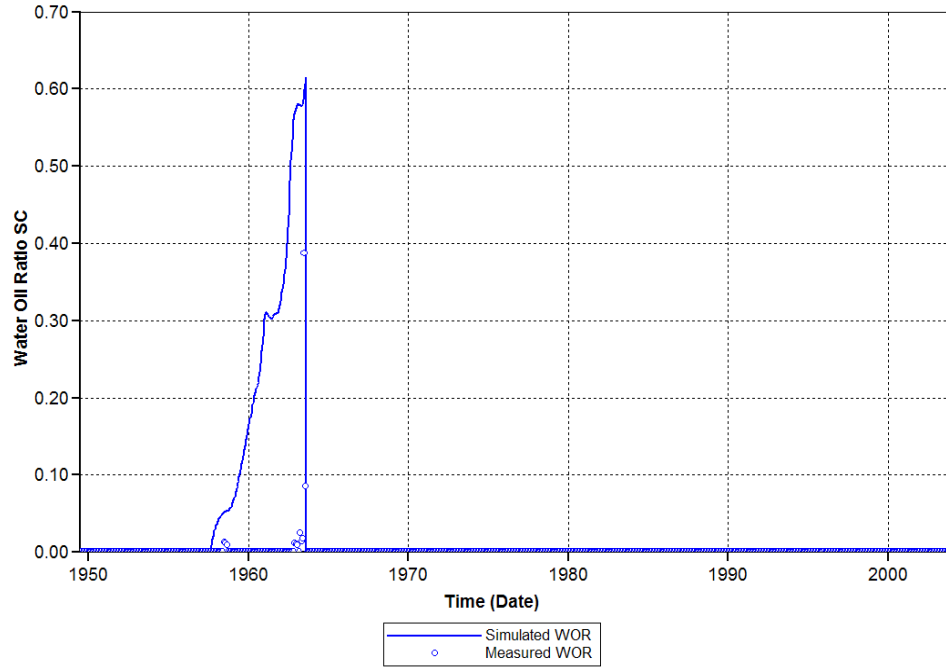


Figure 6.36 - Water-Oil Ratio History Match, 59-2



Figure 6.37 - Reservoir Pressure History Match

Chapter 7: CO₂ FLOOD DESIGN FOR ENHANCED OIL RECOVERY AND CO₂ SEQUESTRATION

7.1 Introduction

Carbon dioxide, CO₂, capture and storage in the deep geological domains is considered to be a practical way to reduce greenhouse gases. Many studies have been performed and several options have been considered to store CO₂ underground. There are many geological domain options for sequestering CO₂ (Han, 2008).

Oil and gas reservoirs have been the main site of CO₂ injection for the purpose of Enhanced Oil Recovery (EOR). Seals in hydrocarbon reservoirs are usually impermeable enough for oil and gas to accumulate and be trapped. Therefore these kinds of reservoirs may prove to be good candidates for storing CO₂ safely. EOR tertiary recovery has proven effective in the oil industry. Injection of CO₂ into deep saline aquifers is another way to store CO₂. However, this method is costly and has associated hazards if injected CO₂ gets into fresh water aquifers.

For the purpose of EOR, wells and processing facilities are also assembled in oil and gas fields to utilize CO₂ injections and on-site storage. Carbon dioxide injection improves oil recovery by reducing the viscosity and density of oil under miscible conditions and enabling it to flow faster. When CO₂ is injected in the reservoir, it contacts oil. Repeated contacts are needed for CO₂ to become totally

miscible and dissolve in oil. After multiple-contacts, the oil-enriched CO₂ rich stream cannot be separated from the CO₂-enriched oil (Jarrell *et al.*, 2002).

In the last decade, oil fields have been considered for performing simultaneous EOR and CO₂ sequestration and both recovering additional oil and sequestration. However, injecting CO₂ for EOR purposes is somewhat different from the projects for both coupled EOR and CO₂ sequestration. Carbon dioxide flooding intended for EOR purposes optimizes the oil recovery by minimizing the volume of CO₂ injected to recover additional oil while the motivation of the injection for sequestration is to expand the CO₂ storage capacity while gaining as much incremental production as possible. Carbon dioxide is considered sequestered only if the injected CO₂ remains contained in the reservoir for significant period of times.

The objective of this research study is to quantify how much additional oil can be recovered while sequestering maximum amount of CO₂ in the oil reservoir. Various well parameters and constraints are considered to study the sensitivity of oil recovery and CO₂ storage.

7.2 CO₂ Flood Design Optimization

A pilot test area model was extracted from the 9 million grid elements of the entire northern platform of SACROC and was established for the preliminary CO₂ flood simulation studies. Its reservoir properties were described and modeled with core data, well logs, stratigraphic interpretation, and seismic data.

Simulation of initial water injection was established for CO₂ flooding and different schemes of CO₂ flooding were performed to determine the best scheme for maximized oil production and CO₂ storage before CO₂ flooding. Water was injected using all four injectors for one whole month and then were terminated. Continuous CO₂ injection started from the time water injection simulation was terminated. To quantify the amount of incremental oil recovery and CO₂ stored, 11 simulation runs were performed. The input well constraints are listed in Table 7.1.

Table 7.1- Description of Input Well Constraints for Simulation Cases

Simulation Run		Input well constraints					
		CO ₂ injection			Oil production		
		Type	max rate	max inj press	(pwf) min	min oil rate	max GOR
			mmscfd	psia		bopd	scf/bbl
Case 1	Scenario 1	continuous	100	5700	Y	50	
Case 1	Scenario 1	continuous	50	5700	Y	50	
Case 1	Scenario 1	continuous	20	5700	Y	50	
Case 1	Scenario 2	WAG	100	5700	Y	50	
Case 1	Scenario 2	WAG	50	5700	Y	50	
Case 1	Scenario 2	WAG	20	5700	Y	50	
Case 2		continuous	5	5700	Y		10000
Case 2		continuous	5	5700	Y		50000
Case 2		continuous	5	5700	Y		100000
Case 3		continuous	5	5700	Y	5	
Case 4		continuous	5	5700	Y	none	

7.3. Case 1: High Injection Rates

In scenario 1 of Case 1, the producer was constrained with a minimum bottomhole pressure and CO₂ was injected continuously (Table 7.1). The injectors

were shut-in when the high, medium and low CO₂ injection rates, 25 MM, 50 MM, and 100 MMscf/day, were reached at the injectors, 56-4, 56-6, 58-2 and 59-2. Scenario 2 focuses on WAG operations. Like scenario 1, different values of CO₂ injection rates were set to determine when CO₂ and water injectors would operate until producers exhibit high water-oil ratios (WOR). Both CO₂ and water injectors were constrained with the maximum parting pressure of 5700 psi. In both scenarios, the producers operate until the reservoir is depleted. However, in both scenarios in Case 1, the oil production rates at the producers were monitored and were shut-in only if the oil rate fell below 50 stb/day. CO₂ injections continued with the above specified injection rates. When parting pressures were reached in this case, the constraints at injectors were converted to pressure controlled. The simulation runs in Case 1 resulted in unrealistic levels in the amount of CO₂ being injected. In the scenario with 25 MMscf/day of continuous CO₂ injection, by end of the CO₂ flood, an additional 6.3 % of OIP was recovered, only 8.9 % of total injected CO₂ was stored, 128 Mscf of CO₂ was injected per barrel of oil produced while 11.4 Mscf of CO₂ was sequestered per each barrel of oil produced. Figure 7.1 indicates incremental cumulative oil recovery of about 4.2, 4.2, and 7.4 MMstb for runs with 100, 50, and 25 MMscf/day injection rates respectively; the cumulative oil production after the history matching was 27.6 MMstb which resulted from all wells in the reservoir model.

Results from Figure 7.1 to 7.3 suggest that injecting 25 MMscf/day helped sweep the reservoir effectively and store higher amounts of CO₂ for each barrel of oil produced. It is also important to note the cumulative CO₂ sequestered in the

first 50 to 100 years of the simulation determined by the difference in the cumulative CO₂ production to the cumulative CO₂ injection (Figure 7.3). However, from the EOR point of view, after 52 years of CO₂ flooding, incremental oil recovery of 5.9 % was achieved in the simulation run with the injection rate of 100 MMscf/day but was slightly less than the case (25 MMscf/day) (Table 7.2).

Table 7.2- Simulation results of injection and production (Scenario 1, Case 1)

Run/Different Scenarios	100 MMscf/D	50 MMscf/D	25 MMscf/D
Cum. Incremental Oil Recovery, MMstb	4.40	4.20	7.40
% OIP	5.90	5.71	6.30
Cum. CO ₂ Injected, MMscf (Tonne)	1220000.00 (2.84×10^{10})	661000.00 (1.54×10^{10})	947000.00 (2.22×10^{10})
CO ₂ Flood Duration, years	52.00	134.00	150.00
CO ₂ Sequestered, MMscf (Tonne)	71700.00 (1.66×10^9)	58700.00 (1.36×10^9)	84200.00 (1.96×10^9)
% of CO ₂ Sequestered	5.88	8.88	8.89
CO ₂ Injected per Barrel of Oil Produced, Mscf/stb (Tonne/stb)	277.27 (6.44×10^3)	157.38 (3.66×10^3)	127.97 (2.98×10^3)
CO ₂ Sequestered per Barrel of Oil Produced, Mscf/stb (Tonne/stb)	16.30 (3.80×10^2)	13.98 (3.26×10^2)	11.38 (2.65×10^2)

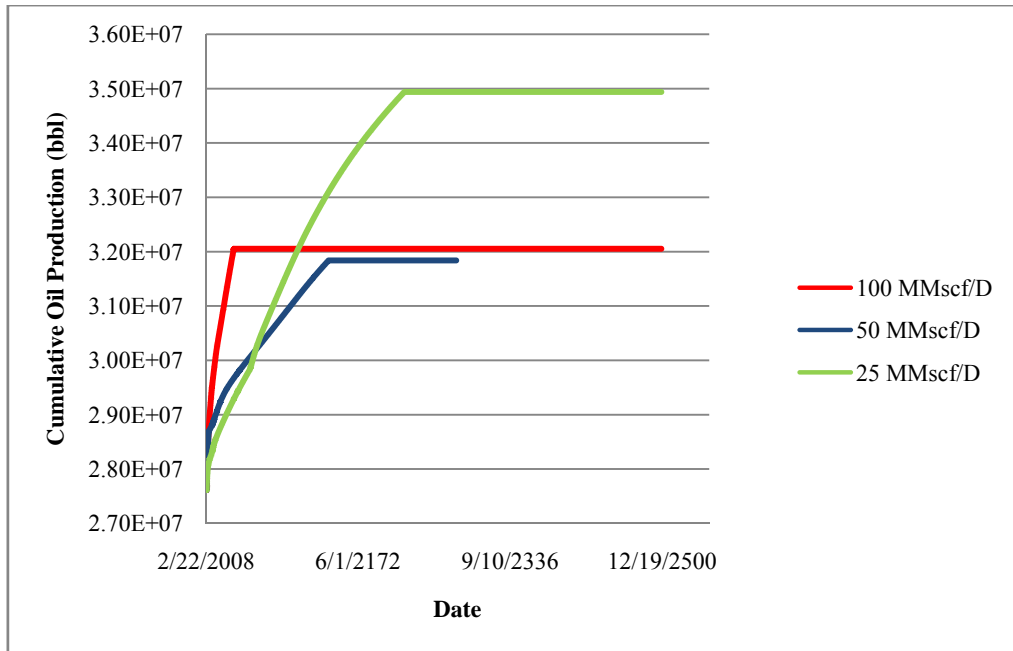


Figure 7.1 - Cumulative Oil Production (Scenario 1, Case 1)

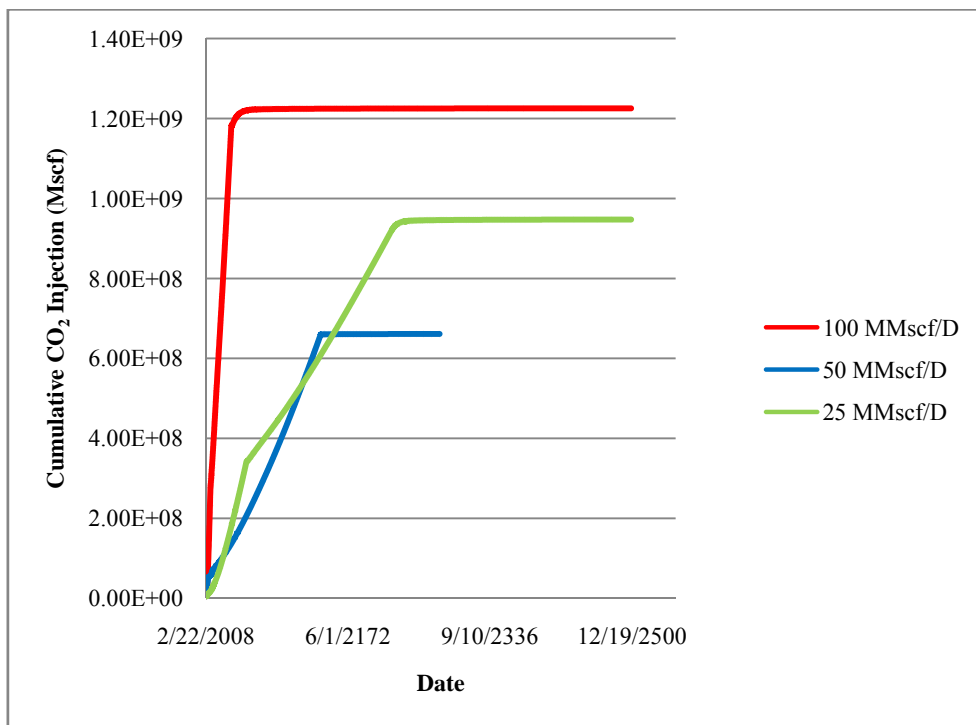


Figure 7.2- Cumulative CO₂ Injection (Scenario 1, Case 1)

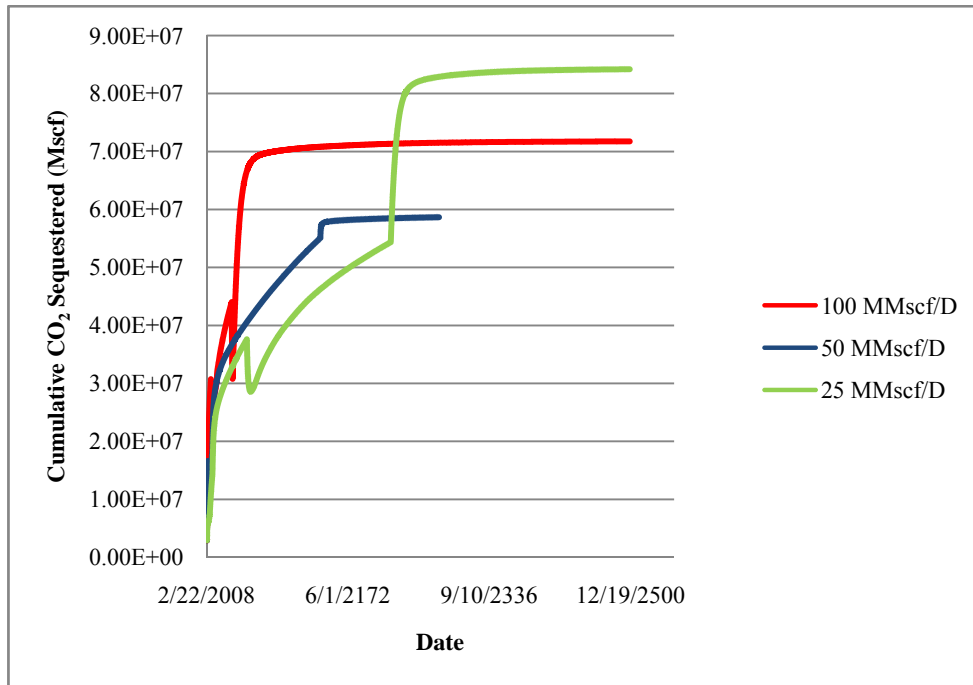


Figure 7.3- Cumulative CO₂ Sequestered (Scenario 1, Case 1)

In scenario 2 of case 1, a WAG operation was applied with the injection rate of 100 MMscf/day. By the end of the CO₂ flood, the oil recovery was highest at 13.5% OIP taking 212 years when only 5 % of total injected CO₂ was stored. However, Table 7.3 indicates that injecting CO₂ with the rates of 50 MMscf/day yielded a much higher percentage of CO₂ stored within 27 years although oil recovery was significantly less compared to the case with 100 MMscf/day. Table 7.3 summarizes the results for all the simulations in scenario 2 of Case 1 and shows that oil production responded well to CO₂ injection and it took 27 years to produce 2.3 % of OOIP.

Table 7.3- Simulation results of injection and production (Scenario 2, Case 1)

Run/Different Scenarios	100 MMSCF/D	50 MMSCF/D	25 MMSCF/D
Cum. Incremental Oil Recovery, MMstb	9.98	1.69	4.40
% OIP	13.50	2.30	5.60
Cum. CO ₂ Injected, MMscf (Tonne)	1210000.00 (2.84×10^{10})	65800.00 (1.53×10^9)	48400.00 (1.12×10^9)
CO ₂ Flood Duration, years	212.00	27.00	104.00
CO ₂ Sequestered, MMscf (Tonne)	58000.00 (1.35×10^9)	17600.00 (4.10×10^8)	9900.00 (2.30×10^8)
% of CO ₂ Sequestered	4.79	26.75	20.45
CO ₂ Injected per Barrel of Oil Produced, Mscf/stb (Tonne/stb)	121.24 (2.82×10^3)	38.93 (9.07×10^2)	11.00 (2.56×10^2)
CO ₂ Sequestered per Barrel of Oil Produced, Mscf/stb (Tonne/stb)	5.81 (1.35×10^2)	10.41 (2.42×10^2)	2.25 (5.24×10^1)

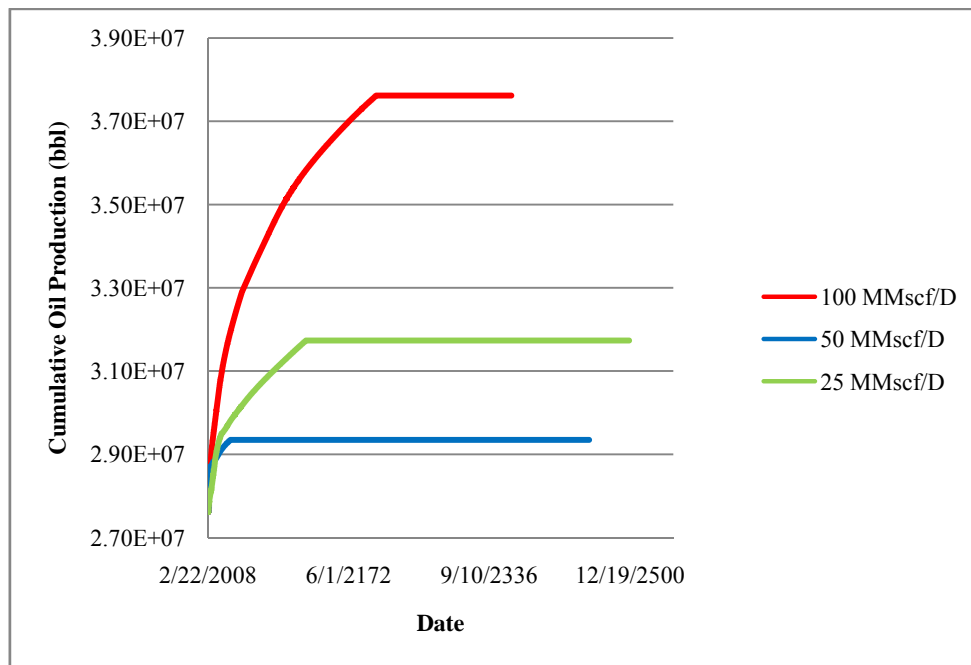


Figure 7.4- Cumulative Oil Production (Scenario 2, Case 1)

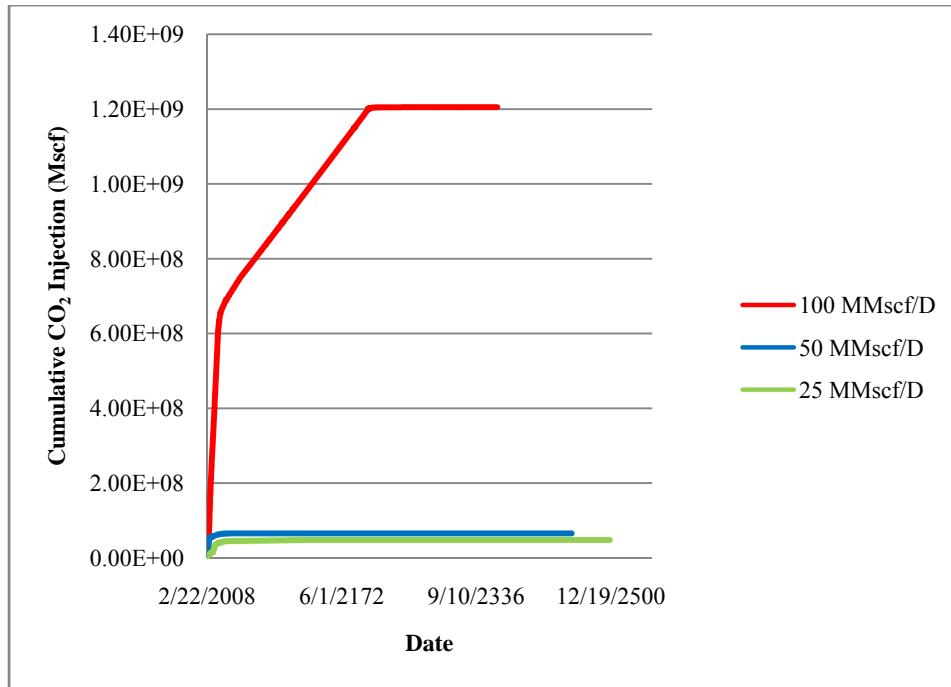


Figure 7.5- Cumulative CO₂ Injection (Scenario 2, Case 1)

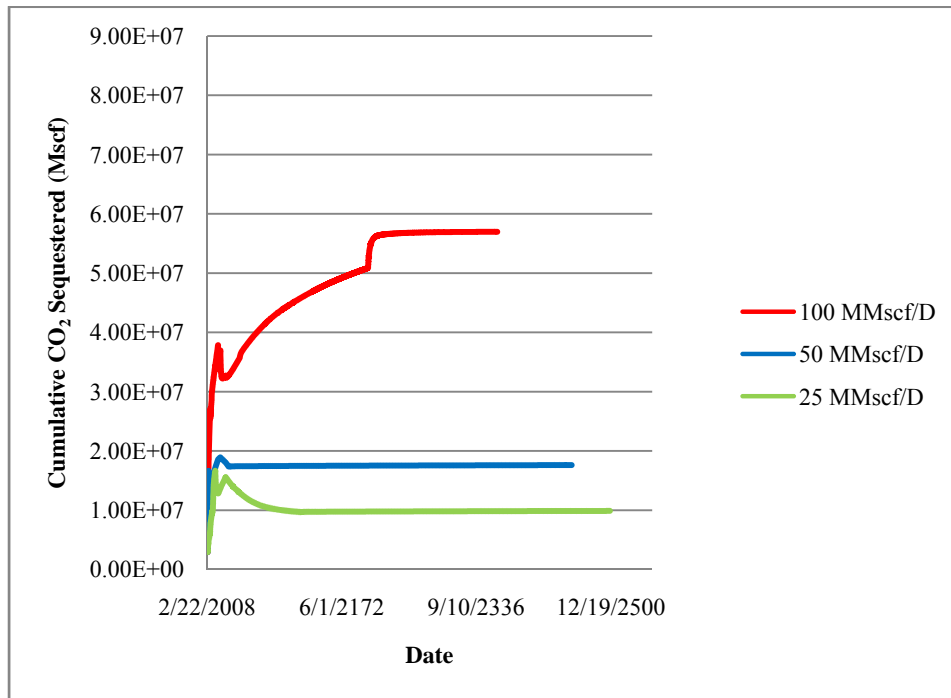


Figure 7.6- Cumulative CO₂ Sequestered (Scenario 2, Case 1)

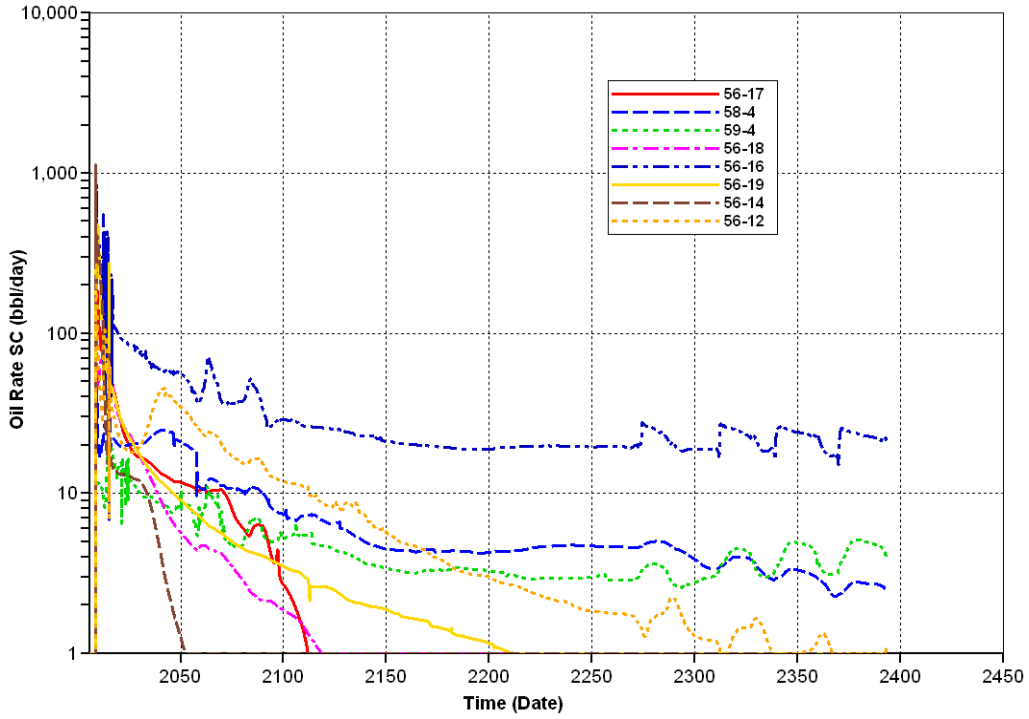


Figure 7.7- Oil Production Rate (Scenario 2, Case 1: 100 MMscf/day)

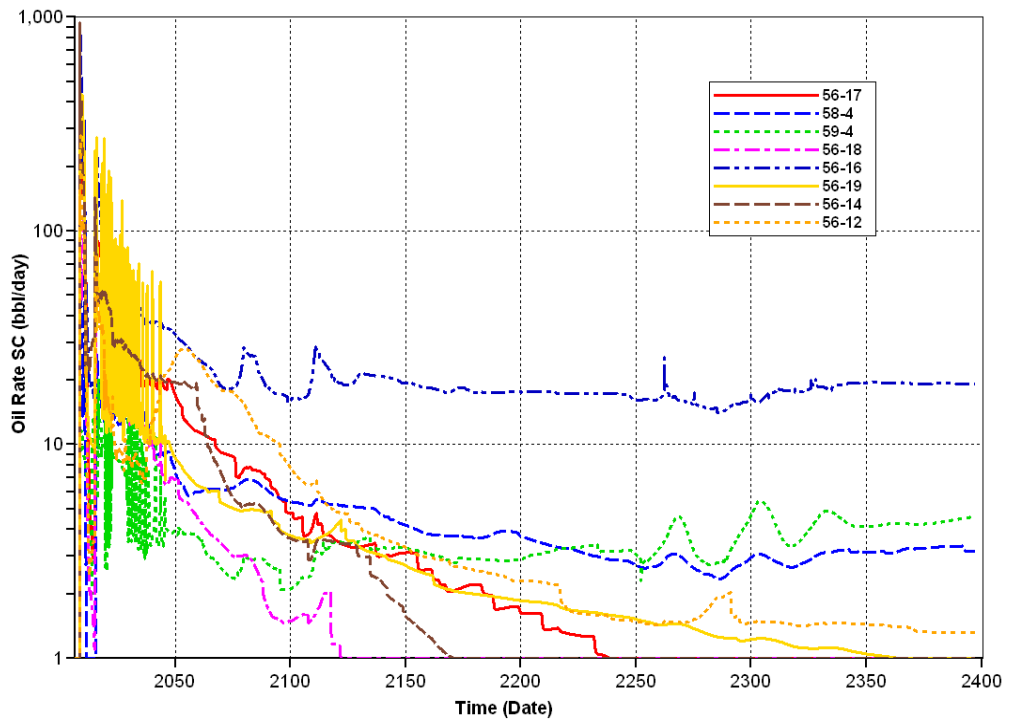


Figure 7.8- Oil Production Rate (Scenario 2, Case 1: 50 MMscf/day)

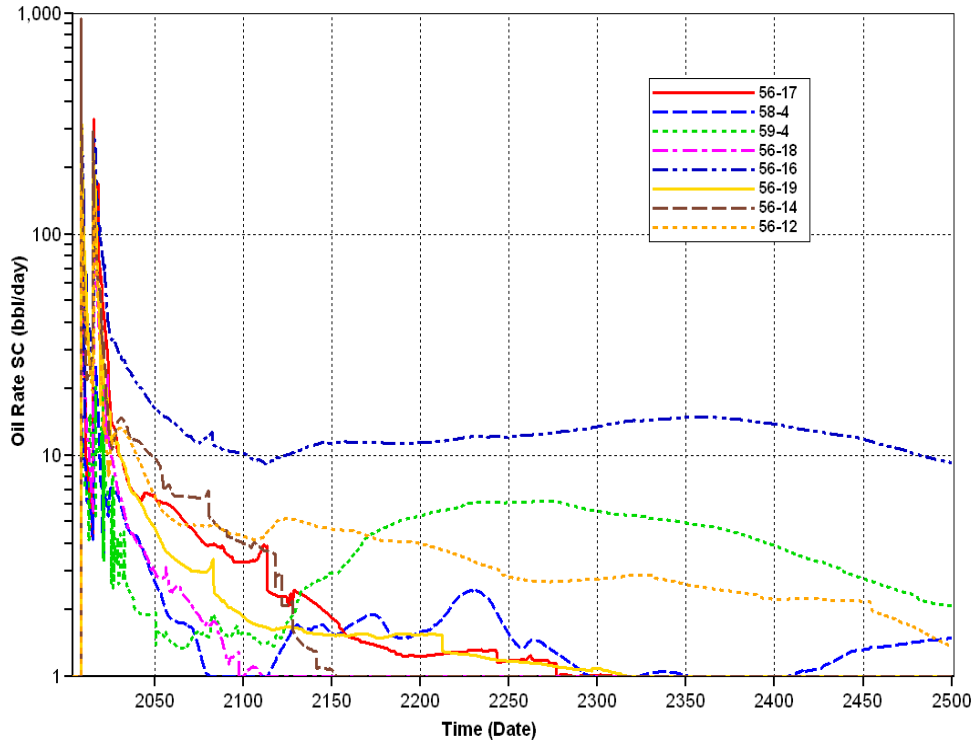


Figure 7.9- Oil Production Rate (Scenario 2, Case 1: 25 MMscf/day)

Figures 7.7 to 7.9 show that oil production continued for a long period of time. This is an indication of how much incremental oil could be recovered if all producers were kept open and no economic consideration was made for all simulation runs. After a predictive simulation was done, a detailed review of CO₂ production from producers indicates that CO₂ breakthrough is within 4 to 5 months in both scenarios of Case 1. In scenario 1 (continuous CO₂ injection), the oil recovery is much higher than Scenario 2 even though the break through time is similar. A slight difference in the peak oil rate for both scenarios was observed. Scenario 2 tends to predict similar oil production rates in a tertiary decline while scenario 1 allows more CO₂ injected in the reservoir and sees some more response of CO₂ injection later in the flood resulting in increased cumulative oil recovery.

Since simulations were run up to 500 calendar years, some plots were shortened or presented in the Appendix.

To determine the optimum oil recovery and amount of CO₂ sequestered, the effect of CO₂ flood design factors in injection processes were simulated and analyzed. Some of the major factors include: produced gas-oil ratio (GOR), constraint for injectors and producers, and WAG or continuous CO₂ injection. As there are many reservoir engineering design variables, efforts were made to select and simulate the most important key design factors.

Case 2: GOR Constraints at Producers

After reviewing the results of the Case 1 scenarios, a new approach, Case 2, was designed. The first scenario using continuous CO₂ injection was simulated and studied. At producers, cutoff GOR values of 10000, 50000, and 100000 scf/bbl were set and monitored (Table 7.1). The injectors were constrained by the parting pressure of 5700 psi and were capped with the maximum CO₂ injection rates of 5 MMscf/day (Table 7.1). Figures 7.10 to 7.12 indicate that some oil producers were shut-in early in the simulation. As a result, production at near-by wells benefited from the shut-in producers indicating a high level of inter-well communication. In all runs with GOR limits, all producers were shut-in by the beginning of 2020 except 59-4. No economics analysis was done in this research project, however; one must determine which GOR constraint to use during CO₂ flood to be able to maximize the oil production while storing maximum amount of CO₂ possible. Figures 7.10 to 7.12 indicate that some wells were shut-in while

producing oil at high daily rates. Therefore, shutting wells that were not producing at lower rates will certainly be beneficial to the oil production at other open producers.

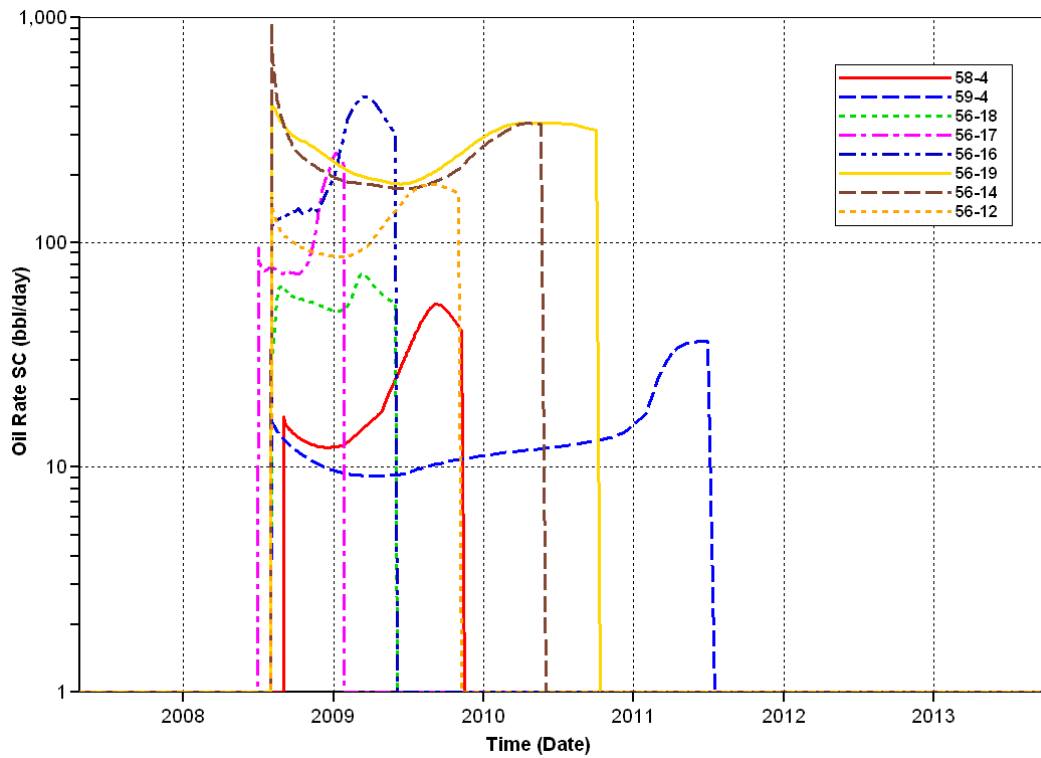


Figure 7.10- Oil Production Rate (Case 2: GOR Constraints 10000 scf/bbl)

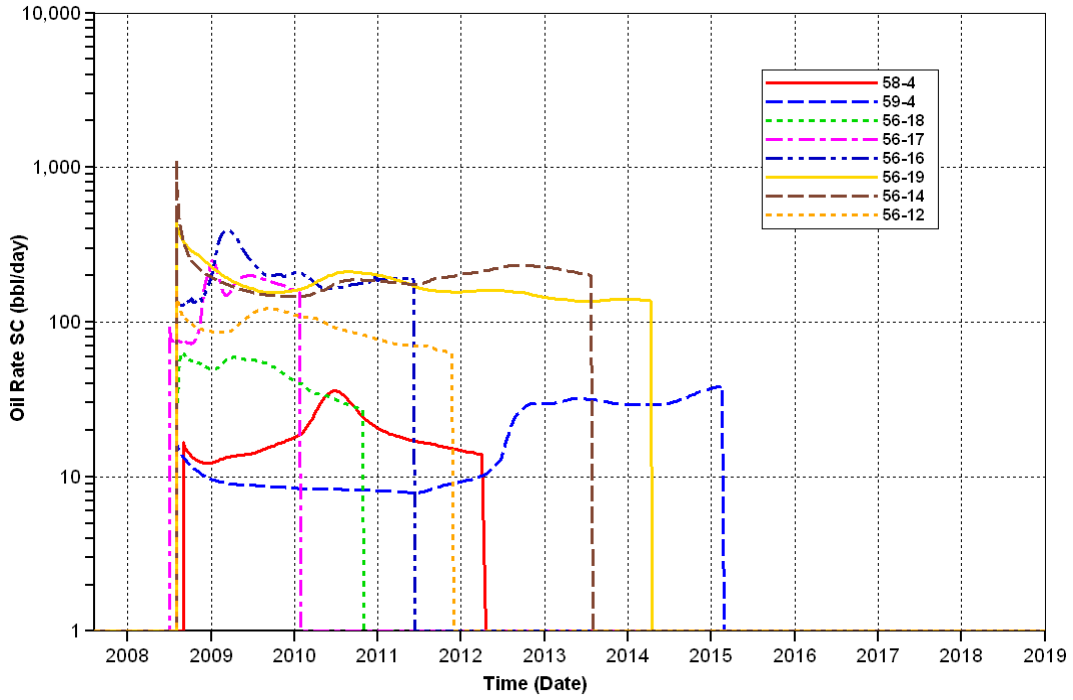


Figure 7.11- Oil Production Rate (Case 2: GOR Constraints 50000 scf/bbl)

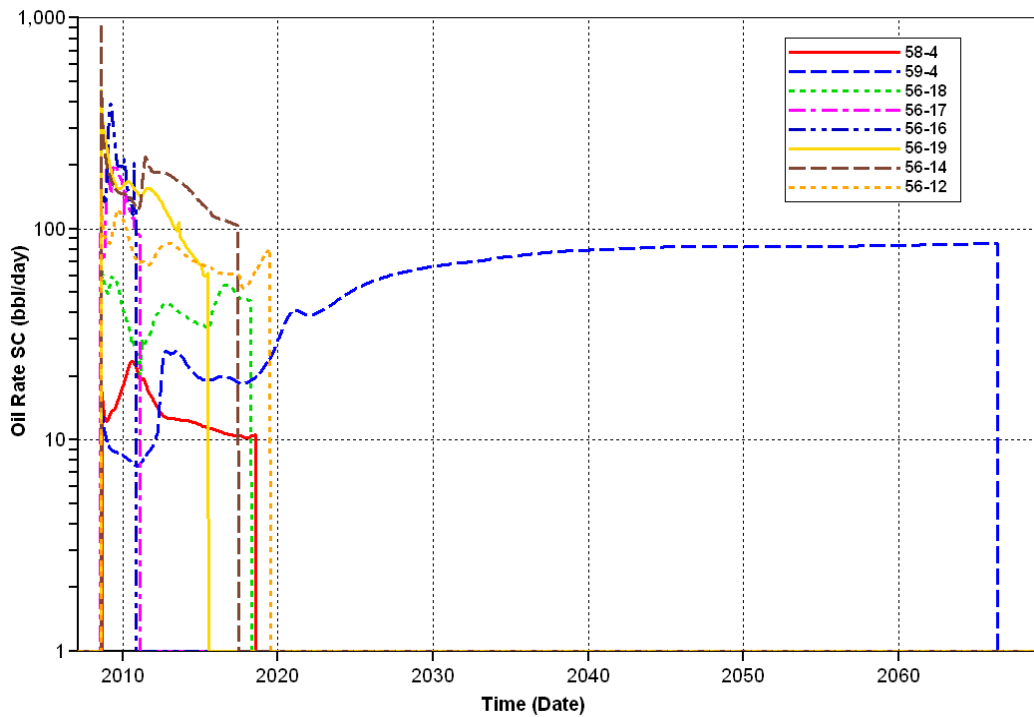


Figure 7.12- Oil Production Rate (Case 2: GOR Constraints 100,000 scf/bbl)

Table 7.4 shows that if producers were kept open for longer period (GOR 100,000 scf/bbl scenario), oil recovery was highest at 4.0% of OIP in Case 2 but only 27.58 % of injected CO₂ was sequestered. On the other hand, applying lower GOR constraint at producers provided less recovery and highest amount of CO₂ stored. In this scenario, an interesting observation can be made that the storage capacity was highest at 93.67 % with the lowest cumulative volume of CO₂ injected if the lowest GOR control of 10,000 scf/bbl was considered. Figures 7.13 to 7.15 also indicates that more oil was produced and higher amount of CO₂ was injected per each barrel of oil produced if producers were kept open longer with the high GOR constraints of 100,000 scf/bbl.

Table 7.4- Simulation results of injection and production (Case 2)

Run/Different Scenarios	10,000 scf/bbl	50,000 scf/bbl	100,000 scf/bbl
Cum. Incremental Oil Recovery, MMstb	0.60	1.30	3.00
% OIP	0.77	1.70	4.00
Cum. CO ₂ Injected, MMscf (Tonne)	27960.00 (6.48 × 10 ⁸)	52260.00 (1.21 × 10 ⁹)	208660.00 (4.85 × 10 ⁹)
CO ₂ Flood Duration, years	52.00	77.00	60.00
CO ₂ Sequestered, MMscf (Tonne)	26190.00 (6.07 × 10 ⁸)	32380.00 (7.52 × 10 ⁸)	57540.00 (1.33 × 10 ⁹)
% of CO ₂ Sequestered	93.67	61.96	27.58
CO ₂ Injected per Barrel of Oil Produced, Mscf/stb (Tonne/stb)	46.60 (1.08 × 10 ³)	40.20 (9.34 × 10 ²)	69.55 (1.62 × 10 ³)
CO ₂ Sequestered per Barrel of Oil Produced, Mscf/stb (Tonne/stb)	43.65 (1.01 × 10 ³)	24.91 (5.82 × 10 ²)	19.18 (4.47 × 10 ²)

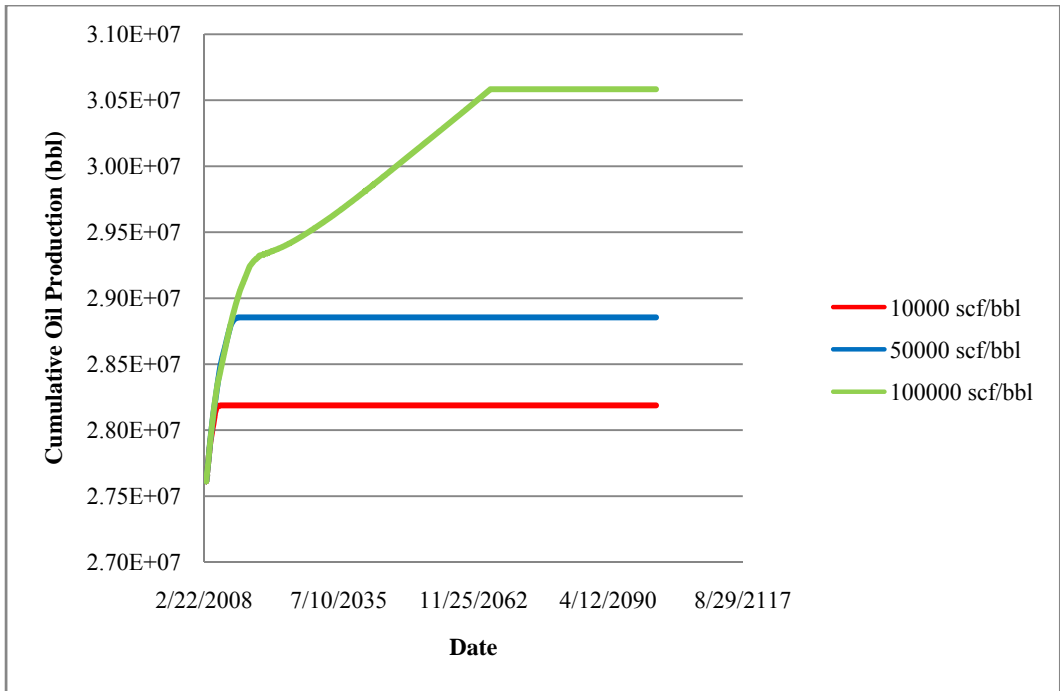


Figure 7.13- Cumulative Oil Production (Case 2)

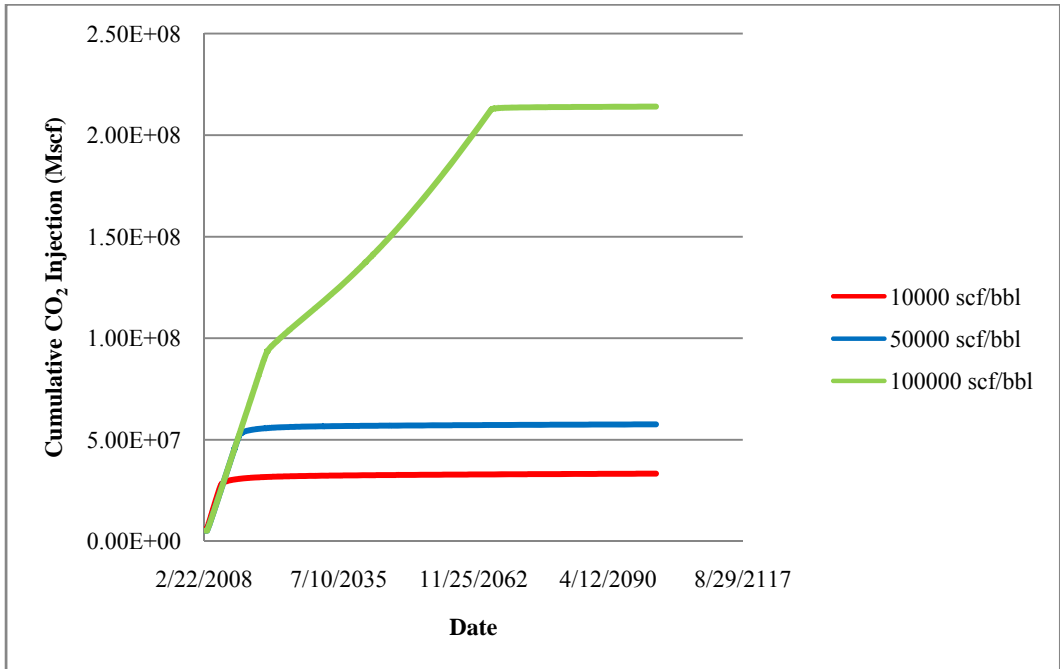


Figure 7.14- Cumulative CO₂ Injection (Case 2)

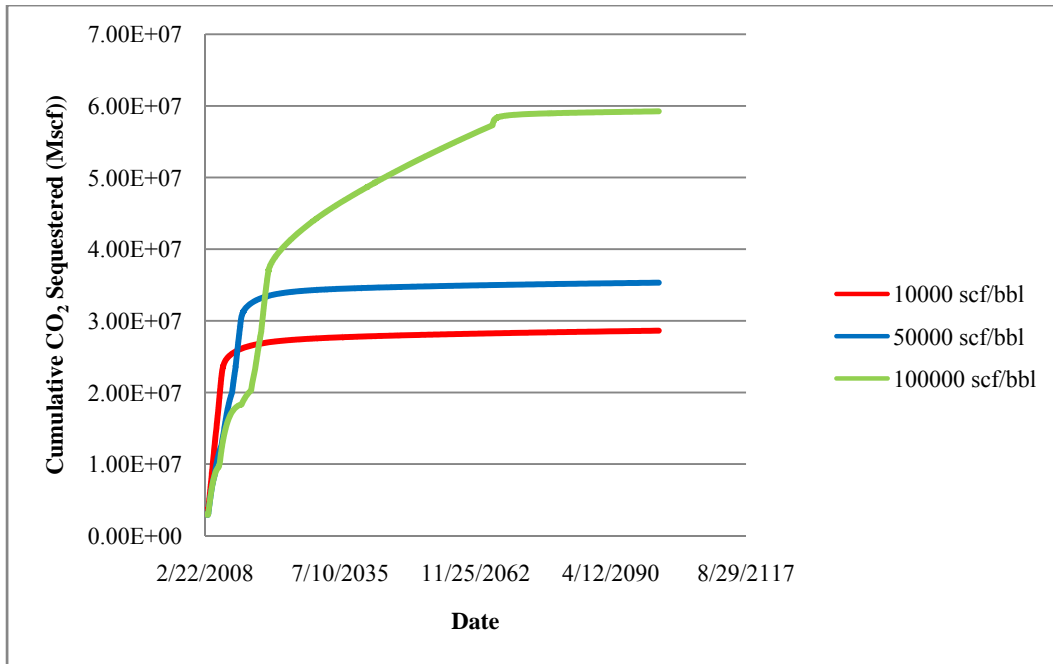


Figure 7.15- Cumulative CO₂ Sequestered (Case 2)

Case 3: Shutting-In When Oil Production Rate Falls 5 stb/day

In Case 3, a minimum oil production limit at 5 stb/day was set and monitored. When the oil rate at a producer dropped, the well was shut-in. CO₂ injectors were constrained with the maximum parting pressure of 5700 psi. An interesting observation is that well 59-4 was producing for many years in the other cases, but in this case it was the earliest well to be shut-in in the year 2013. Figure 7.16 indicates that wells 56-14, 56-16 and 56-19 were able to benefit from shutting in other producers in the field and thus sustained production until 2100. They were able to produce at an average oil rate of 10 stb/day for 80 years, disregarding economics.

Table 7.5 shows that, at the end of CO₂ flood, 3.07 % OIP was recovered, 21.8 % of injected CO₂ was stored, 23.73 Mscf of CO₂ was injected per barrel of oil produced, and 5.17 Mscf of CO₂ was stored per any barrel of oil produced.

Figures 7.17 and 7.18 show that oil production responded well to CO₂ flood. More CO₂ was stored after most producers were shut-in around 2100 (Figure 7.19).

Table 7.5- Simulation results of injection and production (Case 3)

Run/Different Scenarios	Shut-in if < 5 stb
Cum. Incremental Oil Recovery, MMstb	5.80
% OIP	3.07
Cum. CO ₂ Injected, MMscf (Tonne)	137660.00 (3.21×10^9)
CO ₂ Flood Duration, years	35.00
CO ₂ Sequestered, MMscf (Tonne)	30008.00 (6.98×10^8)
% of CO ₂ Sequestered	21.80
CO ₂ Injected per Barrel of Oil Produced, Mscf/stb (Tonne)	23.73 (5.53×10^2)
CO ₂ Sequestered per Barrel of Oil Produced, Mscf/stb (Tonne)	5.17 (1.20×10^2)

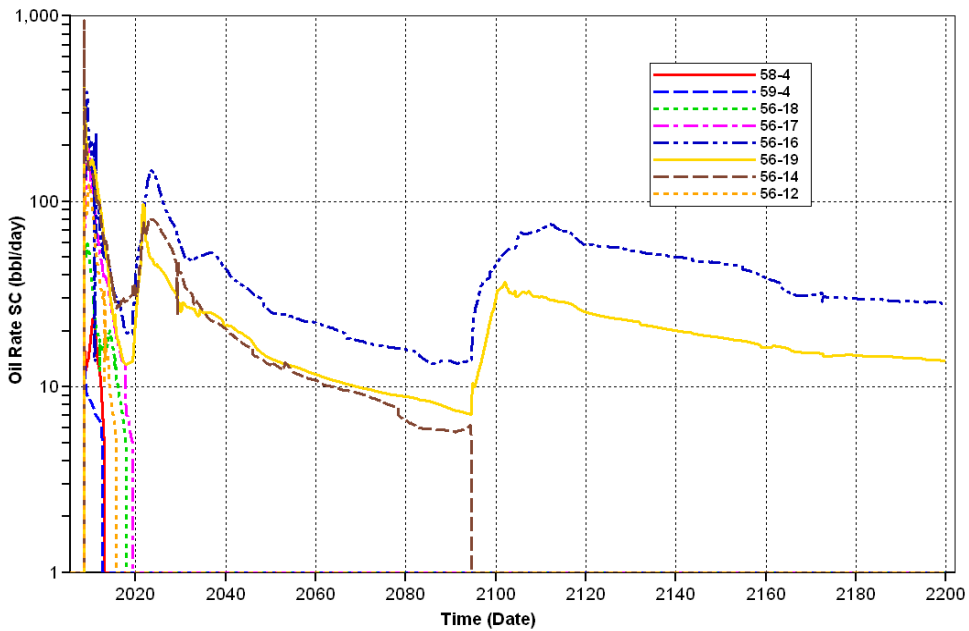


Figure 7.16- Oil Production Rate (Case 3: Shut-in Below 5 stb/day)

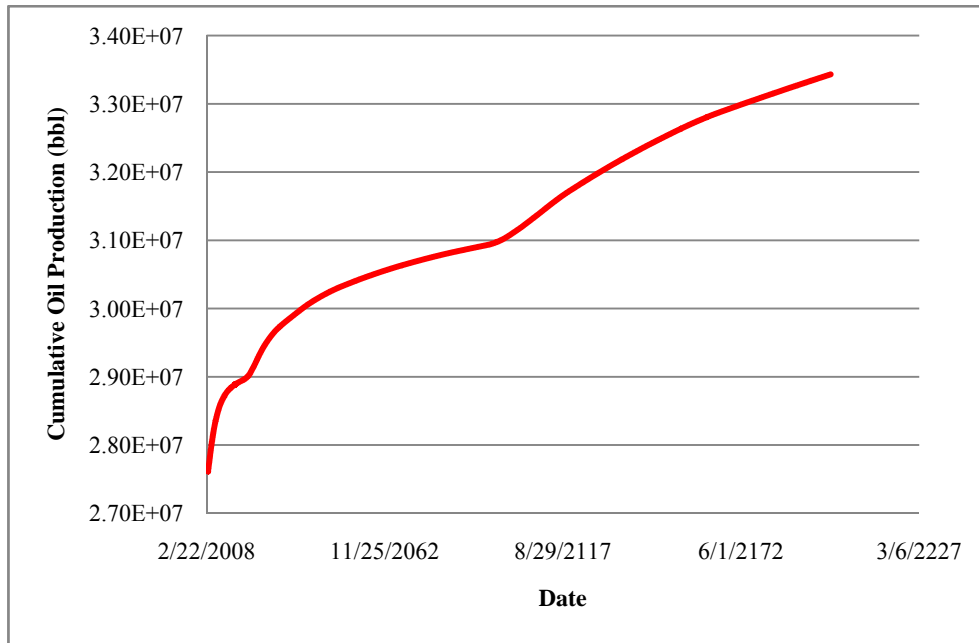


Figure 7.17- Cumulative Oil Production (Case 3: Shut-in Below 5 stb/day)

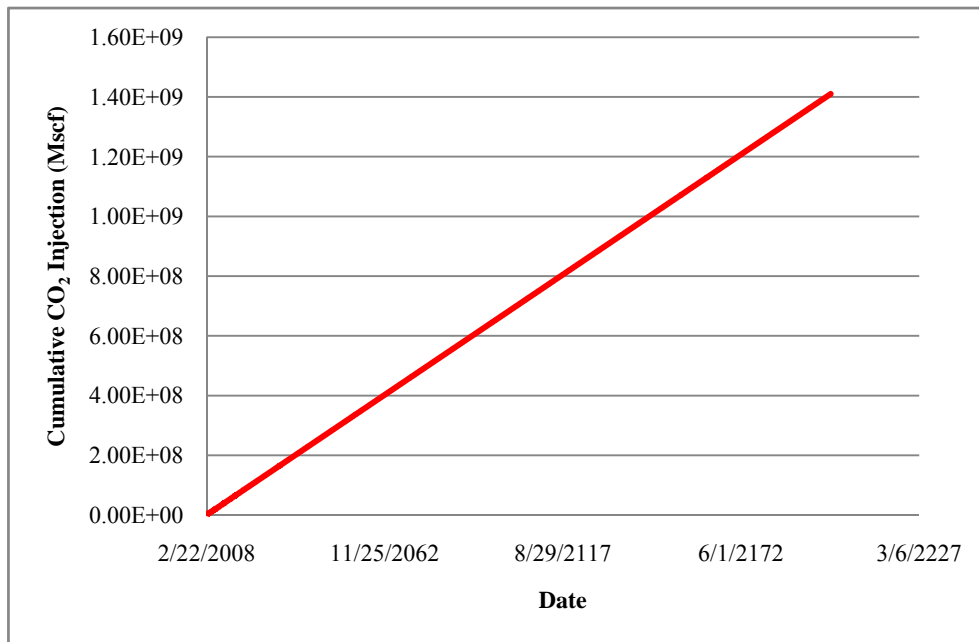


Figure 7.18- Cumulative CO₂ Injection (Case 3: Shut-in Below 5 stb/day)

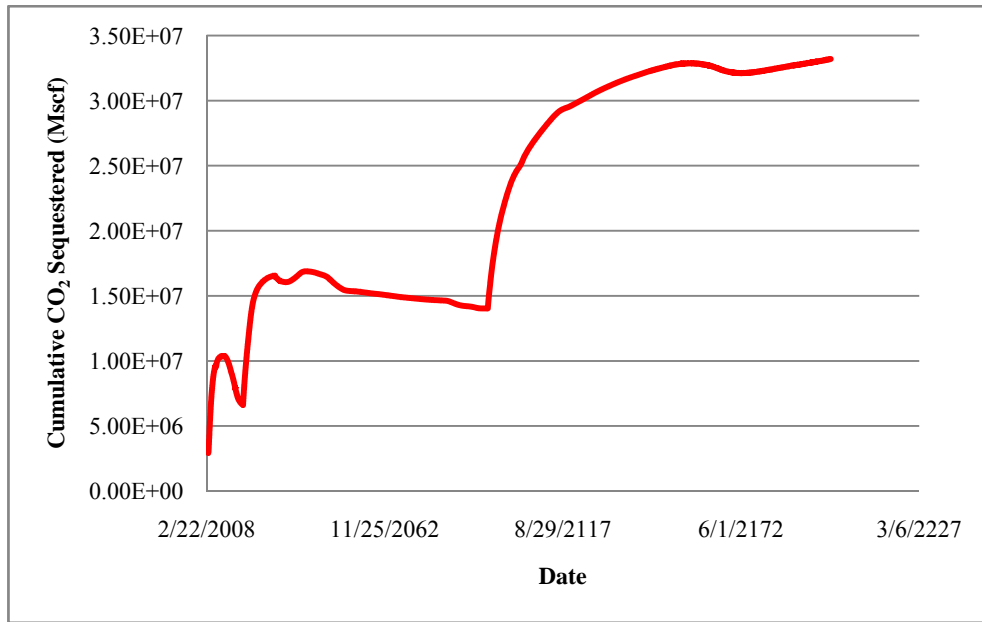


Figure 7.19- Cumulative CO₂ Sequestration (Case 3: Shut-in Below 5 stb/day)

Case 4: No Shut-In

Case 4 simulated a no shut-in constraint on producers as they were kept open to produce oil for the entire simulation run while CO₂ injectors were constrained at the parting pressure of 5700 psi. Being similar to Case 3, Figure 7.20 indicates that wells 56-14, 56-16 and 56-19 were producing much more than the rest of the producers. The simulation ran for 55 years.

Since producers were opened during the entire simulation run, a lot more oil was produced and the reservoir never reached the maximum BHP imposed on the system, however; almost all the injected CO₂ was produced. A thorough economic analysis should be made to determine whether capture and re-injection of the produced CO₂ or shutting in the producers with the low oil production rates is best.

Table 7.6 shows that 2.5 % of OOIP was recovered, only 1.26 % of injected CO₂ was stored, 148 Mscf of CO₂ was injected per each barrel of oil produced, and 1.86 Mscf of CO₂ was stored per each barrel of oil. Figures 7.21 and 7.22 show the cumulative oil production and CO₂ injection of the field. In Figure 7.23, the cumulative volume of CO₂ stored peaked in 2012 and deteriorated later due to high production. As the reservoir pressure fell below MMP which was reported to be 1600 psi, CO₂ that were not miscible in oil were produced quickly.

Table 7.6- Simulation results of injection and production (Case 4)

Run/Different Scenarios	No Shut-In
Cum. Incremental Oil Recovery, MMstb	2.20
% OIP	2.50
Cum. CO ₂ Injected, MMscf (Tonne)	325800.00 (7.57×10^9)
CO ₂ Flood Duration, years	46.00
CO ₂ Sequestered, MMscf (Tonne)	4100.00 (9.57×10^7)
% of CO ₂ Sequestered	1.26
CO ₂ Injected per Barrel of Oil Produced, Mscf/stb (Tonne/stb)	148.09 (3.44×10^3)
CO ₂ Sequestered per Barrel of Oil Produced, Mscf/stb (Tonne/stb)	1.86 (4.33×10^1)

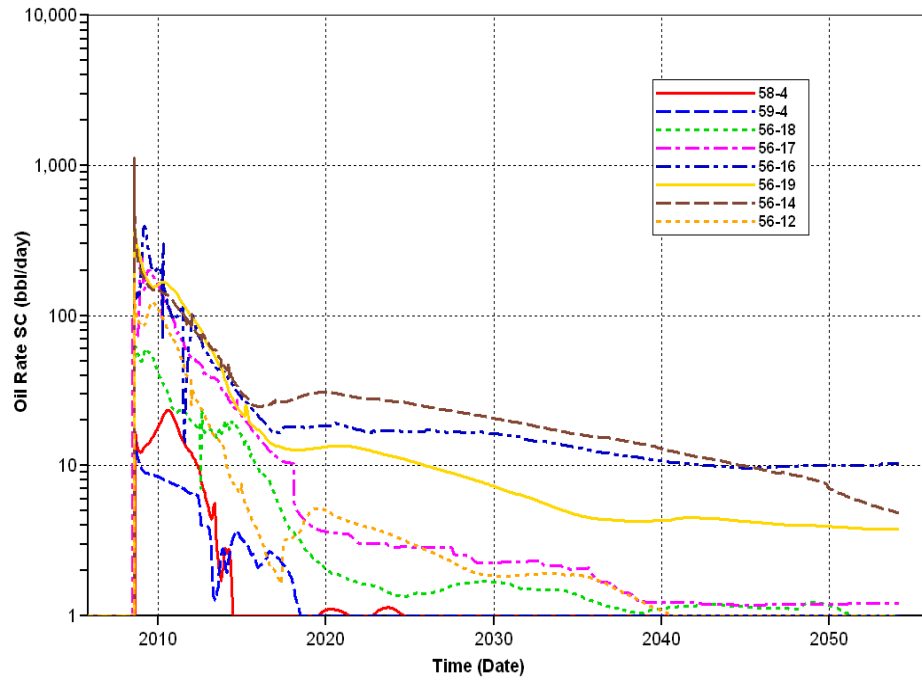


Figure 7.20- Oil Production Rate (Case 4: no shut-in)

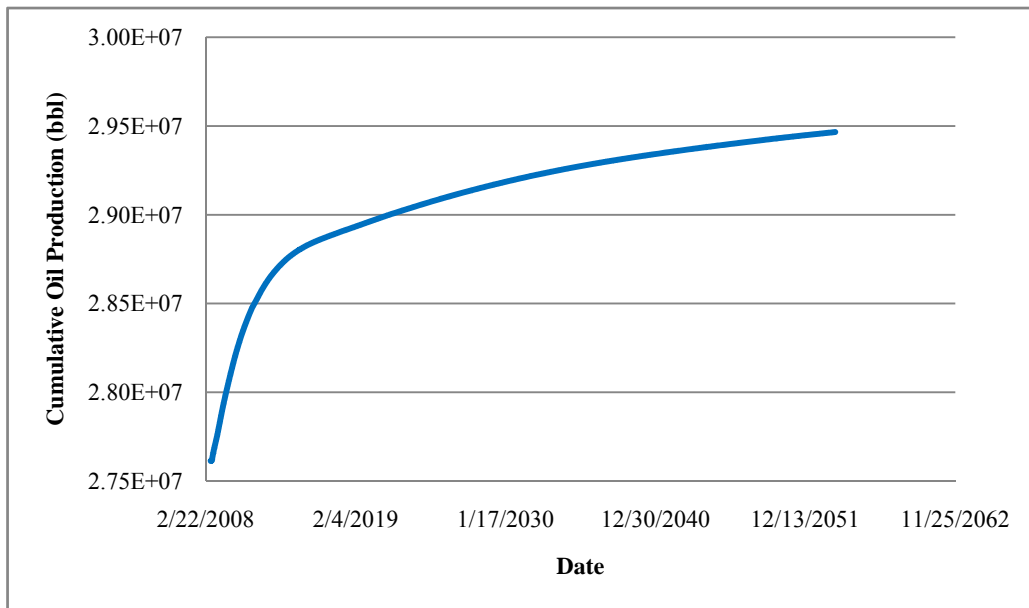


Figure 7.21- Cumulative Oil Production (Case 4: no shut-in)

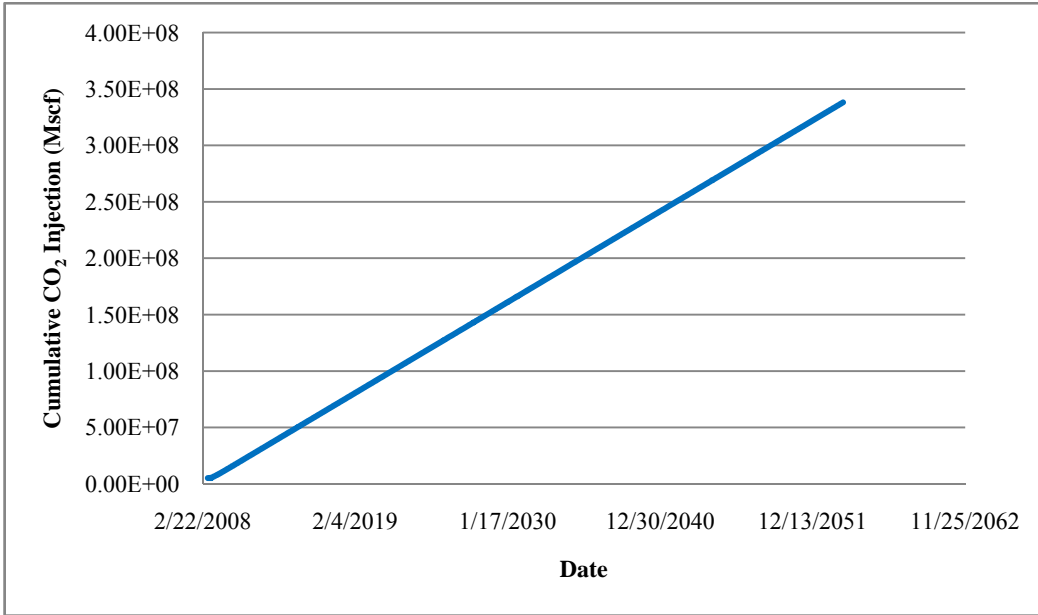


Figure 7.22- Cumulative CO₂ Injection (Case 4: no shut-in)

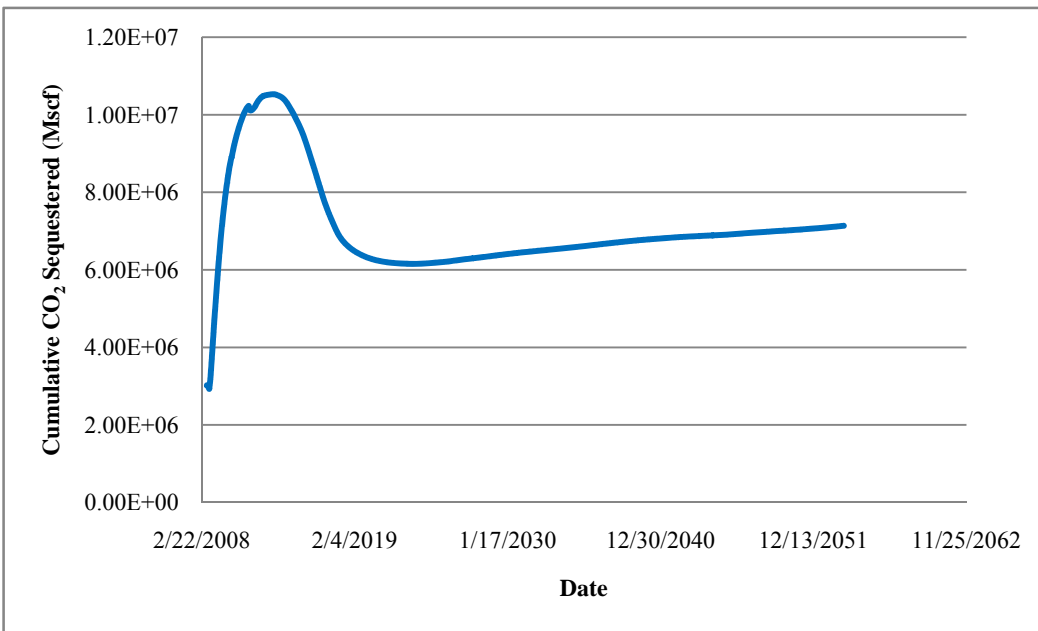


Figure 7.23- Cumulative CO₂ Sequestered (Case 4: no shut-in)

Additional plots on effects of CO₂ injection for coupled enhanced oil recovery and CO₂ sequestration for all cases are provided in Appendix.

Chapter 8: CONCLUSIONS AND FUTURE WORK

8.1 Conclusions

Carbon dioxide emission is generated from the combustion of oil, natural gas, and coal and is expected to rise as world energy needs increase. It may take hundreds of years for CO₂ to decompose once it is emitted into the atmosphere. The atmospheric concentration of CO₂ has increased to 365 parts per million (ppm) with the increment by 1.1 to 6.4° C in the global temperature (Keeling *et al.*, 2000; Metz *et al.*, 2005).

To reduce CO₂ requires reductions in the use of hydrocarbons as fuels or identifying methods to capture and store the released CO₂. World energy demand and the present state of alternative energy resources make it impractical to stop using hydrocarbon fuels. Therefore, carbon capture and storage (CCS) in geological formations may be a key technology if governments choose to reduce CO₂.

Oil production in most reservoirs can only recover 15 to 20 % of original oil in-place (OOIP) after primary recovery. Injecting water and CO₂ consequently can recover the oil remained in the reservoir as secondary and tertiary recovery operations, respectively. Simultaneous EOR and CO₂ sequestration can provide two benefits: additional oil recovery and sequestration in oil fields.

The use of a compositional simulator offers an organized study into the behavior of this subject reservoir. Studying sensitivities of reservoir and wells' parameters allows the engineer to design and predict the best flooding schemes in

CO₂ injection projects. Results from four type cases were presented in this study. The sensitivity of each case has impact on the economics of reservoir management and operations policies within an oil company. It is important to note that some of these cases were selected and evaluated to study phenomena and may not represent economic situations or realistic reservoir management practices.

Table 8.1 - Summary of all Simulation Runs

Simulation Run		Output Results					
		Cumulative CO ₂ Sequestered		Incremental Oil Recovery		CO ₂ Injected per Barrel of Oil Produced	CO ₂ Sequestered per Barrel of Oil Produced
		Bscf (Tons)	%	MMstb	% OIP	Mscf/stb (Tons/stb)	Mscf/stb (Tons/stb)
Case 1	Scenario 1 (100 MMscf/d)	71.7 (4.1 × 10 ⁶)	5.88	4.4	5.9	277.2 (15.9)	16.3 (0.9)
Case 1	Scenario 1 (50 MMscf/d)	58.7 (3.4 × 10 ⁶)	8.88	4.2	5.7	153.3 (8.8)	13.9 (0.8)
Case 1	Scenario 1 (25 MMscf/d)	84.2 (4.8 × 10 ⁶)	8.89	7.4	6.3	127.9 (7.3)	11.3 (0.6)
Case 1	Scenario 2 (100 MMscf/d)	58 (3.3 × 10 ⁶)	4.7	9.9	13.5	121.2 (6.9)	5.8 (0.3)
Case 1	Scenario 2 (50 MMscf/d)	17.6 (1.1 × 10 ⁶)	26.7	1.6	2.3	38.9 (2.2)	10.4 (0.6)
Case 1	Scenario 2 (25 MMscf/d)	9.9 (5.9 × 10 ⁵)	20.4	4.4	5.6	11 (0.6)	2.2 (0.1)
Case 2	10,000 scf/bbl	26.1 (1.5 × 10 ⁶)	93.6	0.6	0.77	46.6 (2.7)	43.6 (2.5)
Case 2	50,000 scf/bbl	32.3 (1.8 × 10 ⁶)	61.9	1.3	1.7	40.2 (2.3)	24.9 (1.4)
Case 2	100,000 scf/bbl	57.5 (3.3 × 10 ⁶)	27.5	3	4	69.5 (3.9)	19.1 (1.1)
Case 3	< 5 stb	30 (1.7 × 10 ⁶)	21.8	5.8	3.07	23.7 (1.36)	5.17 (0.3)
Case 4	No Shut-in	4.1 (2.5 × 10 ⁵)	1.26	2.2	2.5	148.0 (8.5)	1.86 (0.1)

Table 8.1 summarizes the results of key simulation runs made in this study. Scenarios in Case 1 can be considered unrealistic because a large daily rate of CO₂ was injected. Cases 2, 3 and 4 were simulated with injection rates that were closer to those most often used in CO₂ flood projects.

In terms of sequestration efficiency, the best case for CO₂ sequestration among the runs in case 1 is scenario 2 (50 MMscf/d) in which 26.75 % of total injected CO₂ was sequestered. The best case for EOR purpose is scenario 2 of case 1 (100 MMscf/d) in which 13.5 % of OIP was recovered. The balanced case for both EOR and sequestration is scenario 2 of case 1 (25 MMscf/d) in which 5.6 % of OIP was produced and 20.45 % of total injected CO₂ was sequestered. The highest volume of CO₂ sequestered is 84.2 Bscf in scenario 1 of case 1 (25 MMscf/d).

Among the more realistic cases (2, 3 and 4), the best case for CO₂ sequestration is case 2 (GOR limit of 10,000 scf/bbl) in which 93.67 % of total injected CO₂ was stored. The best case for EOR is case 2 (GOR limit of 100,000 scf/bbl) in which additional 4 % of OIP was recovered. The balanced case for both EOR and sequestration is case 3 in which 21.8 % of total injected CO₂ was sequestered and 3.07 % of OIP was produced. The highest volume of CO₂ sequestered is 57.5 Bscf in case 2 (GOR limit of 100,000 scf/bbl). In terms of volume, case 2 (GOR limit of 100,000 scf/bbl) is the run which optimized both EOR and sequestration.

From simulation results, the following conclusions were made:

- An acceptable history match was obtained from 3D reservoir flow simulation constructed by Texas BEG.

- In Case 1, when injection rates were not controlled, the amount of CO₂ injection allowed by the simulator was found to be physically impossible.
- Case 2 results suggest that the maximum storage capacity was reached using a GOR limit of 100,000 scf/bbl as the production constraint, mainly due to a longer period of injection and a subsequent increase in displaced reservoir fluids while providing the highest additional oil recovery.
- In Cases 3 and 4, since producers were open until the oil rates fell below 5 stb/day and were therefore operating for long time periods, a lot more oil was produced and the reservoir never reached the maximum BHP imposed on the system. However, at the same time, almost all the injected CO₂ was produced over the same time period. A thorough economic analysis should be made to determine whether capture and re-injection of the produced CO₂ or shutting in the producers with the low oil production rates is best.

If it is assumed that the project area is a representative sample of how the entire SACROC unit could be developed it is possible to extrapolate the capacity of the entire reservoir to hold CO₂. Table 8.2 compares and contrasts sequestered tons of CO₂ for each model. Also included in Table 8.2 are estimates of CO₂ production rates for coal plants of varying sizes (small, average, and high). Based on the extrapolation, case 2 (GOR limit of 100,000 scf/bbl), which is the best EOR scenario, would store the most CO₂, as measured in years of coal plant

output, by sequestering annual rates of 20, 5, and 1 MMtons for 28, 112, and 560 years, respectively. However, the most efficient case for CO₂ sequestration at 93.6 % is case 2 (GOR limit of 10,000 scf/bbl) which would store emitted CO₂ from plants for 13, 51, and 255 years with the smallest amount of CO₂ at 2.55×10^8 tons. In terms of volume, the balanced case for both EOR and sequestration (case 3) could sequester annual rates of 20, 5, and 1 MMtons for 15, 58, and 292 years. Examination of Figures 8.1 to 8.3 which show the rates of CO₂ sequestration in SACROC and emission rates of power plants indicate that the balanced case (Figure 8.1) would be the best for a sustained sequestration project since the rate produced by the power plants is smaller than the maximum rate accepted by the field in the model for the longest period of time.

**Table 8.2 - Summary of Estimated Years that SACROC Stores CO₂ from
Different Power Plants**

		Estimated Cum. CO ₂ Sequestered in Entire SACROC Unit		Years to Store CO ₂ from a plant which emits 20 MMtons/year	Years to Store CO ₂ from a plant which emits 5 MMtons/year	Years to Store CO ₂ from a plant which emits 1 MMtons/year
		Bscf	Tons			
Case 1	Scenario 1	1.22×10^4	6.99×10^8	35	140	699
Case 1	Scenario 1	9.95×10^3	5.72×10^8	29	114	572
Case 1	Scenario 1	1.43×10^4	8.20×10^8	41	164	820
Case 1	Scenario 2	9.83×10^3	5.65×10^8	28	113	565
Case 1	Scenario 2	2.98×10^3	1.71×10^8	9	34	171
Case 1	Scenario 2	1.68×10^3	9.65×10^7	5	19	96
Case 2		4.44×10^3	2.55×10^8	13	51	255
Case 2		5.49×10^3	3.16×10^8	16	63	316
Case 2		9.75×10^3	5.60×10^8	28	112	560
Case 3		5.09×10^3	2.92×10^8	15	58	292
Case 4		6.95×10^3	4.00×10^7	2	8	40

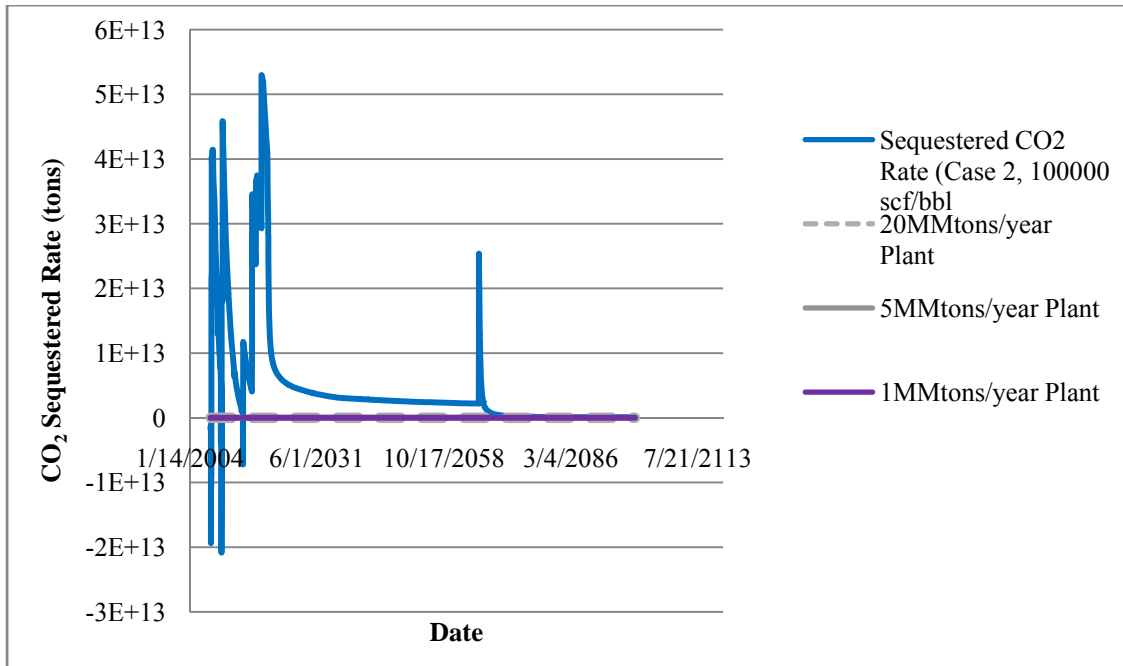


Figure 8.1- CO₂ sequestered rate vs. CO₂ emission rates from plants (Case 2, 100000 scf/bbl)

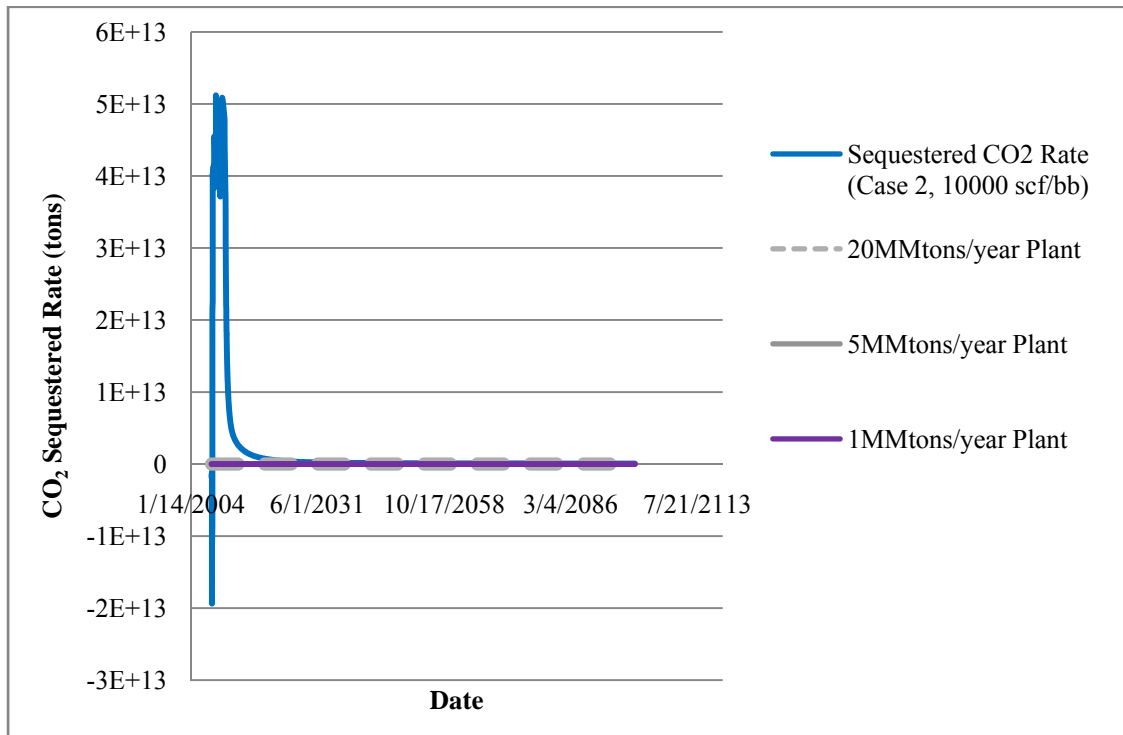


Figure 8.2- CO₂ sequestered rate vs. CO₂ emission rates from plants (Case 2, 10000 scf/bbl)

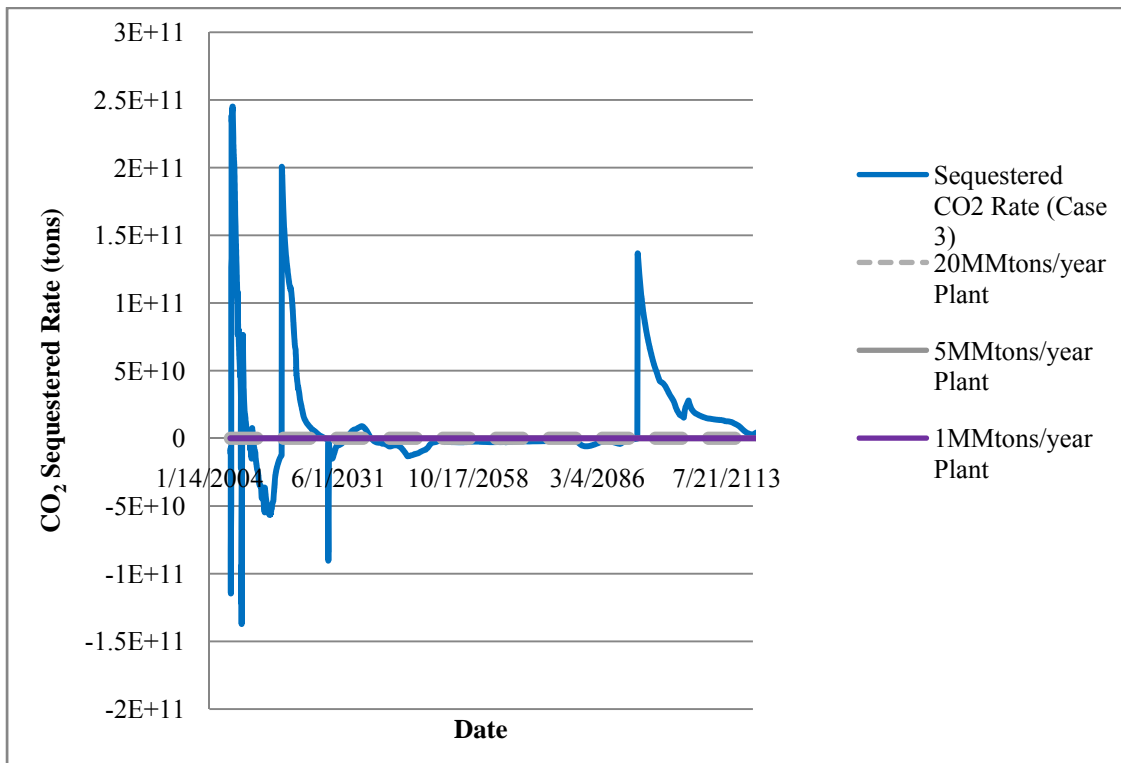


Figure 8.3- CO₂ sequestered rate vs. CO₂ emission rates from plants (Case 3)

8.2 Future Work and Recommendations

A set of relative permeability experiments on a carbonate from West Texas was used to simulate the fluid flows in this study. Experiments to measure the relative permeability of a SACROC rock are recommended.

This simulation study did not focus on trapping mechanisms to evaluate the amount of CO₂ sequestered. However, the GEM simulator provides limited results on CO₂ sequestered trapped by solubility and mineral trapping mechanisms, but not on specific trapping mechanisms such as hydrodynamic and residual trapping. Additional techniques are required to quantify these results.

Future work may also include various runs with mobility control programs such as water alternating gas (WAG) injection schemes to avoid the early CO₂ breakthrough and sustain oil production. Different WAG ratios, CO₂ slug size, and relative permeability hysteresis need to be analyzed to see their effects on the amount of CO₂ injected and produced. To analyze the trapping of CO₂ as residual gas, effects of hysteresis should be accounted.

Other flood design parameters such as well spacing, production and injection well types, injection scheme (WAG or continuous CO₂ injection), shut-in and open status, and recycling the produced CO₂ should be studied in the future.

REFERENCES

- Aziz, K., Settari, A.: "Petroleum Reservoir Simulation," Elsevier, NY, 1979.
- Bennion, B., Bachu, S.: "Relative Permeability Characteristics for Supercritical CO₂ Displacing Water in a Variety of Potential Sequestration Zones in the Western Canada Sedimentary Basin," *Society of Petroleum Engineers Journal* 95547, 2005.
- Chang, K.W.: "A Simulation Study of Injected CO₂ Migration in the Faulted Reservoir," MS thesis, The University of Texas at Austin, 2007.
- Computer Modeling Group, 2007. User's Guide GEM, Advanced Compositional Reservoir Simulator (version 2007). Computer Modeling Group Ltd., 2007.
- Dicharry, R.M., Pettyman, T.L., Ronquille, J.D.: "Evaluation and Design of a CO₂ Miscible Flood Project- SACROC Unit, Kelly-Snyder Field," *Society of Petroleum Engineers Journal* 1147, 1973.
- International Energy Annual.: "World Carbon Dioxide Emissions from the Use of Fossil Fuels," Energy Information Administration, Available at <http://www.eia.doe.gov/iea/carbon.html>, August, 2009.
- Ghomian, Y.: "Reservoir Simulation Studies for Coupled CO₂ Sequestration and Enhanced Oil Recovery," PhD Dissertation, The University of Texas at Austin, 2008.
- Han, W.S.: "Evaluation of CO₂ Trapping Mechanisms at the SACROC Northern Platform: Site of 35 years of CO₂ Injection," PhD Dissertation, New Mexico Institute of Mining and Technology, Socorro, New Mexico, 2008.
- Jarrell, P.M., Fox, C.E., Stein M.H., and Webb, S.L., "Practical Aspects of CO₂ Flooding," SPE Monograph Series, Richardson, Texas, 2002.

- Keeling, C.D., and Whorf, T.P.: "Atmospheric CO₂ records from sites in the SIO air sampling network," *Trends: A Compendium of Data on Global Change*, Information Analysis Center, Oak Ridge National Laboratory, U.S. Department of Energy, 1998.
- Langston, M.V., Hoadley, S.F., Young, D.N.: "Definitive CO₂ Flooding Response in the SACROC Unit," *Society of Petroleum Engineers Journal* 17321, 1988.
- Li, Y.-K., Nghiem, L.X.: "Phase Equilibria of Oil, Gas, and Water/Brine Mixtures from a Cubic Equation of State and Henry's law," *Canadian Journal of Chemical Engineering* 486-496, 1986.
- Metz, B., Davidson, O., Coninck, H. C., Loos, M., Meyer, L.A.: "IPCC Special Report on Carbon Dioxide Capture and Storage," Cambridge University Press, Cambridge, United Kingdom and New York, USA, 2005.
- Nghiem, L., Sammon, P., Grabenstetter, J., Ohkuma, H.: "Modeling CO₂ Storage in Aquifers with a Fully-coupled Geochemical EOS Compositional Simulator," *Society of Petroleum Engineers Journal* 89474, 2004.
- Park, S.: "Influence of Relative Permeability Curves on Extent of CO₂ Plume during Injection into Deep Saline Aquifers," MS thesis, The University of Texas at Austin, 2007.
- Pruess, K., Xu, T., Apps, J., and Garcia, J.: "Numerical Modeling of Aquifer Disposal of CO₂ ," *Society of Petroleum Engineers Journal*, 49-60, March 2003.
- Reichle D., Houghton J., Kane B., Ekmann J., Benson S., Clarke J., Dahlman R., Hendry G., Herzog H., Hunter-Cevera J., Jacobs G., Judkins R., Ogden J., Palmisano A., Socolow R., Stringer J., Surles T., Wolsky A., Woodward N., York M. Carbon Sequestration Research and Development, *U.S. Department of Energy Report DOE/SC/FE-1*. Available at www.ornl.gov/carbon_sequestration/, 1999.

Saller, A.H., Walden, S., Robertson, S., Nims, R., Schwab, J., Hagiwara, H., and Mizohata, S., "Three-Dimensional Seismic Imaging and Reservoir Modeling of an Upper Paleozoic "Reefal" Buildup, Reinecke Field, West Texas, United States," *Search and Discovery Article 20044*, Available at <http://www.searchanddiscovery.com/documents/2006/06144saller/index.htm>, 2006.

Vest, E.L.Jr.: "Oil Fields of Pennsylvanian-Permian Horseshoe Atoll, West Texas in Halbouty, Michael T. (ed.) *Geology of Giant Petroleum Fields*," *AAPG Memoir # 14*. American Association of Petroleum Geologists, Tulsa, Oklahoma, 185-203, 1970

Appendix

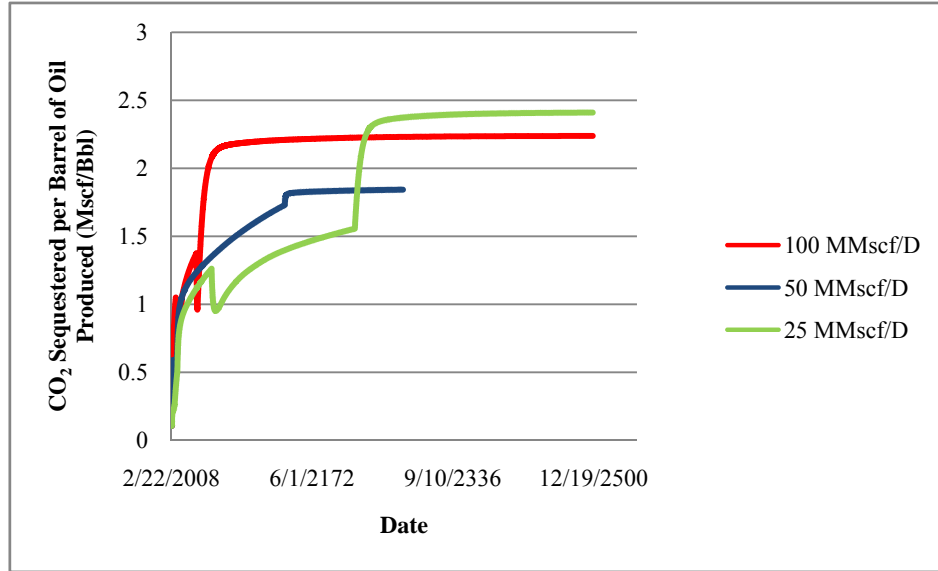


Figure A.1 - CO₂ Sequestered per Barrel of Oil Produced (Scenario 1, Case 1)

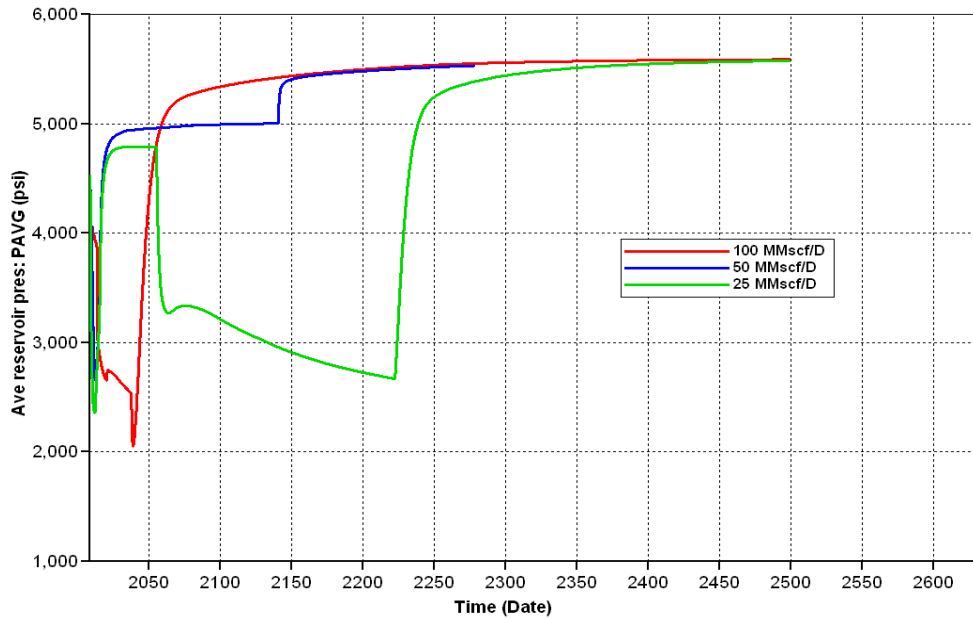


Figure A.2 - Average Reservoir Pressure (Scenario 1, Case 1)

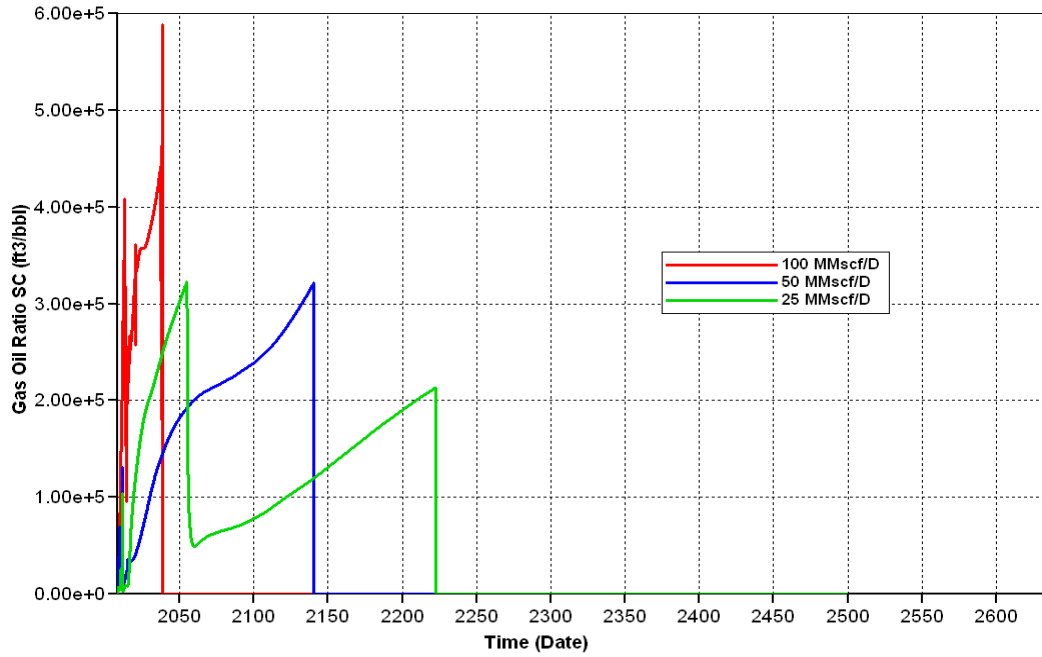


Figure A.3 - Gas Oil Ratio (Scenario 1, Case 1)

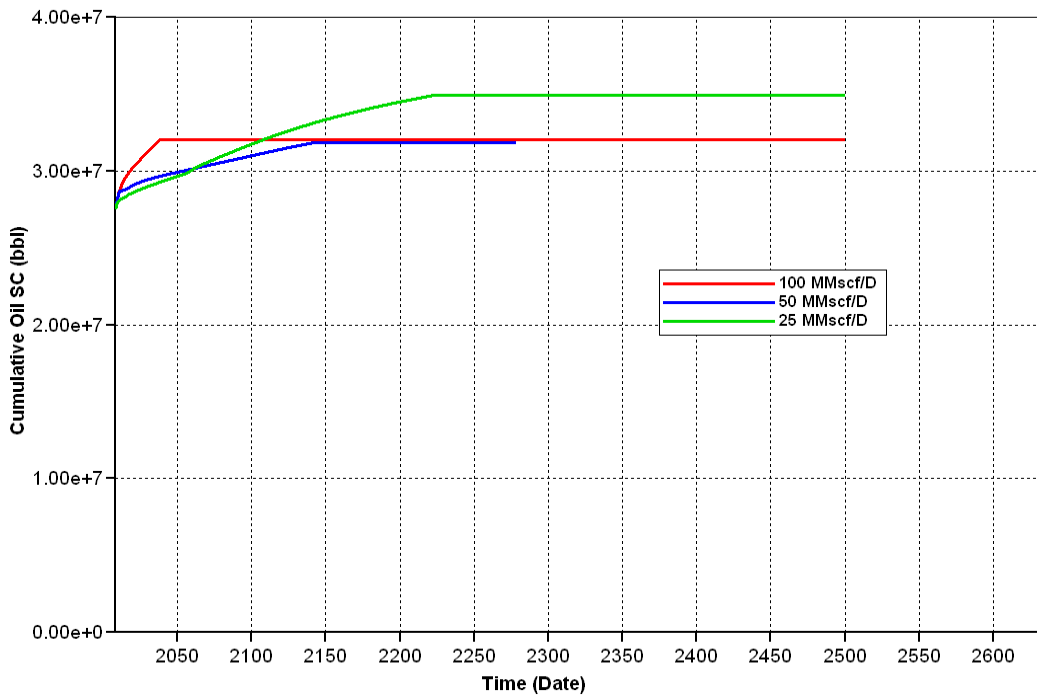


Figure A.3 - Cumulative Oil Production (Scenario 1, Case 1)

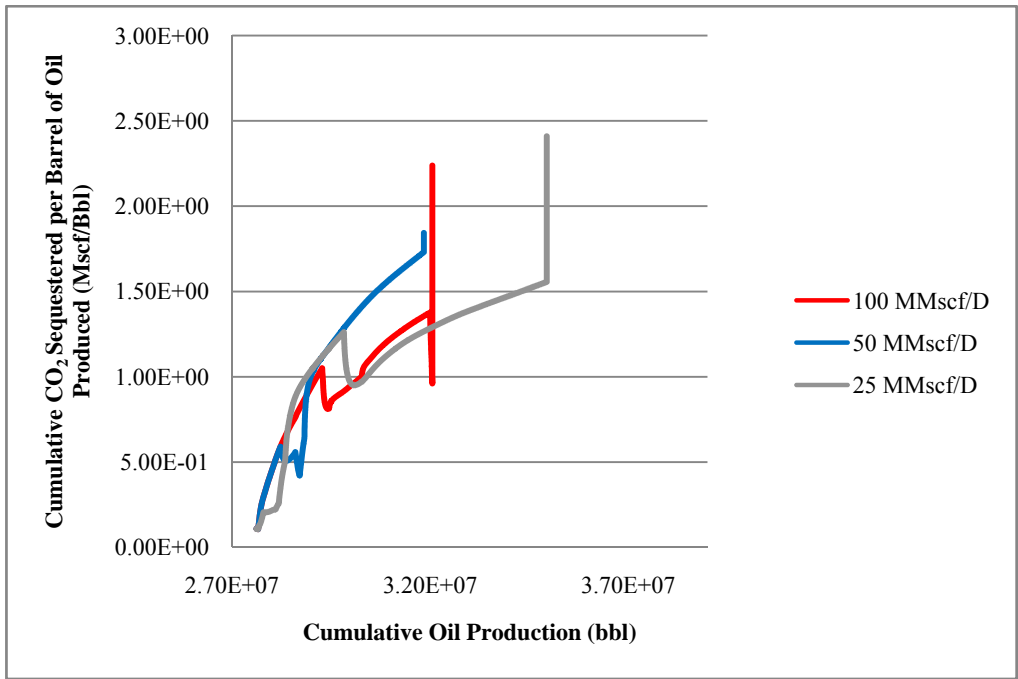


Figure A.4 - Cumulative CO₂ Sequestered per Barrel of Oil Produced VS. Cumulative Oil Production (Scenario 1, Case 1)

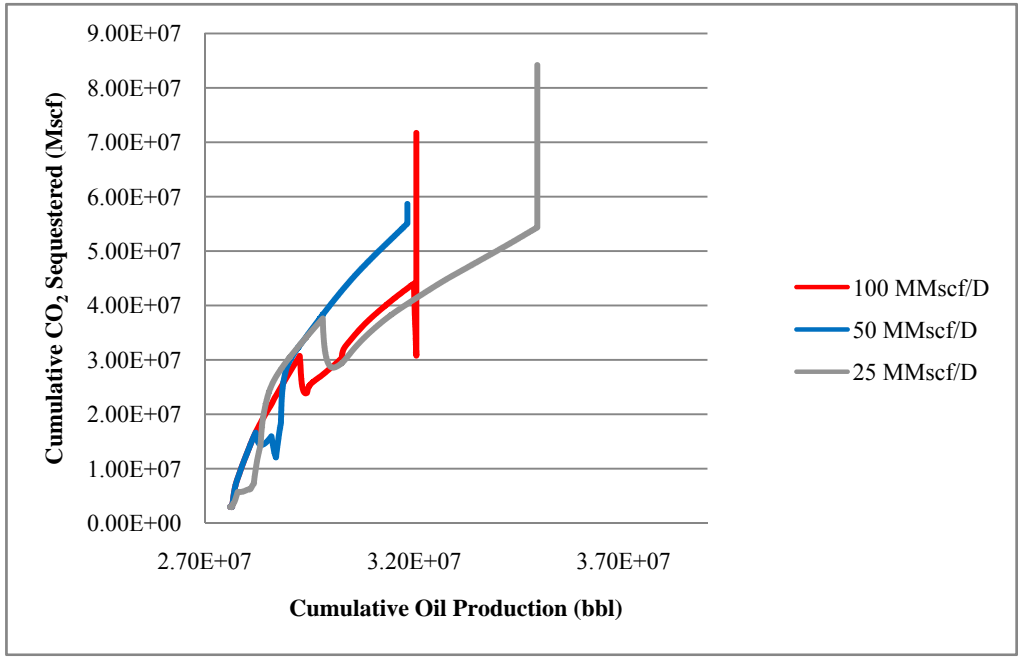


Figure A.5 - Cumulative CO₂ Sequestered VS. Cumulative Oil Production (Scenario 1, Case 1)

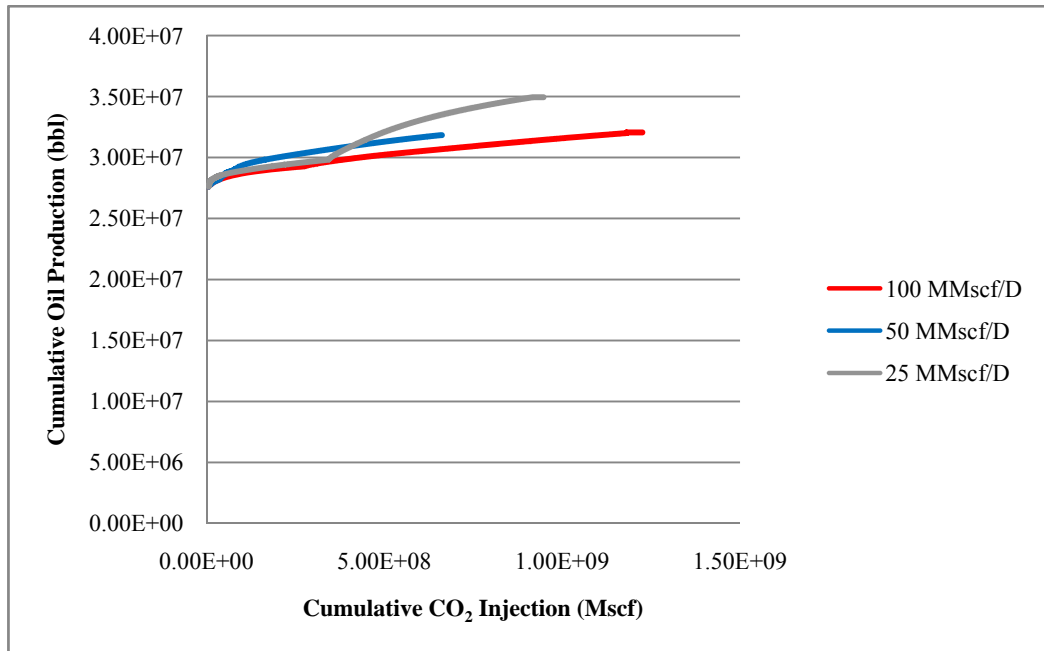


Figure A.6 - Cumulative Oil Production VS. Cumulative CO₂ Injection (Scenario 1, Case 1)

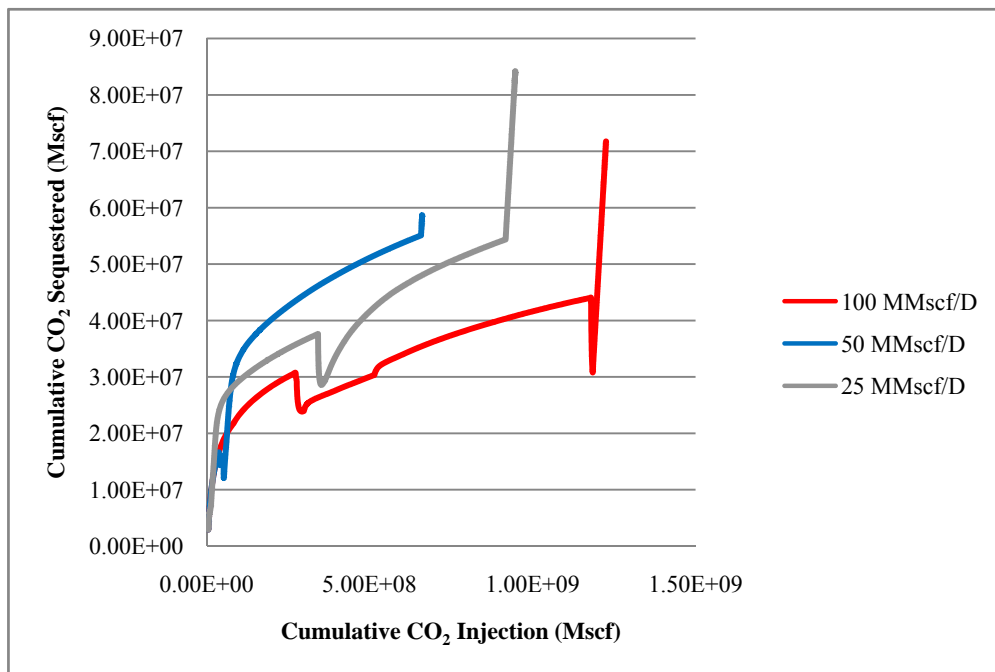


Figure A.7 - Cumulative CO₂ Sequestered VS. Cumulative CO₂ Injection (Scenario 1, Case 1)

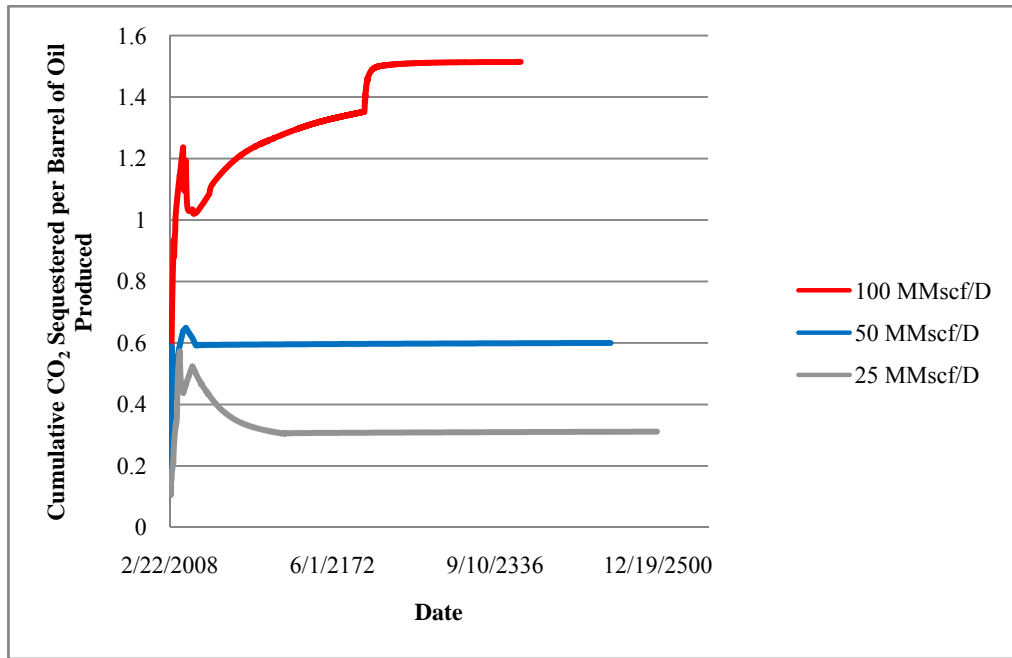


Figure A.8 - Cumulative CO₂ Sequestered per Barrel of Oil Produced (Scenario 2, Case 1)

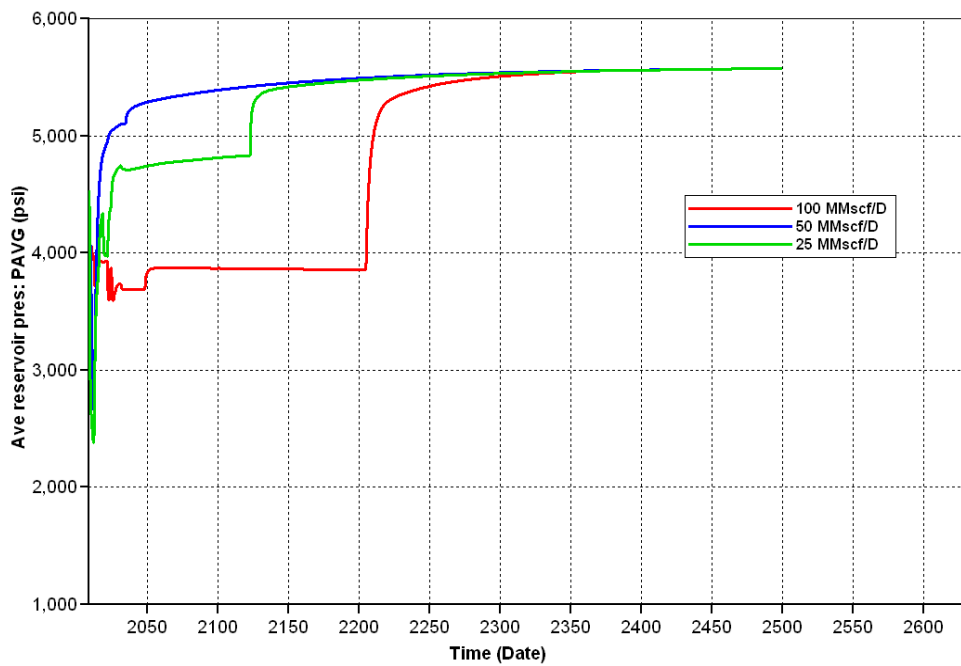


Figure A.9 - Average Reservoir Pressure (Scenario 2, Case 1)

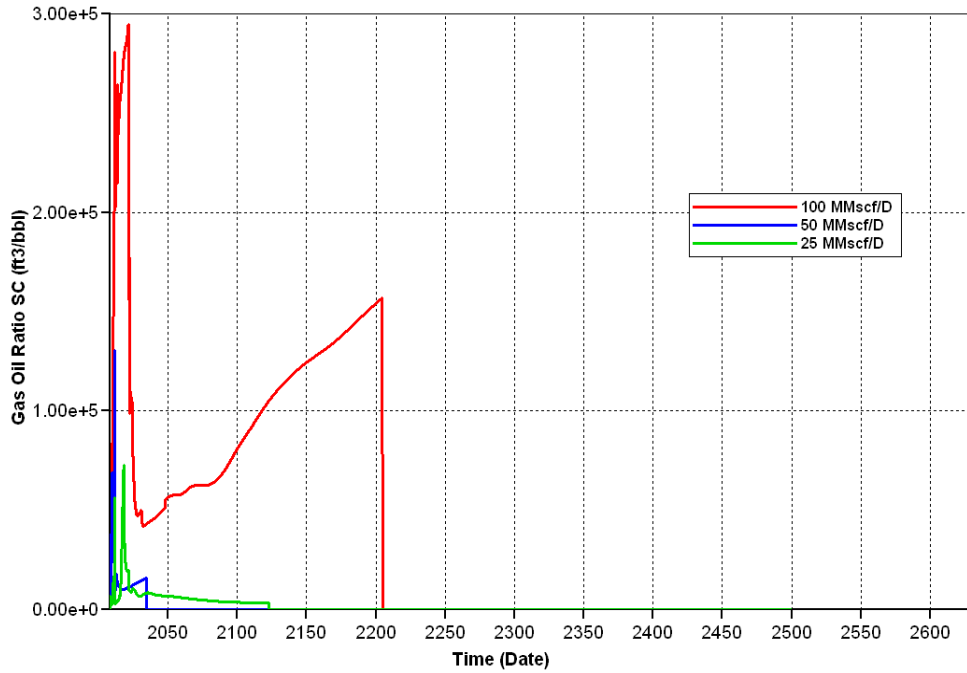


Figure A.10 - Gas Oil Ratio (Scenario 2, Case 1)

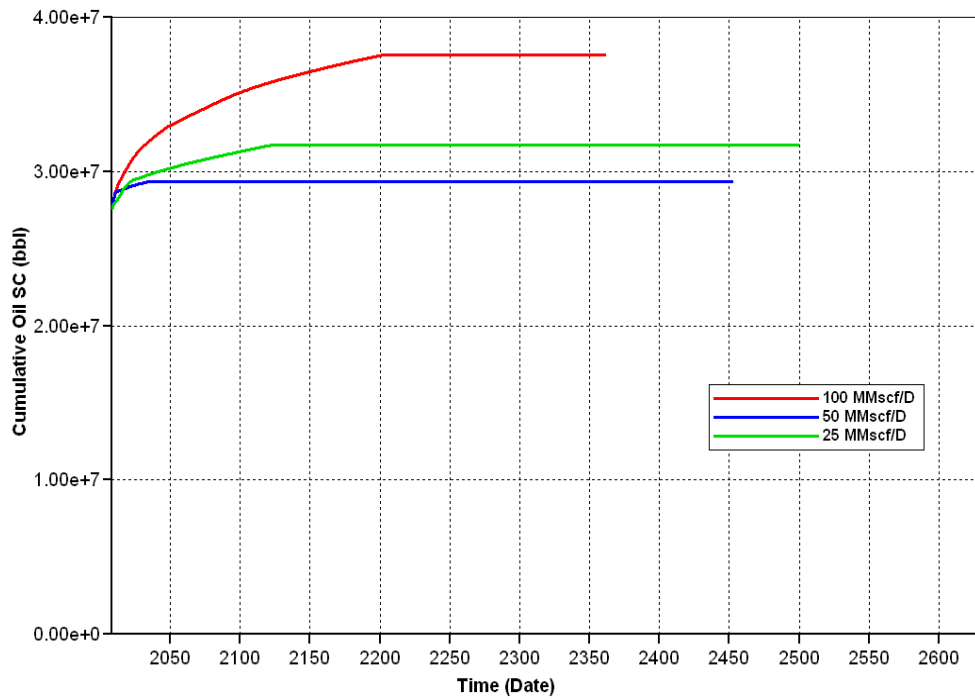


Figure A.11 - Cumulative Oil Production (Scenario 2, Case 1)

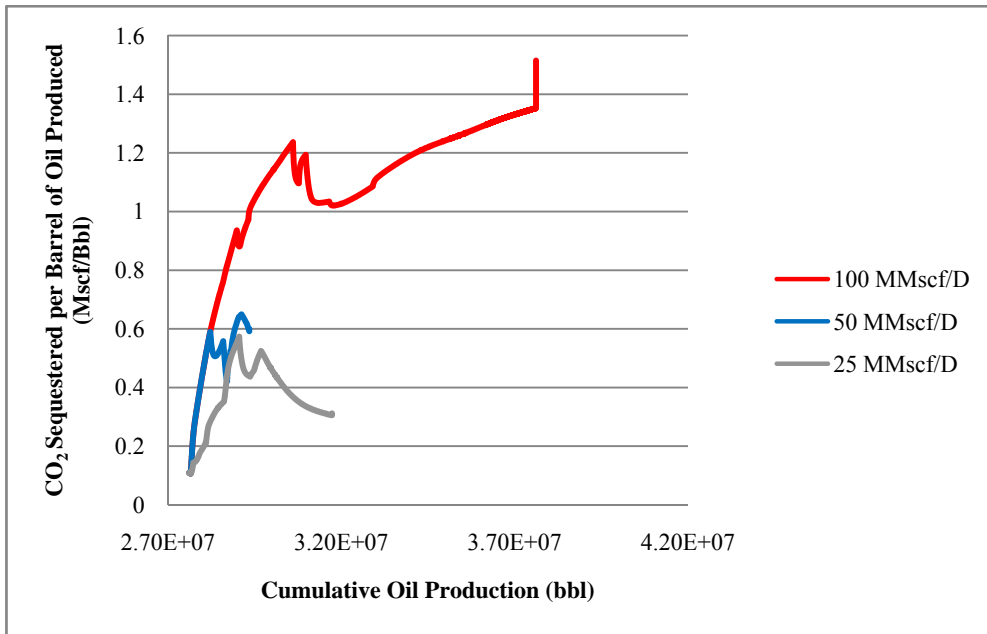


Figure A.12 - Cumulative Oil Production VS CO₂ Sequestered per Barrel of Oil Produced (Scenario 2, Case 1)

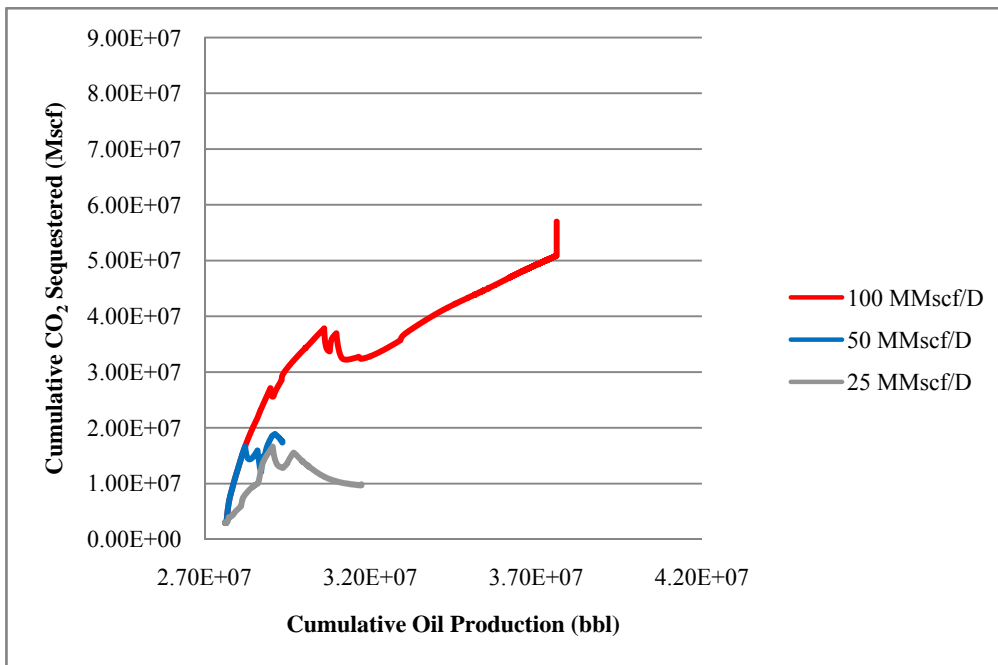


Figure A.13 - Cumulative CO₂ Sequestered VS Cumulative Oil Production (Scenario 2, Case 1)

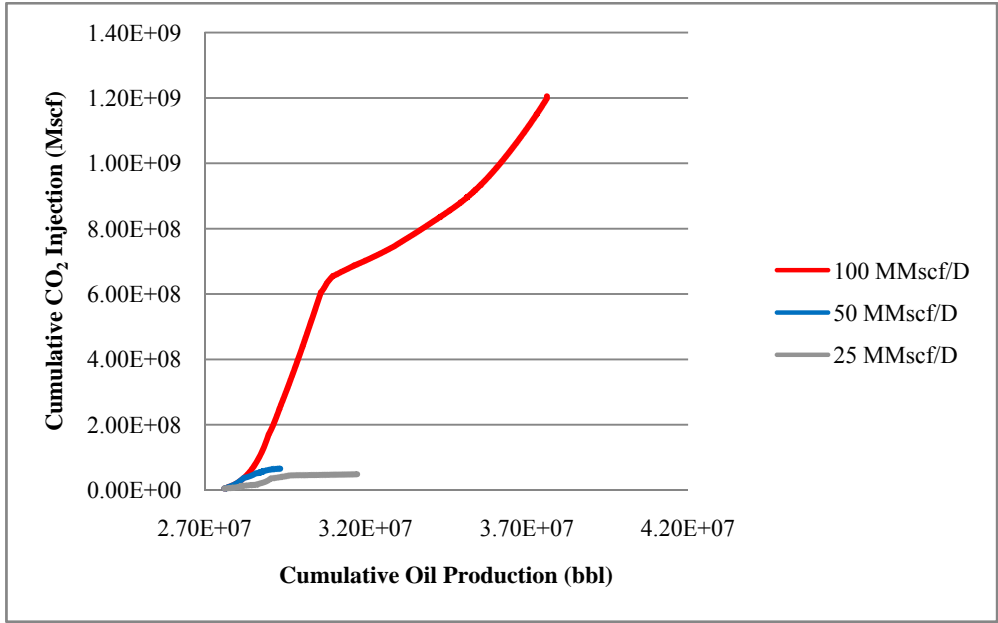


Figure A.14 - Cumulative CO₂ Injection VS Cumulative Oil Production (Scenario 2, Case 1)

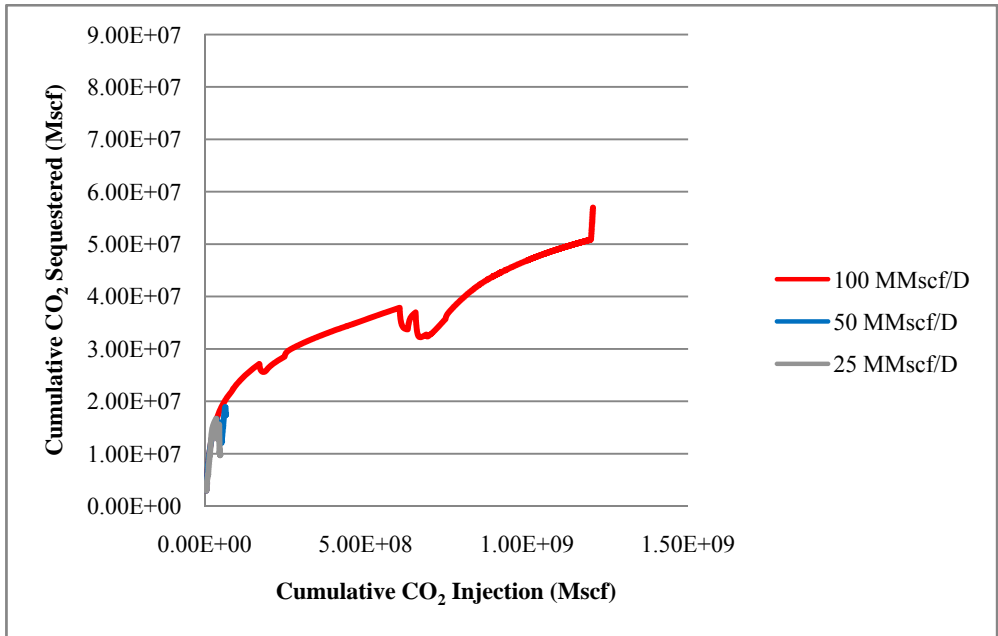


Figure A.15 - Cumulative CO₂ Sequestered VS Cumulative CO₂ Injection (Scenario 2, Case 1)

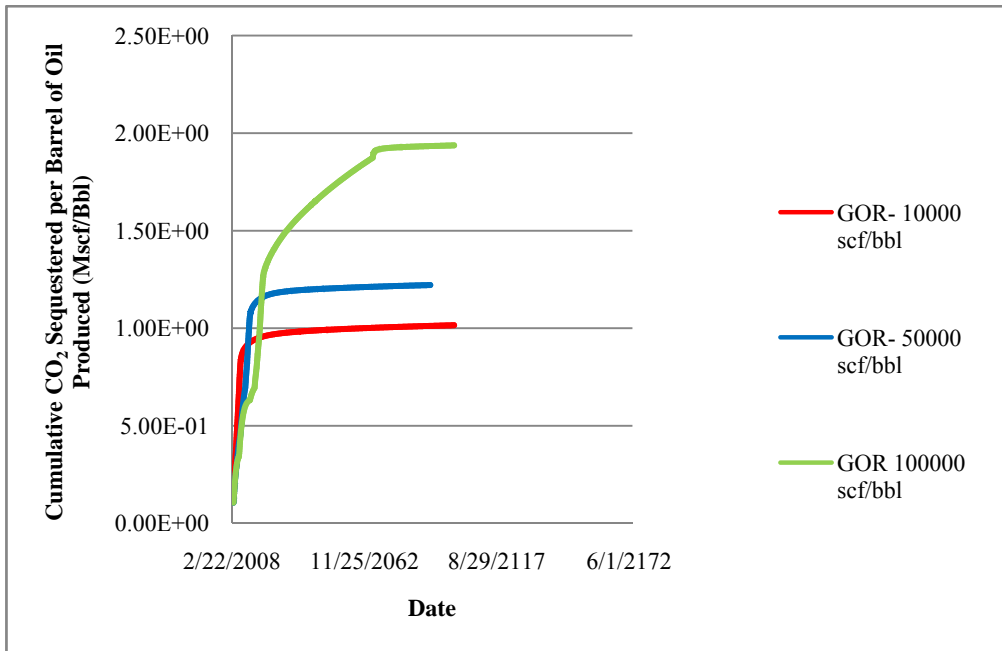


Figure A.16 - Cumulative CO₂ Sequestered per Barrel of Oil Produced (Case 2)

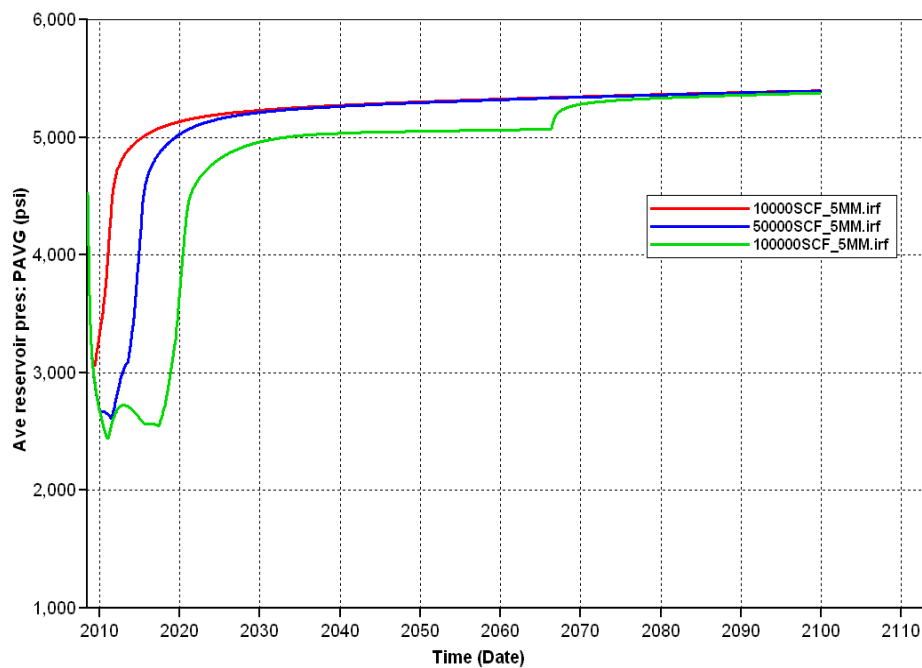


Figure A.17 - Average Reservoir Pressure (Case 2)

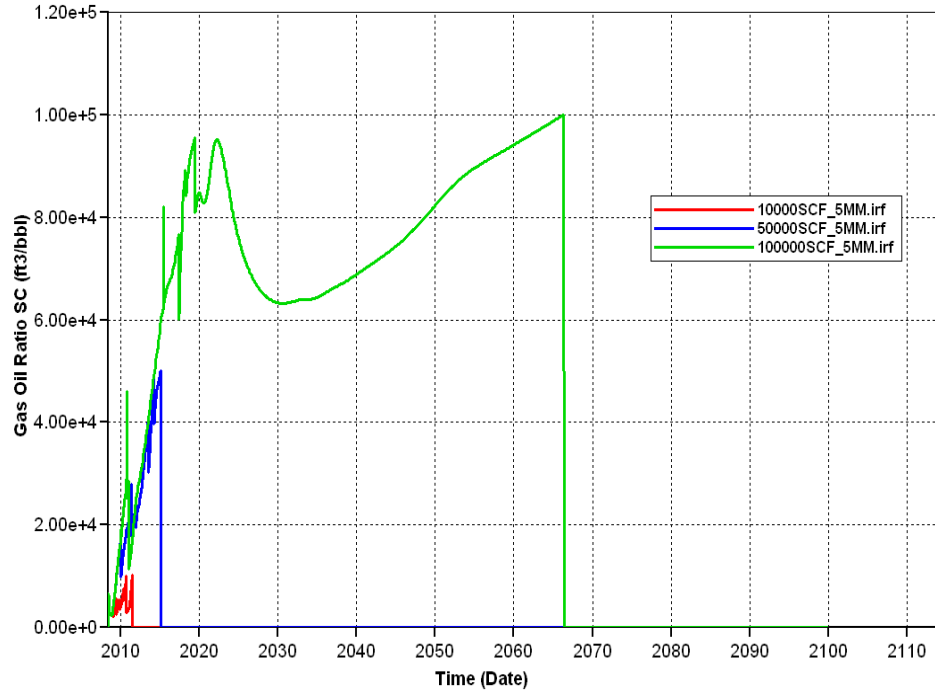


Figure A.18 - Gas Oil Ratio (Case 2)

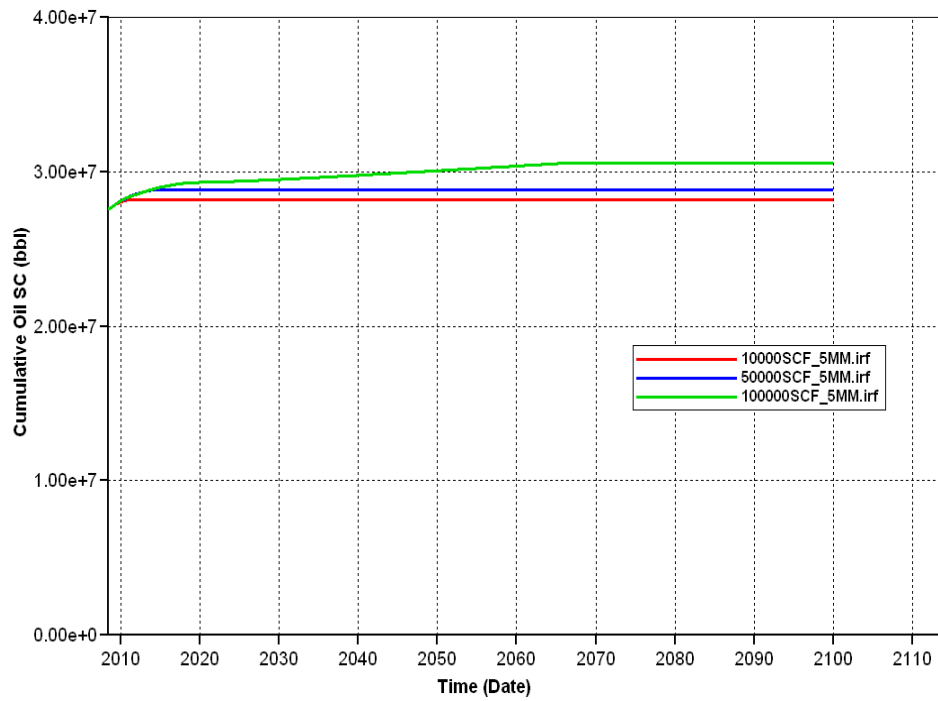


Figure A.19 - Cumulative Oil Production (Case 2)

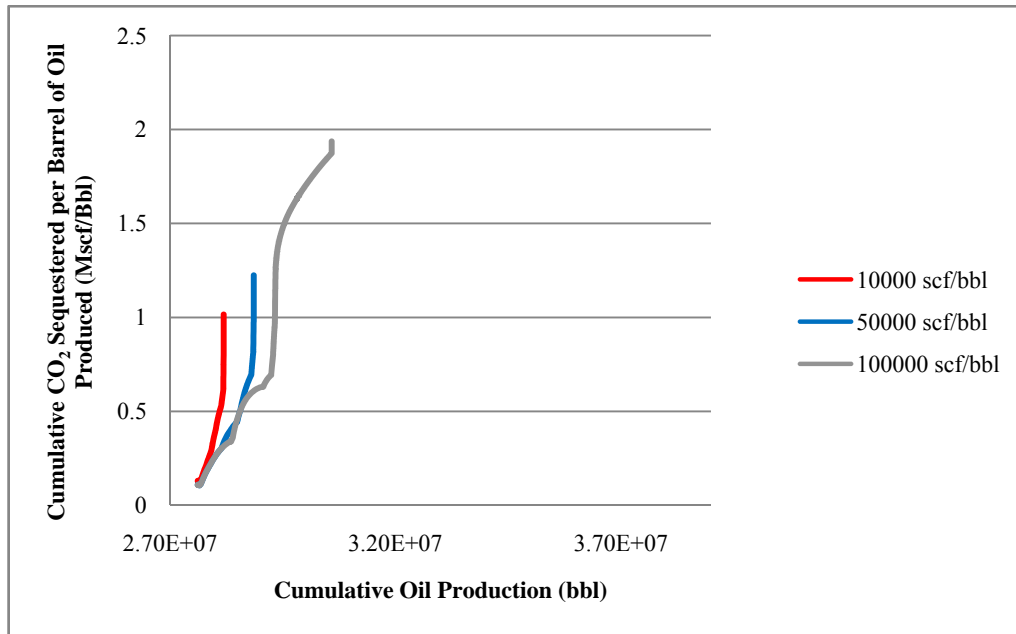


Figure A.20 - Cumulative CO₂ Sequestered per Barrel of Oil Produced VS Oil Production (Case 2)

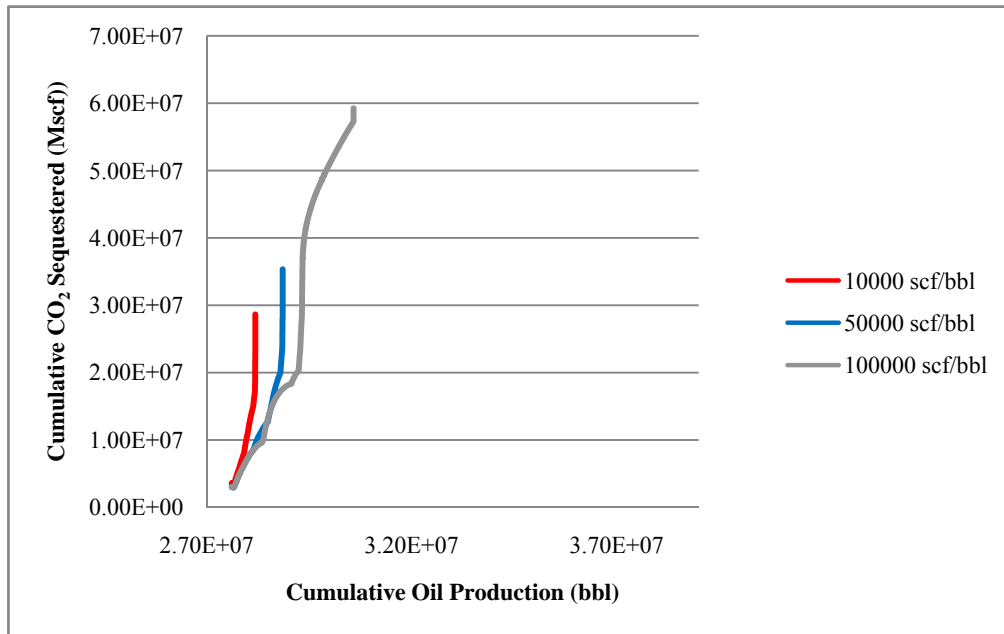


Figure A.21 - Cumulative CO₂ Sequestered VS Oil Production (Case 2)

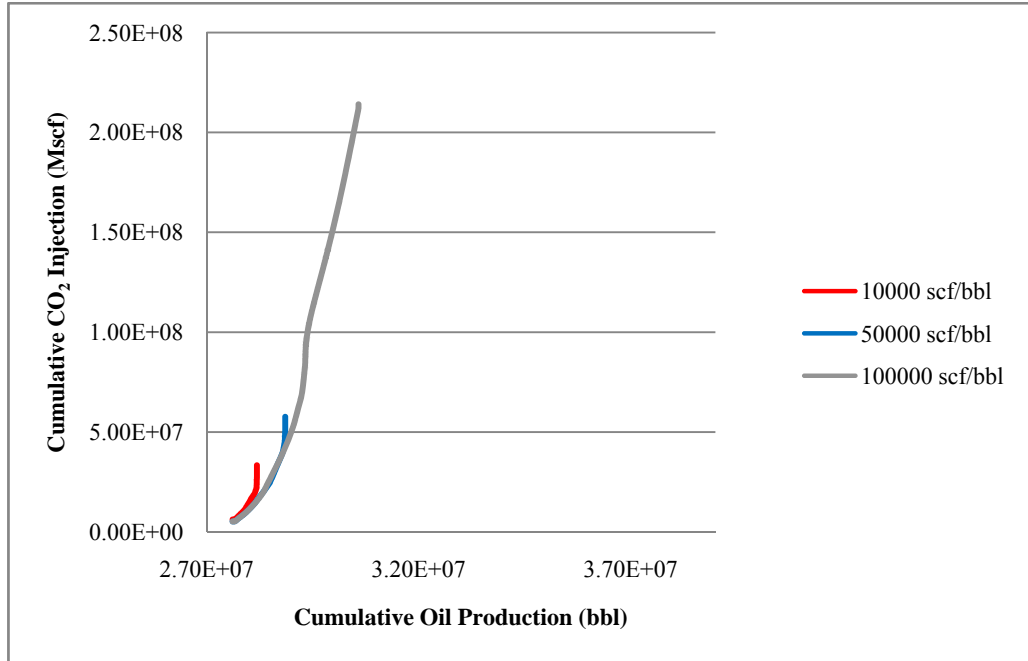


Figure A.22 - Cumulative CO₂ Injection VS Cumulative Oil Production (Case 2)

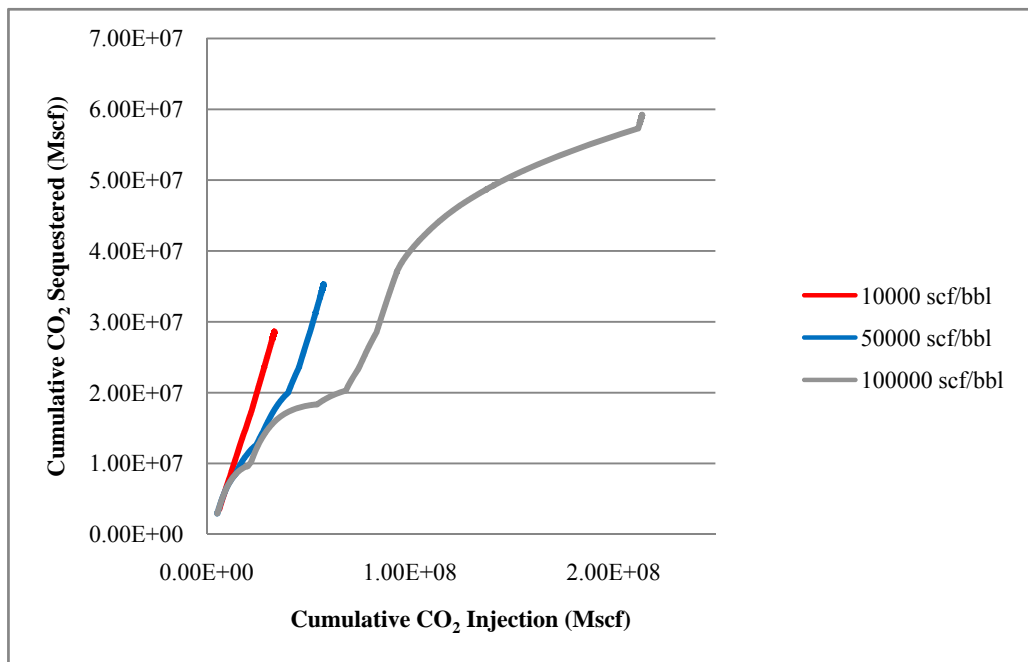


Figure A.23 - Cumulative CO₂ Sequestered VS Cumulative CO₂ Injection (Case 2)

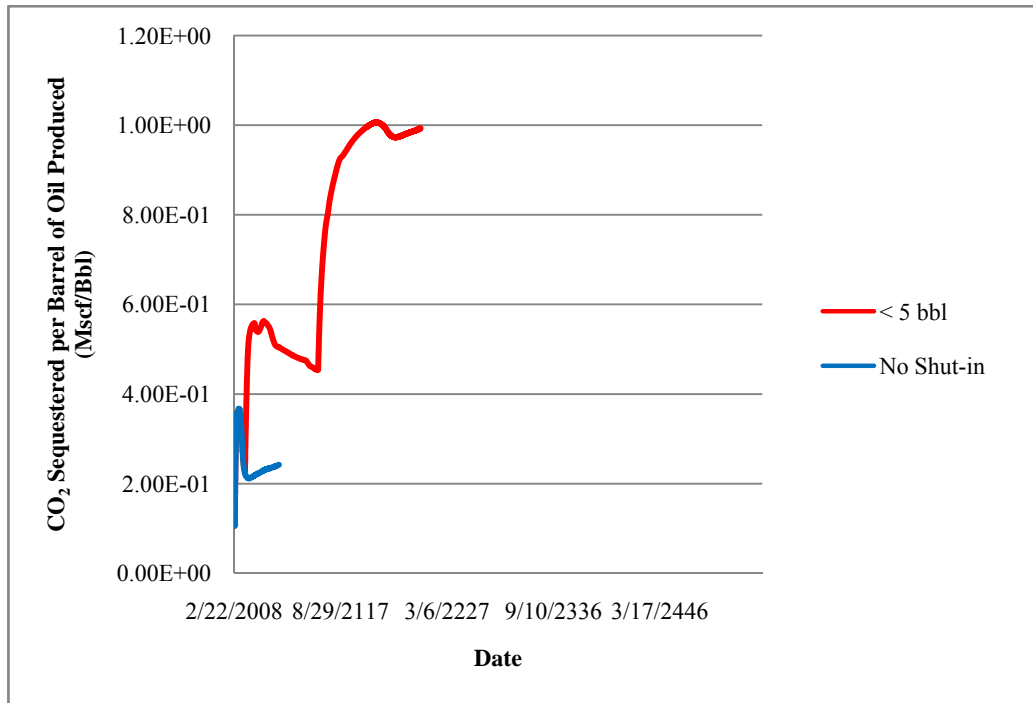


Figure A.24 - Cumulative CO₂ Sequestered per Barrel of Oil Produced (Case 3 and 4)

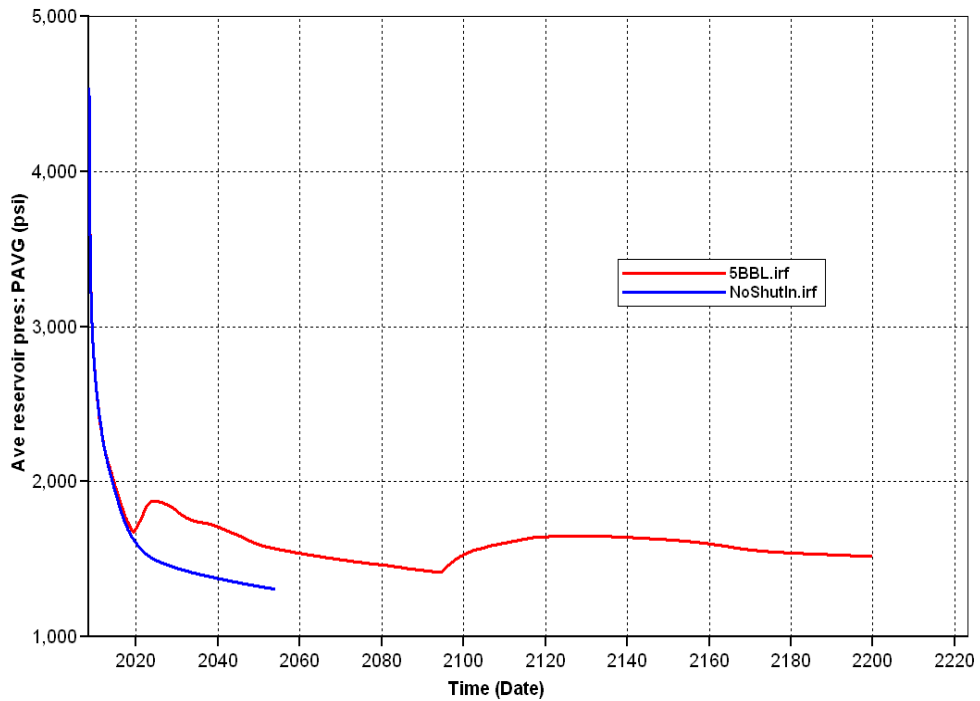


Figure A.25 - Average Reservoir Pressure (Case 3 and 4)

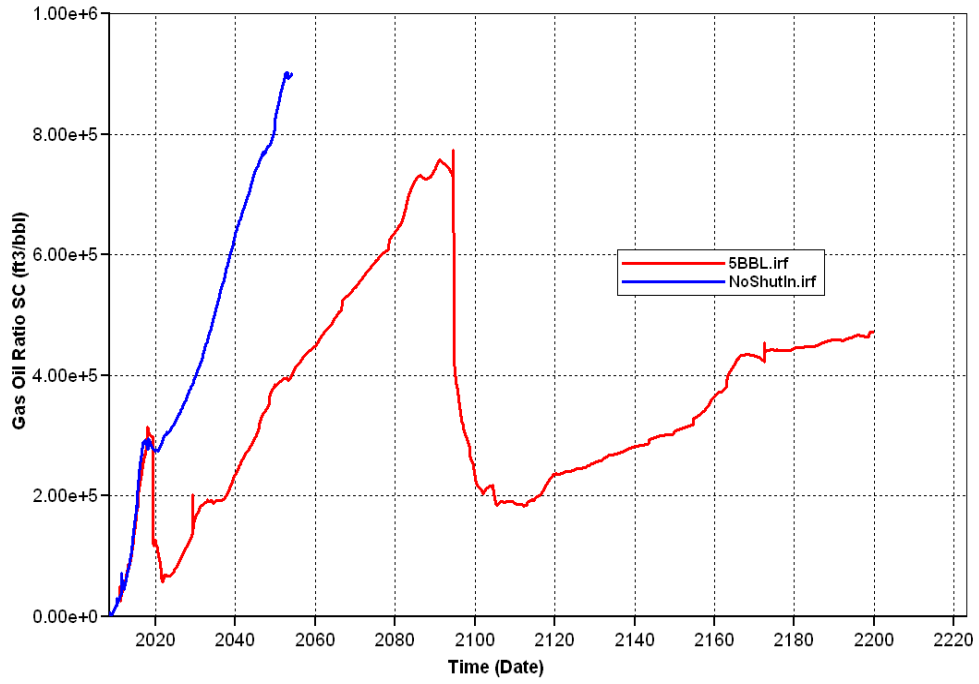


Figure A.26 - Gas Oil Ratio (Case 3 and 4)

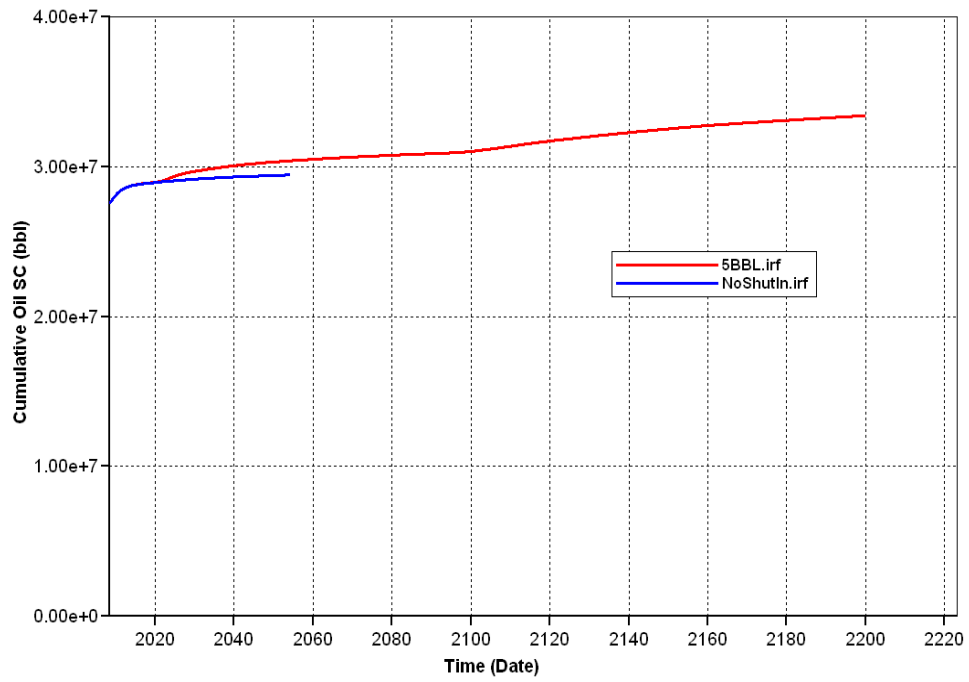


Figure A.27 - Cumulative Oil Production (Case 3 and 4)

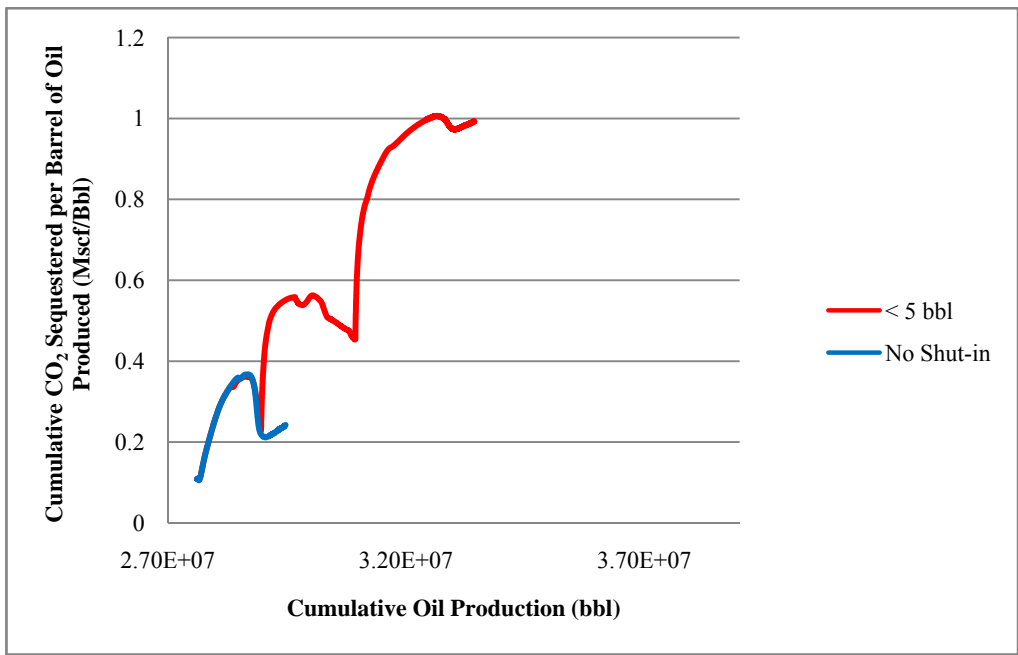


Figure A.28 - Cumulative CO₂ Sequestered per Barrel of Oil Produced VS Cumulative Oil Production (Case 3 and 4)

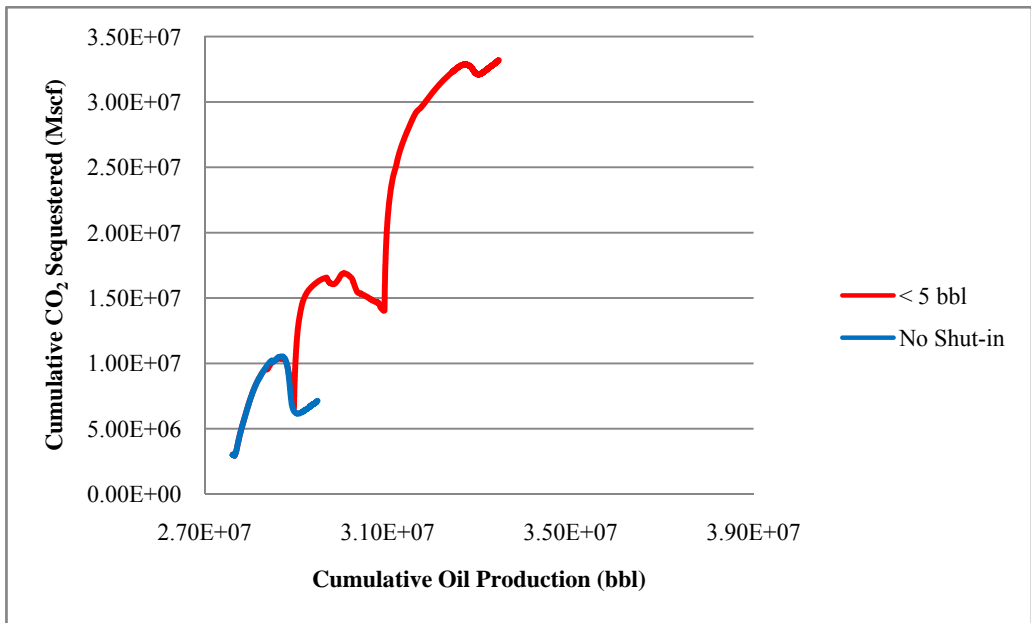


Figure A.29 - Cumulative CO₂ Sequestered VS Cumulative Oil Production (Case 3 and 4)

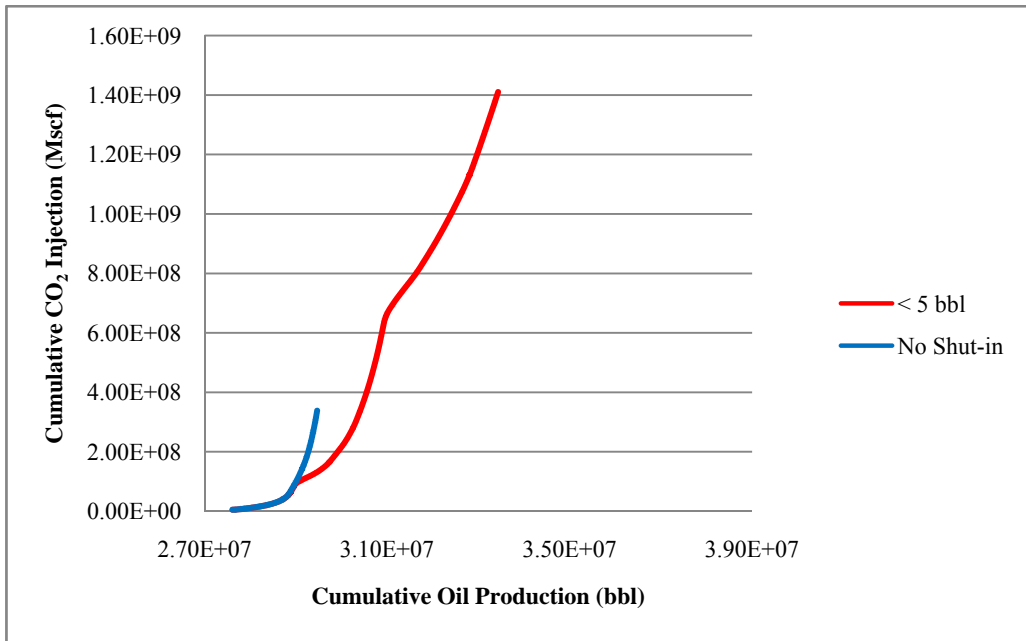


Figure A.30 - Cumulative CO₂ Injection VS Cumulative Oil Production (Case 3 and 4)

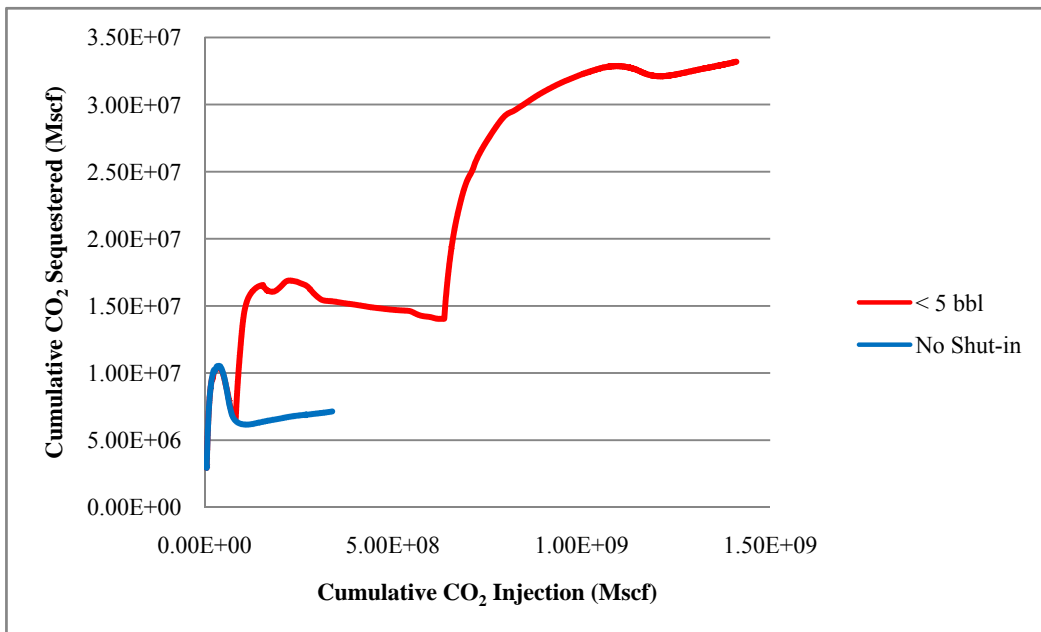


Figure A.31 - Cumulative CO₂ Sequestered VS Cumulative CO₂ Injection (Case 3 and 4)